Power Quality Improvements of Wind Farms

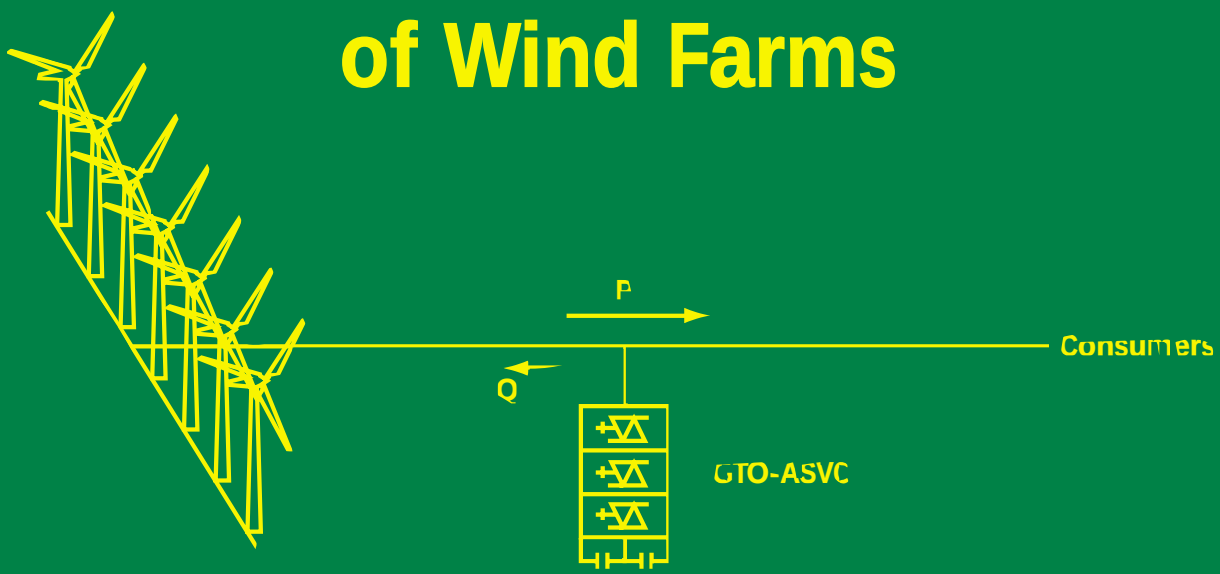

Power Quality Improvements of Wind Farms

Power Quality Improvements of Wind Farms

Fredericia, June 1998

Towards Sustainable Development for the Next Generation

ISBN No.:
87-90707-05-2

Type:
Formata
Excelsior

Layout and text:
Eltra . Information

Repro and printing:
Søndergaard Bogtryk og Offset

Binding:
J.P. Møller, Haderslev

Paper:
115 g mat offset
130 g silkmat coated offset

Impression:
200 copies

Preface

The project described in this book was carried out successfully, thanks mainly to exemplary co-operation in the project team comprising participants from a manufacturer of electrical equipment, the utilities and two universities:

Siemens, Power Transmission and Distribution, Erlangen
UMIST, Department of Electrical Engineering and Electronics, Manchester
National Wind Power, UK
The Technical University of Denmark
Sønderjyllands Højspændingsværk (SH), Denmark
Eltra, Denmark

The project was supported financially by the European Commission under the Fourth Framework, the Joule Non-Nuclear R&D Programme.

Siemens, Germany, was represented by Mr Ralf Stöber as project manager, Dr Michael Weinholdt, Mr Frank Schettler, Mr Heinz Tyll, Mr Klaus Bergmann and Mr Reinhard Brieden. Besides, Mr Peter Jensen and later Mr Bjarne Reeuwijk participated as the local project co-ordinators for Siemens in Denmark.

Dr Nick Jenkins from the Manchester Centre for Electrical Energy contributed to the system studies and Mr Magnus Davidson from National Wind Power participated in the project as subcontractor.

The Technical University of Denmark was represented by three assistant professors; Mr Kaas Pedersen, Mr Erik Andersen and Dr Knud Ole Helgesen, all from the Department of Electric Power Engineering.

The participants from Eltra (formerly Elsam) were Mr J.J. Rype, who conducted the civil works, and Mr Tonny Rasmussen, who was involved as part of his Ph.D. study at the beginning of the project.

Finally, Mr Jacob Rath from SH and Mr Frede Nielsen from the local distribution undertaking of EASV contributed to the project.
Many people have been involved in the project. However, my task as project coordinator was not a difficult one, thanks to the dedication to and involvement of all project partners. Great efforts have been made to cope with the time schedule whenever there were unforeseen delays because of uncertainties, which cannot be avoided in a complicated development project like this.

The contract with the European Commission came into force on January 1, 1996, which was the official starting date of the project. However, intensive negotiations with Siemens and the basic system studies were carried out well before the EC contract came into force.

The first task was to determine the system design. Our first idea was to have two 4 Mvar ASVCs, one connected to each of the two busbars in the switchgear. Preliminary studies indicated that with this solution the harmonic distortion was acceptable.

However, detailed studies showed that under worst case conditions the distortion was too high when all wind turbines were running on one busbar and only one wind turbine was running on the other busbar. The harmonic studies showed that shunt capacitors for no-load compensation in the wind turbines function like a filter, which will absorb all harmonics and may cause overload of the shunt capacitors.

The solution was to connect the two ASVCs in a 12-pulse configuration via a three-winding transformer and to increase the series inductance between the ASVC and the network. Also the ASVC pulse pattern was changed to reduce the harmonic distortion.

Since the grass root movements put the environmental issue on the political agenda, adoption of drastic measures will be required by the power industry. Today, environmental issues and the Danish government's strategy for reduction of the emissions of carbon dioxide will eventually introduce large offshore wind farms into the electrical power system.

To be ready for a deregulated marked, the former power pool of Elsam was divided into two separate companies on January 1, 1998; an independent production company, which will keep the name of Elsam, and a new transmission company with the name of Eltra. Apart from being a transmission company Eltra will bear the overall responsibility for the electrical system. Third-party access to the transmission system, trade in electricity and public resistance to new overhead lines are some of the challenges Eltra will be confronted with. Therefore, from a Danish point of view this project may be seen as part of a strategy for meeting the future challenges and for integrating a large number of offshore wind farms into the Danish electrical power system.

I wish to thank the European Commission for their financial support for the project, and Mr K. Diamantaras, DG XII, for his help and guidance. I also give my warmest thanks to all the people who have contributed to the project and to the creation of this book. I feel that close relationships were established and strong friendships were developed between the partners across the borders of the European Union. Last, but not least, I also want to thank Mr Valdemar Legaard from the graphical department of Eltra, who has made a very great effort putting all the material together and creating the final layout of this book.

Kent H. Søbrink
Project co-ordinator
Fredericia, June 1998

Kent H. Søbrink
I/S Eltra
Fjordvejen 1-11
P.O. Box 140
DK-7000, Fredericia
Denmark

Frank Schettler
SIEMENS, Power Transmission
and Distribution
Erlangen
Germany

Klaus Bergmann
SIEMENS, Power Transmission
and Distribution
Erlangen
Germany

Ralf Stöber
SIEMENS, Power Transmission
and Distribution
Erlangen
Germany

Nicholas Jenkins
Department of Electrical
Engineering and Electronics
UMIST
PO Box 88
Manchester
M60 1QD
ENGLAND

Janaka Ekanayake
UMIST Visitor
Department of Electrical and
Electronic Engineering
Faculty of Engineering
University of Peradeniya
Peradeniya
Sri Lanka

Jørgen Kaas Pedersen
Technical University of Denmark
Department of Electrical Power
Engineering
DK-2800 Lyngby

Knud Ole Helgesen Pedersen
Technical University of Denmark
Department of Electrical Power
Engineering
DK-2800 Lyngby

Zouhir Saad-Saoud,
Maria Luiza Lisboa,
Goran Strbac
Department of Electrical
Engineering and Electronics
UMIST
PO Box 88
Manchester
M60 1QD
ENGLAND

Table of Contents

Chapter 1

Introduction

Nicholas Jenkins
Department of Electrical Engineering and Electronics
UMIST
PO Box 88
Manchester
M60 1QD
ENGLAND

1.1 Introduction to the Book

This book was written at the conclusion of a project to install and monitor the performance of an 8 MVAr Advanced Static VAr Compensator (ASVC) at the Rejsby Hede wind farm in Jutland, Denmark. The book is intended both to record the main achievements of the project but also to illustrate how this new type of power electronic equipment might be applied in other situations to improve the quality of electrical power delivered to the distribution network from renewable generation sources embedded within it.

Many changes occurred during the course of the project. A small change was that it was decided internationally to refer to Advanced Static VAr Compensators (ASVCs) as STATCOMs (Static Compensators). However as this change occurred part way during the project the old name is retained in this book. Of more consequence, the UN Climate Change Conference took place in Kyoto, Japan and further increased the determination of European Governments to reduce gaseous emissions. The installed capacity of wind turbines in Germany exceeded 2000 MW and in Denmark 1000 MW. The installation of large arrays of wind turbines offshore started to appear to be a practical proposition and was encouraged by Danish Government policy. The separation of power utilities into network and generation businesses continued world-wide and the host utility of the project was split into two parts. Finally, progress was maintained in the technology of power electronic devices and systems.

All these changes served only to confirm the importance of the project. Wind turbines and other forms of renewable generation embedded in the electricity distribution networks will continue to play an important part in reducing the CO_2 emissions of European countries. The impact of wind farms on distribution networks can be minimised and hence the connection costs reduced only if effective reactive power schemes are in place. The separation of the power utilities into a number of business units increases the requirements of the transmission and distribution operator for independent control of reactive power, while the continuing developments in power electronics offer the potential for cheaper and more effective compensators.

1.2 Introduction to the Project

The main objective of the project was to investigate how the power quality of the electrical output of wind farms could be improved by the use of modern high power electronic technology. Although the research is of direct application to wind energy it will also be relevant to many other types of small-scale generation embedded in utility distribution networks.

The operation of wind turbines with asynchronous generators requires reactive power which, if supplied from the network, leads to low voltages and increased losses. In order to improve the power factor of the generation, fixed capacitors are usually used to provide reactive power. However, if they are sized for the full requirement of the wind farm, they can cause self-excitation and potentially damaging and hazardous overvoltages if the wind turbines' connection with the network is interrupted and they become islanded.

The reactive power consumption of wind turbines consists of a constant no-load demand and a requirement which varies proportionally with the output of the generator. In weak networks in particular this results in varying voltages and poor power quality. The voltage quality can be improved considerably if the wind turbines' varying reactive power consumption is provided from a dynamic compensator which supplies reactive power corresponding to the varying consumption of the induction generators whereas only the constant no-load consumption is provided from fixed capacitors. In this way the risk of overvoltages due to islanding can also be eliminated.

An advanced Static VAr Compensator (ASVC) uses a power electronic converter to generate or absorb reactive power. They can be used to provide reactive power with rapid control and with only modestly sized passive components (i.e. small capacitors and reactors). The objective of the project was to combine research and development of this novel form of electronic equipment with its application to increase the use of renewable energy, and wind power in particular, in the European Union.

1.3 Introduction to the Project Partners

The partners in the project were:

1.3.1 ELSAM – ELTRA

At the start of the project ELSAM was the integrated Jutland-Funen power pool and transmission authority. However, towards the end of the project the organisation was split into its constituents parts and the project was completed by the transmission utility which was renamed ELTRA.

ELSAM was the initiator and co-ordinator of the project. Local support for the project was provided by one of the 6 Jutland-Funen electrical utilities Sønderjyllands Højspændinsværk.

1.3.2 SIEMENS

After extensive analysis of the wind farm system and associated network with respect to impedans, harmonics and load flow, Siemens Power Quality Management designed and manufactured the ASVC at their facilities at Erlangen, Germany.

1.3.3 Technical University of Denmark (DTU)

The Technical University of Denmark designed and installed the measurement equipment to monitor the performance of the ASVC.

1.3.4 University of Manchester Institute of Science and Technology (UMIST)

The role of UMIST was to undertake power systems analysis and simulations in order to investigate the wider applications of ASVCs to wind farms. The studies were carried out in collaboration with National Wind Power who provided details of typical wind farms connected to weak distribution networks.

Chapter 2

Rejsby Hede Wind Farm

Kent H. Søbrink
I/S Eltra
Fjordvejen 1-11
P.O. Box 140
DK-7000, Fredericia
Denmark

2.1 Introduction

Wind power is one of the most promising sources of renewable energy, and the application of wind turbines is one of the cheapest alternatives to reduce CO_2 emissions from electrical power production. The disadvantages of wind turbines are that it is impossible to control their power output and difficult to predict their production of electrical power, as their production profile is only determined by the wind speed. In addition, wind turbines with asynchronous generators also have an impact on the voltage quality in the network to which they are connected. This project addresses the last mentioned problem and demonstrates how the power quality may be improved by using power electronic equipment – Advanced Static VAr Compensators (ASVCs).

The goal of the Danish government is to reduce CO_2 emissions by 20 % by the year 2005 compared to the 1988 level and to halve emissions by the year 2030. One of the important strategies to achieve this goal, is to promote electrical wind power. Today, the total installed wind power capacity in the western part of Denmark is 731.4 MW generated by more than 3,500 wind turbines, and the yearly energy production is approximately 1,200 GWh. The total capacity in 2005 is estimated to be 1,500 MW and the potential capacity is estimated to be 4,000 MW in total – mainly based on offshore wind farms.

Experience with offshore wind farms has shown that they are more efficient than expected, and under certain circumstances, they are economically feasible as a means to reduce CO_2 emissions.

A commission with members from the Danish Ministry of Energy, the National Forest and Nature Agency and the power industry proposed the erection of 4,000 MW of offshore wind farms within the next 25 to 30 years; 1,500 MW before 2015 and 1,750 MW before 2030.

Therefore, the Danish electrical power industry recently announced their active support for the Government's strategy concerning more wind farms. The Commission has pointed out three offshore areas; two areas with a potential capacity of 800 MW of wind power each, and a third area with a potential capacity of 1,400 MW of wind power.

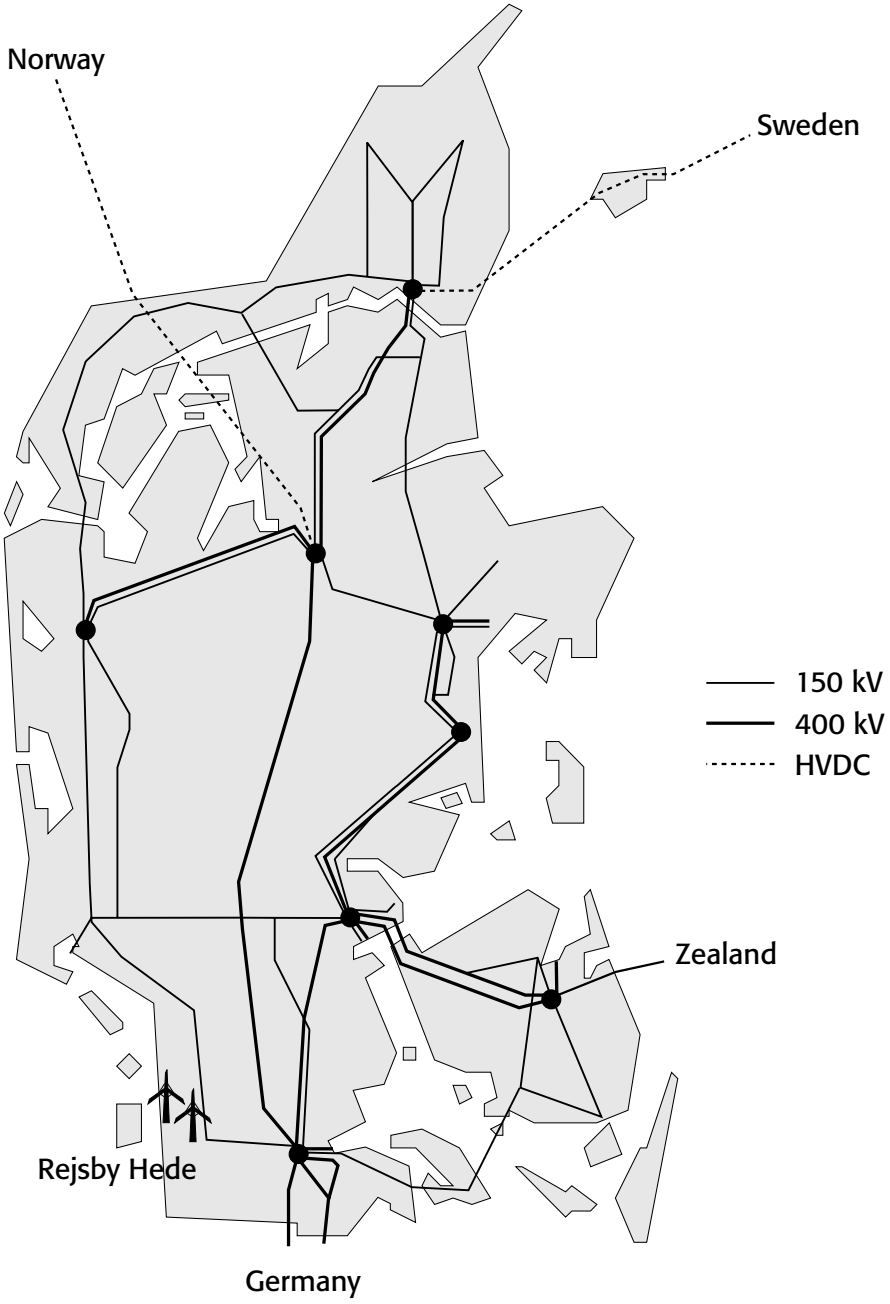

Figure 2.1: Map of the Danish Jutland peninsula.

2.2 The Rejsby Hede Wind Farm

The Rejsby Hede wind farm with a total capacity of 24 MW has been erected in the southwestern part of Jutland by the local power production company Sønderjyllands Højspændingsværk as part of the Danish energy plan "Energy 2000". Figure 2.1 shows the map of the Danish Jutland peninsula, showing the main electrical circuits.

2.2.1 Description of the Wind Farm

The Rejsby Hede wind farm is located in a flat, high wind speed area near the west coast. Because the energy content of the wind increases with the third power of the wind speed careful location of wind turbines is vital for the economical exploitation of the wind power. After a prolonged local planning period, the 40 wind turbines were brought into service at Rejsby Hede in 1995.

No. of wind turbines	40
Wind turbine type	M 1500 - 600/150 kW, MICON
Hub height	46 m
Rotor diameter/area	43.5m /1,452 m^2
Blade type	LM 19.1 m, with Vortex-generator, stall-regulated
Gearbox	FLENDER, PEAK 4280 - combined planet wheel and cogwheel
Generator	ELIN, MCT-445J21F9N, asynchronous multiple-speed
Wind roughness class	1 - 2.5
Total installed power	24 MW
Expected yearly production	58,500 MWh

Table 2.1: Main data for the Rejsby Hede wind farm.

The wind farm consists of 40 Micon 600 kW turbines, of which one is privately owned. The wind turbines are mounted on tubular towers at a hub height of 46 m. The three-bladed rotor is 43.5 m in diameter. The foundation of each turbine consists of 70 m^3 of concrete and 8 tonnes of steel reinforcement and takes up an underground area of 100 m^2. Table 2.1 gives details of the main data of the wind farm.

The first wind turbine was erected during May 1995 and the last one was set up during July. The period from July to October was used for testing, and the production figures for this period were lower than expected for full operation. The production figures from October to November 1995 were assumed to be representative of normal operation. Based on commercial operating experience in 1995, it was expected that the wind farm was to yield a total annual energy production of 58.5 TWh. Table 2.2 shows the actual energy production of 48.7

TWh in 1996, which was lower than expected. Year 1996 was also less windy than usual.

The wind farm output during the month of August of 1996 is shown in Figure 2.2. The curve is based on measurements on each quarter of an hour, and the power output is shown in percentage of the installed capacity of the wind farm (23.4 MW). Figure 2.3 shows the power duration and power loss curve for the year 1996. The power duration curve is formed by normalising the power output P/P_{max}, i.e. dividing the measured power output values P by the installed power capacity P_{max}, and then by arranging all normalised power output values in descending order.

The network losses increase with the square of the current (losses = R x I^2), which means that if the power factor is constant then the losses increase in proportion to the square of the power. Therefore, the loss curve is obtained by taking the square of the normalised power, i.e. the power duration curve.

The area below the power duration curve is equal the power duration time T_d, which expresses how long it takes to produce the actual yearly energy production at full output power. Power duration time for 1996 was T_d = 2080 h, which corresponds to utilisation percentage of 23.7 % (= 2080 x 100 / 8760) of a maximum possible yearly production which is equal 8760 h multiplied by P_{max}.

Similarly the area below the loss curve is equal to the loss factor or the loss duration T_l, which expresses how long it takes to generate the actual yearly losses at P_{max}. The loss duration time for 1996 was 1062 h. The loss duration T_l is less than the power duration T_d, because the losses increase with the square of the power, so the yearly power losses are generated in a shorter time at P_{max}.

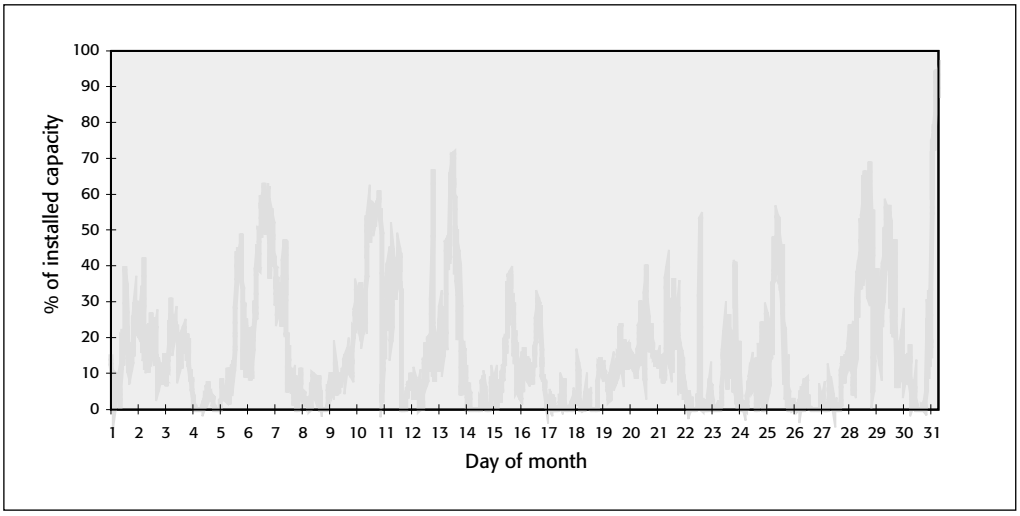

Figure 2.2: Wind farm power output in August 1996.

Month	Energy production (MWh)	Peak power (MW)
January	5,210	23,621
February	5,317	23,394
March	5,285	21,607
April	1,859	18,953
May	4,143	23,454
June	4,182	22,038
July	4,071	19,778
August	2,826	22,117
September	3,211	22,107
October	4,015	23,949
November	5,277	24,387
December	3,280	22,979
Total	48,676	24,387

Table 2.2: Energy production 1996.

If the losses Pl_{max} are known at P_{max} and if T_l is known, then the capitalised value of the losses may approximately be calculated as T_l x Pl_{max} x Q, where Q is the average marginal production price.

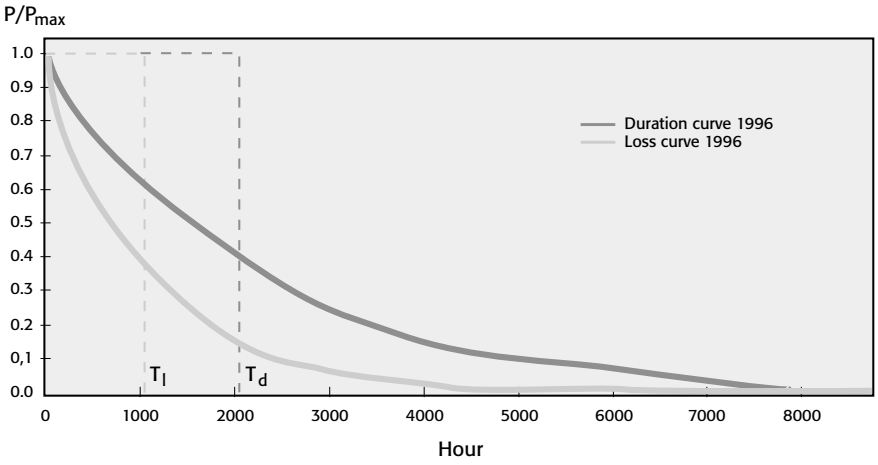

Figure 2.3: The power duration and power loss curves, 1996.

2.2.2 Description of the Turbines

The turbines are up-wind, horizontal-axis, stall-regulated machines. Figure 2.4 shows components of the nacelle of each wind turbine. Each turbine drives a dual-power, two-speed, asynchronous induction generator with an output of 150 kW at wind speeds of up to 7-8 m/s. The generator automatically switches to 600 kW at higher wind speeds. For each turbine three 50 kVAr shunt capacitors are provided for compensation of the no-load reactive consumption of the asynchronous generators. When a turbine is operated with its 150 kW generator one capacitor (50 kVAr) is switched in, and when a turbine is operated with the 600 kW generator three capacitors (total 150 kVAr) are switched in.

A purpose-made electronic unit controls each turbine and all the wind turbines are connected to the local distribution company's control centre at Skærbæk. The system provides control for all the functions of the turbines, records details of production and faults, and provides status reports.

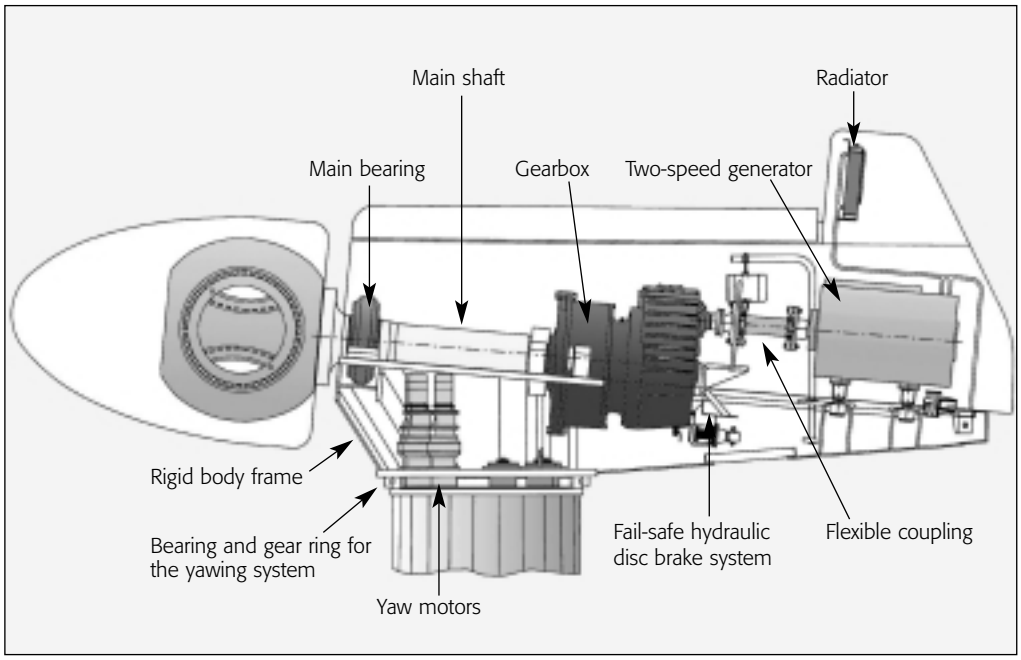

Figure 2.4: Components of the nacelle.

2.2.3 Description of the Local Network

The Rejsby Hede wind farm is connected to a 60 kV substation in a radial distribution network which is supplied from a 60/150 kV substation in Bredebro as shown in Figure 2.5. Apart from the Rejsby Hede wind farm, the 60 kV distribution network supplies two villages Højer and Ballum. Normally, the loads in Højer and Ballum are less than the wind farm production, which is why the

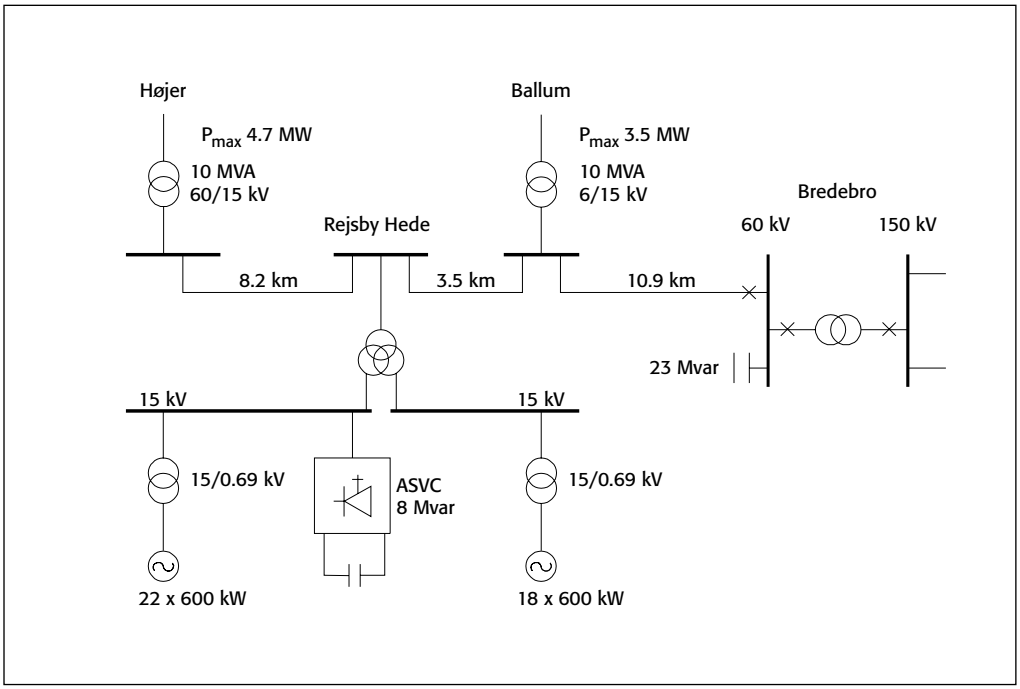

Figure 2.5: Single-line diagram of the 15 kV and 60 kV networks.

excess power production from the Rejsby Hede wind farm is fed into the 150 kV network in Bredebro.

Figure 2.5 shows that the 60 kV substation in Bredebro is provided with a 23 MVAr shunt capacitor. This means that if the wind farm together with the consumers in Ballum and Højer are isolated from the 150 kV network, i.e. if the transformer breaker in Bredebro trips, the presence of the 23 MVAr capacitor in Bredebro may give rise to self-excitation of the wind turbine generators. Then, the wind farm becomes overcompensated, which leads to excessive overvoltage and the danger that the consumers' electrical equipment may be destroyed.

In the wind farm, each wind turbine generator is equipped with a 0.69/15 kV step-up transformer. All transformers are connected to the local 15 kV network cable which consists of five radial feeders, of which two are connected to nine generators each. Of the remaining three feeders, one is connected to six generators and the remaining two are connected to eight generators each. In order to reduce the short-circuit level, the 15 kV switchgear is split into two busbars. Two feeders with 18 generators are connected to one of the 15 kV busbars while the remaining three feeders with 22 generators are connected to the other busbar. The two 15 kV busbars are connected to the 60 kV substation through a 15/15/60 kV three-winding step-up transformer.

2.2.4 Need for Reactive Compensation

The need for reactive power in electrical networks is due to energy stored in electrical and magnetic fields in the network components such as overhead lines, cables, capacitors, reactors, transformers and motors. Models of such network components contain voltage and current sources and pure passive components which are either Resistors (R), Inductors (L), Capacitors (C) or a combination of any of them.

Figure 2.6 shows the relationship between current and voltage for a resistive, an inductive and a capacitive component. The current flowing through a resistor and the voltage across it are in phase. Therefore, the electrical power in a resistor, equal to current multiplied by voltage, is dissipated as heat.

In a capacitor, the current leads the voltage by 90 degrees. This means that when the a.c current is at its maximum the voltage is zero, and when the voltage is at its maximum the current is zero. Therefore, no power is dissipated in a pure capacitor. However, energy is stored in the electric field in the capacitor. The capacitor alternately takes up energy and gives off energy as the a.c voltage across the capacitor alternates between plus and minus.

In a inductor, the current lags the voltage 90 degrees. As with capacitors, no heat is dissipated in an inductor. However, energy is stored in the magnetic field in the inductor. The inductor alternately takes up energy and gives off energy as the a.c. current in the inductor alternates between plus and minus.

Inductive and capacitive currents are in opposite phases which means that the electrical energy in capacitors and the magnetic energy in inductors are overlapping in an a.c network. When inductors deliver energy, capacitors consume

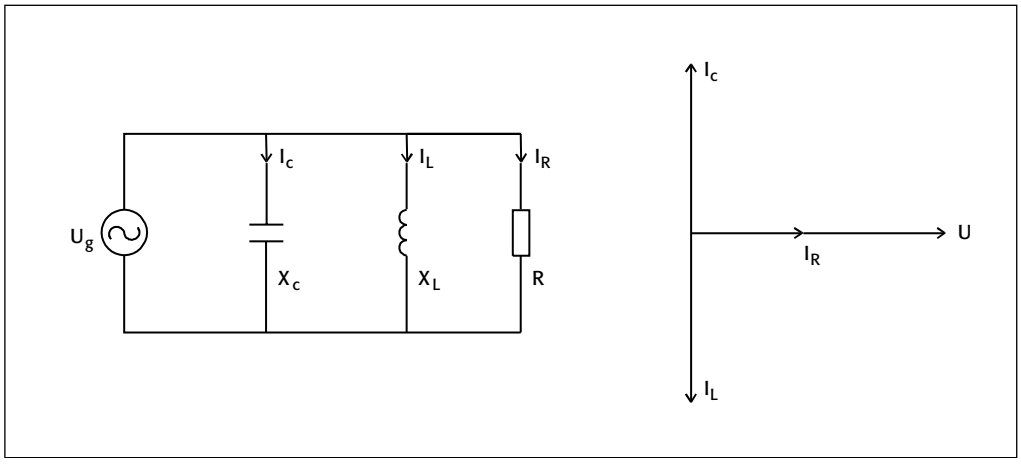

Figure 2.6: AC voltage and current in RLC components.

energy and vice versa. By definition, reactive power in capacitors is negative and is calculated as $Q_c = \omega C U^2$, whereas reactive power in inductors is positive and calculated as

$$Q_L = \frac{U^2}{\omega L} .$$

It is said that capacitors generate reactive power whereas inductors absorb reactive power.

If there was no resistance in the network, this flow of magnetic and electric energy or generation and absorption of reactive power would persist without losses. However, except for super conducting material, all electrical components have some resistance, which means that the transfer of reactive power from capacitors to inductors causes losses in resistances in the network. If an inductor is connected to an a.c. network, it will absorb reactive power from the network, which will cause losses and voltage drops in the network. However, if a capacitor is connected close to the inductor, the capacitor can deliver the reactive power required by the inductor.

Figure 2.7 shows an example in which a reactive load (R_L, X_L) is compensated with a shunt capacitor Q_C. If the reactive power from the shunt capacitor Q_C is equal to the reactive power required by the load, the transfer of reactive power from the generator (Q_L-Q_C) is zero, which means that losses and voltage drop, in the line impedance (R_L, X_L), caused by this transfer of reactive power from the generator are eliminated. The reactive power is transferred over a much shorter distance from the shunt capacitor to the inductive load.

As mentioned above, models of network devices may be represented by RLC components. The wind turbines are equipped with induction generators, which

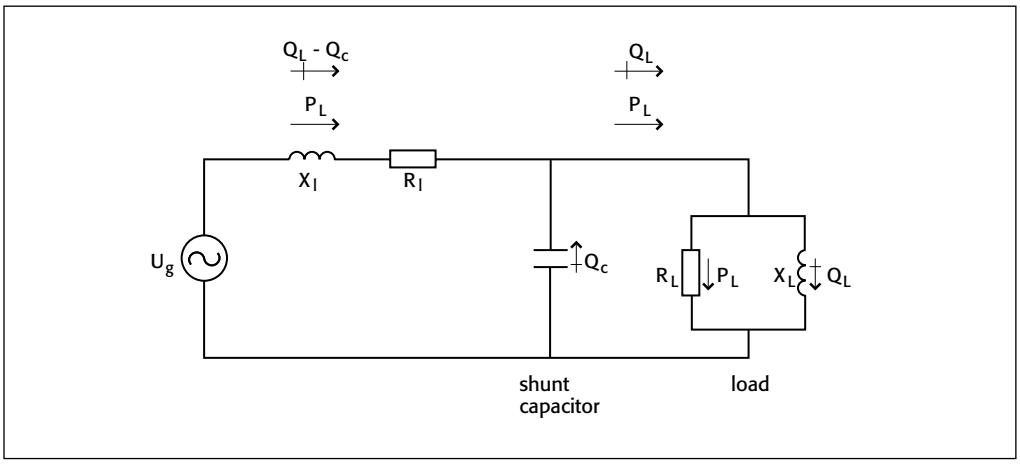

Figure 2.7: Reactive power compensation with a shunt capacitor.

have a very simple, robust and reliable construction. An induction generator consists of stator windings and rotor windings. The stator windings are embedded in the stator, which is the non-rotating part of the machine, whereas the rotor windings are wound on the rotor, which is the rotating part of the machine. The rotor windings are short-circuited. If the stator winding is connected to a balanced three-phase a.c. network, it creates a magnetic field which rotates in synchronism with the network frequency. The rotating field created by the stator induces voltages and currents in the rotor. The rotor currents react with the rotating field and create torque, which accelerates the rotor in the direction of the rotating field. The induced voltage in the rotor depends on the relative speed between the rotating field and the rotating rotor. When the rotor accelerates, the relative speed between rotor and the rotating field decreases and if the relative speed is zero no voltage and current are induced in the rotor. In order to produce torque the speed of the rotor must differ from the speed of the rotating magnetic field.

The rotational speed for a P-pole machine is given by

$$n_s = \frac{120f}{P},$$

where n_s is in rad/min, and P is the number of poles. The rotor speed n_r must be different from n_s in order to create torque in the air gap between the rotor and the stator. The per-unit slip of the rotor is defined as

$$s = \frac{n_s - n_r}{n_s}.$$

If n_r is less than n_s, then the slip is positive and the induction machine is driven as a motor. If n_s is greater than n_r, the slip is negative and the induction machine is driven as a generator where external mechanical torque is applied to the rotor, which is the case of wind turbine generators.

Figure 2.8 shows the equivalent circuit of an induction machine with all quantities referred to the stator. R_s is the stator resistance, X_s is the stator leakage reactance, R_r is the rotor resistance and X_r is the rotor reactance. X_m is the magnetising reactance and s the rotational slip speed. P_a is the power transferred across the air gap and P_s is the mechanical power on the shaft of the induction machine. As can be seen from the equivalent circuit, the induction machine has a constant reactive power consumption which corresponds to X_m, and a variable reactive power consumption which varies with the load.

The constant reactive power consumption is also known as no-load reactive power consumption. The no-load reactive power depends only on the terminal voltage and is therefore easy to compensate with a shunt capacitor connected at the terminals of the induction machine. To prevent overcompensation, which may lead to self-excitation and overvoltages, normally only 80 to 90 % of the constant no-load consumption is compensated with shunt capacitors.

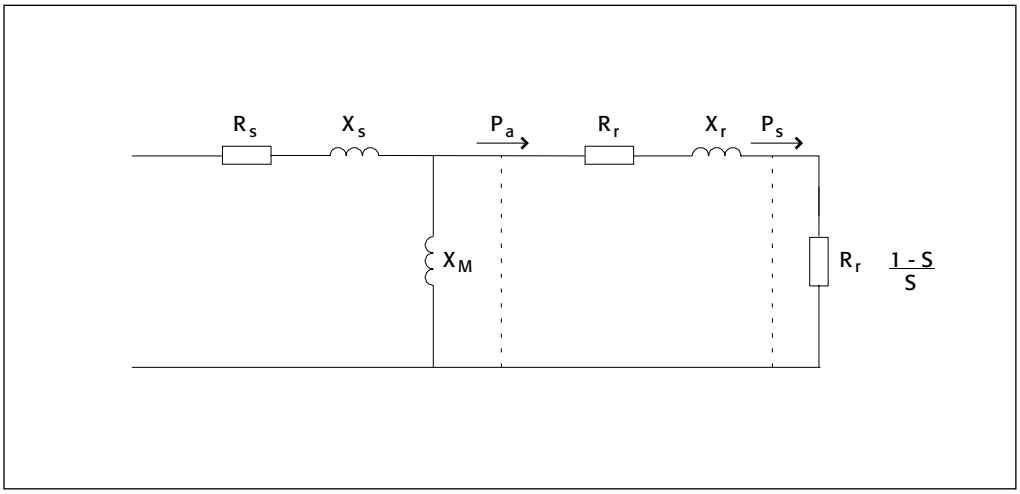

Figure 2.8: Equivalent circuit of an induction machine.

The reactive power consumption corresponding to Xs and Xr varies with the loading of the induction machine. This variable consumption is not easy to compensate and so it is usually drawn from the network. This causes voltage drops and losses due to the reactive power flow in the network. Therefore, it would be an advantage if this reactive power could be provided from a variable source such as an Advanced Static VAr Compensator (ASVC).

The main consumers of reactive power in the wind farm are the induction generators, whereas reactive losses in the lines are negligible. The reactive consumption of each 600 kW generator is 219 kVAr at no-load and 372 kVAr at full load, as given in Table 2.3. For the 150 kW generator the reactive consumption is 87 kVAr at no-load and 124 kVAr at full load (see Table 2.3 for full details of the machine). The total reactive power required by the wind farm is 8,760 MVAr at no-load and 14,880 MAVr at full load.

For no-load compensation, three 50 kVAr shunt capacitors are connected across the terminals of each wind turbine generator. When the wind turbine is operated with the 150 kW generator, only one 50 kVAr capacitor is connected. When the wind turbine is operated with the 600 kW generator, all three 50 kVAr (150 kVAr) shunt capacitors are connected.

In total the wind farm is provided with 6 MVAr shunt capacitors for no-load compensation. Compared with the total no-load consumption of the wind farm, the compensation ratio is 68.5 per cent.

The wind farm operates with any mixture of 150 kW and 600 kW generators and the variable reactive power requirement ranges from 0 to 8.880 MVAr.

Nominal power	600 kW	150 kW
Nominal apparent power	706 kVA	195 kVA
Number of poles	4	6
Coupling star star		
Nominal voltage	690 V	690 V
No-load voltage	715 V	715 V
Frequency	50 Hz	50 Hz
Synchronous rev.	1500 rpm	1000 rpm
Full-load rev.	1605.7 rpm	1004.4 rpm
Efficiency 4/4	0.9732 ohm	0.9594 ohm
Slip	0.4 %	0.37 %
No-load consumption	219 kVAr	87 kVAr
Full-load consumption	372 kVAr	124 kVAr
No-load current	183 A	81 A
Full-load current	581.1 A	158.02 A
Cos phi 100 %	0.85	0.77

Table 2.3: Main data for the MICON 600/150 kV induction generator.

However, an 8 MVAr ASVC, which is a standard size, was chosen. At full power output from the wind farm, there is a reactive power deficit of 880 kVAr. This is drawn from the network with no real impact on the voltage quality. Moreover, the wind farm is only operated for a few hours per year at full output power according to the power duration curve depicted in Figure 2.3.

Chapter 3

Reactive Compensation for Wind Farms

Janaka Ekanayake
UMIST Visitor
Department of Electrical and Electronic Engineering
Faculty of Engineering
University of Peradeniya
Peradeniya
Sri Lanka

Nicholas Jenkins
Department of Electrical Engineering and Electronics
UMIST
PO Box 88
Manchester
M60 1QD
ENGLAND

3.1 Introduction to Reactive Power Compensation [1]

Reactive power compensation is the absorption or generation of reactive power to maintain efficient and reliable operation of the power system and its loads. It can be used to: (1) maintain load voltages and/or voltages of a transmission network within maximum and minimum limits, (2) increase the power transmission capability of lines while maintaining stability of the power system and (3) minimise the reactive power flow in the circuits, by compensating large reactive power consuming loads locally, and thus reduce the network losses.

Reactive power compensation has often been used in transmission systems to improve network voltages and power transfer capability and also in distribution networks to compensate large reactive power consumers. Large reactive power consumers are encouraged by the power utility to increase their power factor, thereby reducing the reactive power demand on the network. The result is a better voltage profile, reduced losses and increased stability of the system.

Wind farms are a rather unusual type of large reactive power consumer as they import reactive power while generating active power. Many of the electrical networks, to which wind farms are connected, are ‘weak’ with high source impedances. The output of a wind farm changes constantly with wind conditions and so it draws varying amounts of reactive power from the utility network resulting in variations in the voltage at the point of connection. A reactive power compensator can be connected to the wind farm to supply this reactive power locally and thus improve the steady state voltage profile at the point of connection.

Another problem with wind farms is that, rapidly changing wind conditions may create an objectionable “voltage flicker” condition. In this case the magnitude of the voltage variations are relatively small but occur at a frequency which causes severe annoyance to the human eye. In such cases, a compensator of appropriate rating may be employed to compensate the voltage changes and hence eliminate flicker.

A reactive power compensator can also be connected to improve the steady state stability limit of the network to which the wind farm is connected. Effective voltage control through reactive power compensation enables the connection of medium-size and large wind turbines to ‘weak’ networks.

3.2 Impact of Reactive Power Flows on a Simple Circuit [2]

The basic circuit shown in Fig 3.1 can be considered to demonstrate the impact of reactive power flow and how a reactive power compensator can be used to minimise them.

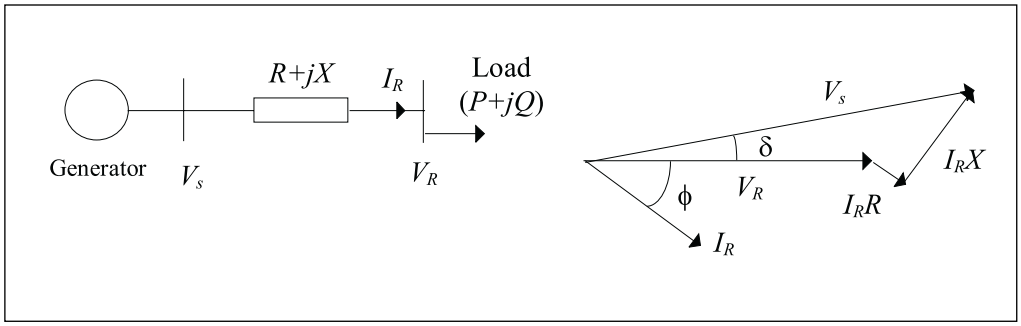

Fig 3.1: Simple electrical power system.

Assuming the power flow in the line is P+jQ:

$$\underline{V_R} I_R^* = P + jQ \tag{3.1}$$

$$I_R = \frac{P - jQ}{V_R^*} \tag{3.2}$$

Then

$$\begin{aligned} \underline{V_s} &= \underline{V_R} + (R + jX)\underline{I_R} \\ &= \underline{V_R} + (R + jX)\left(\frac{P - jQ}{V_R^*}\right) \end{aligned} \tag{3.3}$$

According to the phasor diagram,

if $\underline{V_R} = V_R \angle 0°$, then $\underline{V_S} = V_S \angle \delta$

with usual complex notation. Then from equation (3.3), equating real and imaginary parts the following equations can be obtained.

$$V_s \cos\delta - V_R = \frac{PR + QX}{V_R} \tag{3.4}$$

$$V_s \sin\delta = \frac{PX - QR}{V_R} \tag{3.5}$$

As δ is very small, from equation (3.4)

$$\text{Voltage drop across the line} = V_S - V_R = \frac{PR + QX}{V_R} \tag{3.6}$$

Generally for transmission networks, R is much less than X and from equation (3.5)

$$P = \frac{V_S V_R \sin\delta}{X} \tag{3.7}$$

For a circuit with a small resistance, R, it is clear that the voltage drop across the line mainly depends upon the reactance of the line, X, and the reactive power flow, Q. If the reactive power requirement of the load can be supplied locally by connecting a reactive power compensator at the load bus, the voltage drop across the line can be reduced, the steady state voltage at the load bus can be raised and any flicker can be improved.

3.3 Conventional Methods of Shunt Reactive Power Compensation

Reactive power compensation can be achieved with a variety of shunt devices. The simplest method is to connect a capacitor or an inductor in parallel with the network. As the reactive power output of these component is not controllable, devices such as synchronous condensers and saturable reactor compensators have also been used. However when a consumer creates rapidly varying voltage fluctuations, it is not possible to improve the quality of power supply with the aid of simple compensators. Therefore fast control reactive power compensators, employing solid state devices, have emerged to supersede the earlier technologies.

3.3.1 Shunt Capacitors and Reactors

Shunt capacitors and reactors may be used to supply or absorb reactive power. In most cases they are connected to the power system by a circuit breaker either directly or via a transformer and switched in and out when needed. As

the dynamic response of these shunt devices is determined by the time and permitted frequency of operation of the circuit breaker, the usefulness of these devices is limited. Another major drawback of them is that the reactive power produced or absorbed by them falls as the voltage drops, leading to reduced effectiveness when they are needed most.

3.3.2 Synchronous Condenser

A synchronous condenser is a synchronous motor running without a mechanical load. Depending on the value of excitation, it can absorb or generate reactive power. The synchronous condenser exhibits great advantages such as flexibility of operation in all load conditions and an essentially inductive source impedance that cannot cause harmonic resonances with the transmission network. However it suffers from a number of shortcomings, such as slow response (the average response time is around one second), requirement for significant starting and protection equipment and high maintenance.

3.3.3 Thyristor Controlled Reactor (TCR)

The basic elements of a TCR are a reactor in series with a bi-directional thyristor pair as shown in Fig 3.2(a). The thyristors conduct on alternative half-cycles of the supply frequency. The current flow in the inductor (L) is controlled by adjusting the conduction interval of the back to back connected thyristors. This is achieved by delaying the closure of the thyristor switch by an angle a, which is referred to as the firing angle, in each half cycle with respect to the voltage zero. When α=90°, the current is essentially reactive and sinusoidal. Partial conduction is obtained with firing angles between 90° and 180°. Outside the control range, when the thyristor is continuously conducting, the TCR behaves simply as a linear reactor. The voltage current characteristics for the TCR is shown in Fig 3.2(a).

It is important to note that the TCR current always lags the voltage, so that reactive power can only be absorbed. However, the TCR compensator can be biased by shunt capacitors so that its overall power factor can either be lagging or leading. The voltage current characteristic of a TCR with a fixed or switched capacitor is shown in Fig 3.2(b).

A slope characteristic, k_s, shown in Fig 3.2(b), is used to control the voltage at the point of connection (PC) of the TCR and any fixed or switched capacitor arrangement (This combination is normally called as a static VAr compensator - SVC). The electric power system when viewed from the PC busbar can be represented by a Thevenin equivalent circuit with an equivalent reactance X_{TH}. The power system characteristics can be represented by a straight line with slope X_{TH} as also shown in Fig 3.2(b). To limit the voltage variation at the PC with the set point voltage, V_o, the value of k_s is selected to be less than X_{TH}, which results in voltage control with a droop [3].

Under the phase control mode, the TCR generates higher harmonic currents. In three phase applications, the third harmonic components can be cancelled out

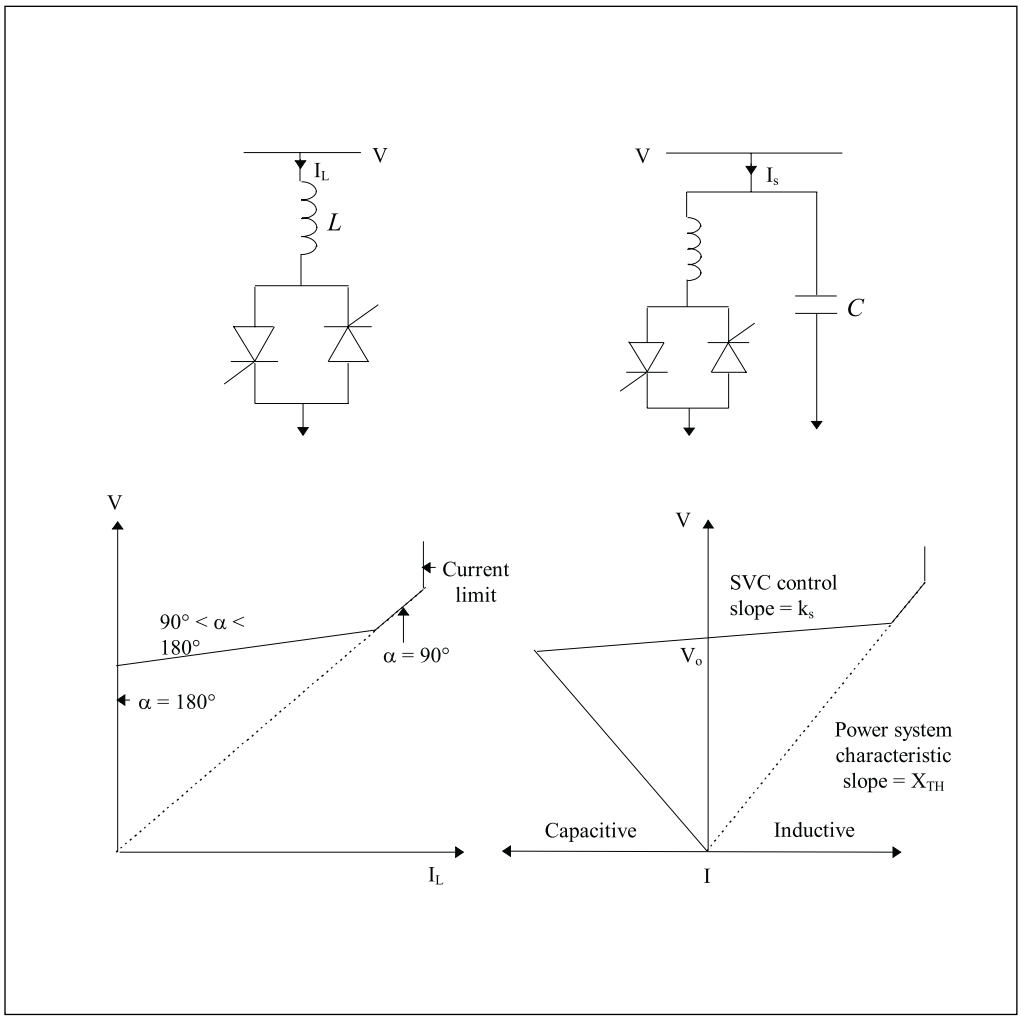

Fig 3.2(a): Output characteristic of TCR.
Fig 3.2(b): Output characteristic of a TCR with capacitors.

by connecting the basic TCR elements in delta through a transformer. The transformer is necessary for matching the mains voltage to the thyristor valve voltage. Further elimination of harmonics can be achieved by using two delta connected TCRs of equal rating fed from two secondary windings of the step-down transformer, one connected in star and other in delta. This forms a 12 pulse TCR as shown in Fig 3.3. Moreover the harmonics in the line current can be reduced by replacing the fixed capacitors, associated with reactive power generation, with a filter network. The filter can be designed to draw the same fundamental current as the fixed capacitors at the system frequency and provide low-impedance shunt paths at the harmonic frequencies.

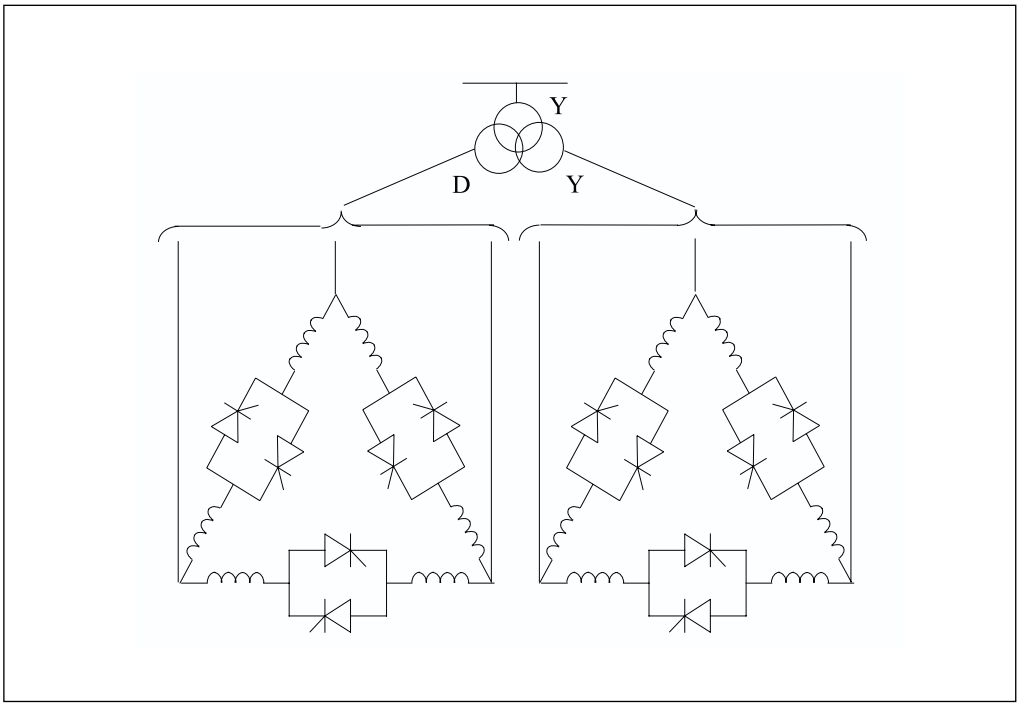

Fig 3.3: 12 - pulse TCR arrangement.

3.3.4 Thyristor Switched Capacitor (TSC)
The basic elements of a TSC are a capacitor in series with a bi-directional thyristor pair and a small reactor. The purpose of the reactor is to limit switching transients, to damp inrush currents and may be used to form a filter for harmonics coming from the power system. In three phase applications the basic TSC elements are usually connected in delta. The susceptance is adjusted by controlling the number of parallel capacitors connected in shunt. Each capacitor always conducts for an integral number of half cycles. The total susceptance thus varies in a stepwise manner. The one line diagram of the TSC scheme is shown in Fig 3.4(a). The output characteristic is discontinuous and determined by the rating and number of parallel connected units. Therefore the voltage support provided is discontinuous as shown in Fig 3.4(b).

The switching of capacitors excites transients and it is necessary to switch the capacitors at a point where switching transients are minimum. This can be achieved by pre-charging the capacitor to the crest value of the supply voltage and by choosing the switching instant when the voltage across the thyristor switch is minimum, i.e. at the crest value of the supply voltage. The switch off period corresponds to a current zero after an integral number of half cycles. More detailed analysis of transients associated with the TSC can be found in [1 & 4].

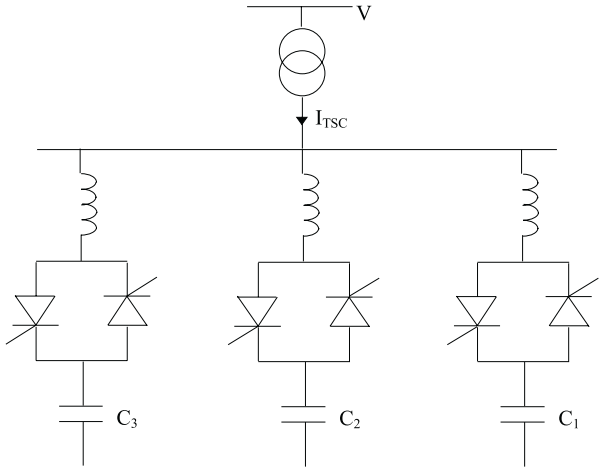

Fig 3.4(a)

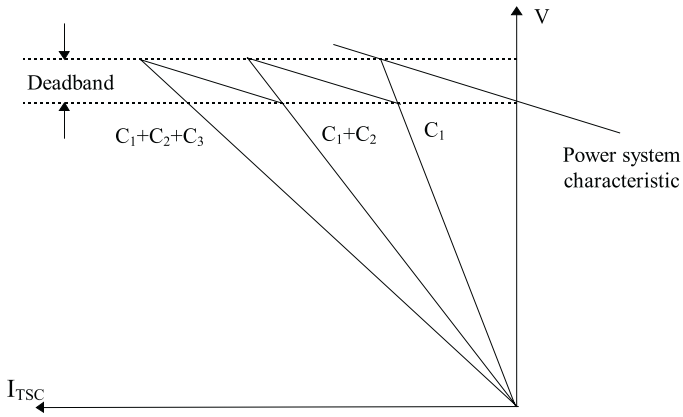

Fig 3.4(b)

Fig 3.4: TSC scheme and its output characteristics.

3.4 Advanced Static VAr Compensator (ASVC)

3.4.1 Introduction

Over the last few decades, the power handling capability of power electronic devices has increased and new solid state switches with turn-off capability have emerged. This has led to a reduction in the number of switching devices required for a high power static VAr compensator and a corresponding

decrease in the cost of power electronic control [5]. This falling tendency in specific price and introduction of new devices with turn-off capability is likely to encourage a shift towards the increase use of solid state means for both the generation (or absorption) and control of reactive power. As a results of this trend all solid state reactive power compensators have started emerging. One of the more developed of this type of reactive power compensator is the ASVC based on the voltage source inverter (VSI).

3.4.2 Six-pulse Voltage Source Inverter Operating with Fundamental Frequency Modulation

This is the simplest form of three phase dc to ac inverter and can be considered as a basic building block of an ASVC. The power circuit of the six-pulse VSI is shown in Fig 3.5 together with its output voltages. This circuit consists of six power electronic switches with both turn-on and turn-off capability and six diodes. In Fig 3.5, the power electronic switches are shown by an arrow with arrowhead indicating the direction of current flow. The basic square wave output, shown in Fig 3.5, can be obtained by operating the six switches in the sequence, $S_1S_2S_3$, $S_2S_3S_4$, $S_3S_4S_5$, $S_4S_5S_6$, $S_5S_6S_1$ and $S_6S_1S_2$. From Fourier analysis, it can be shown that, for an ideal wave shape, only harmonics of order of $6k\pm1$, where k = 1, 2, 3..., remain in the output waveform. For the ideal circuit, the k^{th} harmonic component has an amplitude 1/k relative to the fundamental component. When the inverter is operating with this switching pattern, the dc side current pulsates six times during one cycle of the alternative voltage and therefore this circuit is called a six-pulse inverter.

3.4.3 Principle of Operation of a Six-pulse VSI based ASVC

The ASVC consists of a voltage source inverter whose DC side is connected to a capacitor. The inverter is connected to the supply system via a transformer. A basic ASVC circuit is shown in Fig 3.6(a), in which transformer leakage reactance is represented by X. If the fundamental of the phase output voltages of the inverter is in phase with the corresponding system voltage, the line current flowing into or out of the VSI is always at 90° to the network voltage due to the reactive coupling. When the fundamental of the inverter voltage is less than the ac system voltage, reactive power is absorbed by the ASVC. On the other hand, when the ASVC voltage is higher than the system voltage, reactive power flows from the ASVC to the system. This is shown in Fig 3.6(b) and (c). The magnitude of the ASVC output voltage can be varied by controlling the dc capacitor voltage. If the switching devices of the inverter are operated to obtain the fundamental of the ASVC output voltage leading or lagging the ac system voltage by a small angle, a net amount of real power flows between the system and the ASVC. This in turn decreases or increases the dc capacitor voltage.

The harmonic distortion at the output of this six-pulse inverter based ASVC is very high and the circuit is not used for practical applications. Various other inverters have emerged which operate either at the fundamental frequency or at higher frequencies. In next few sections, these types of inverters are discussed.

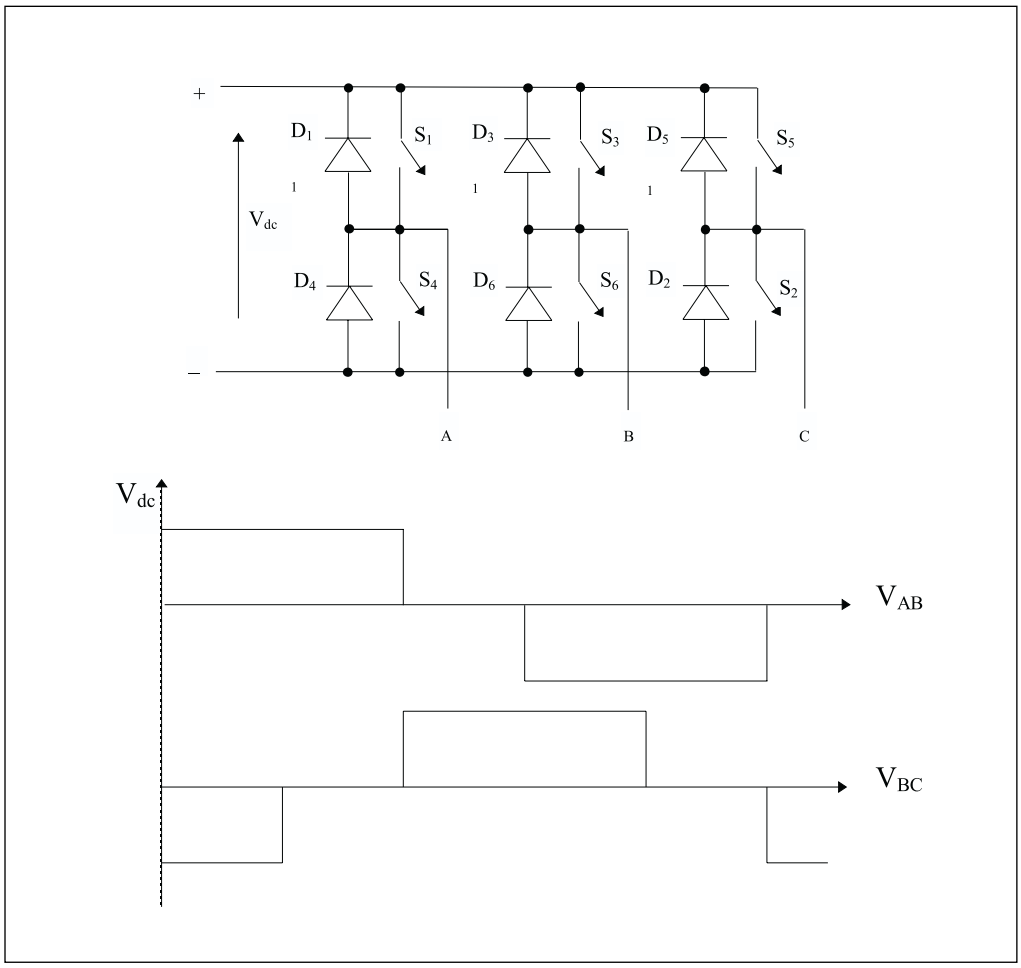

Fig 3.5: Six-pulse voltage source inverter and its line voltages.

3.4.4 Multi-phase Configuration

A block diagram of this circuit configuration is shown in Fig 3.7. A 6P – pulse inverter (where P is an integer) can be obtained by connecting P six-pulse inverters having a $2\pi/6P$ phase displacement between each other, through a transformer array. This transformer array has a complex winding arrangement which is used to cancel the phase displacement of the inverter outputs. In-phase transformed outputs of all the inverters are summed by the connection of the windings. Each of the P transformers required for this arrangement is rated at 1/P of the total MVA output of the inverter.

If this 6P-pulse inverter is connected to a network having a frequency f, the output frequency of each harmonic present in the ac side is $(6Pk\pm1)f$, where k is a positive integer.

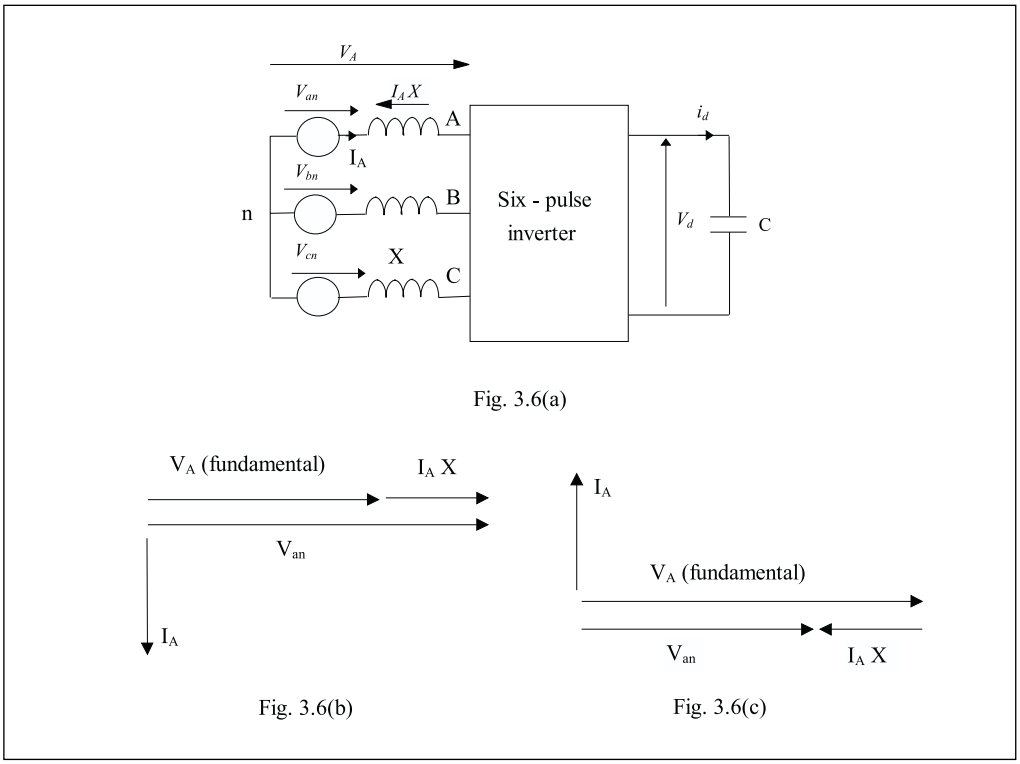

Fig 3.6: Six - pulse inverter as an ASVC.

Examples of a 24-pulse inverter configuration and a 48-pulse configuration can be found in references [5] and [6] respectively.

3.4.5 Multi-level Configuration [7]

A simplified schematic of a multi-level inverter having an arbitrary number of levels is shown in Fig 3.8(a). Fig 3.8(b) shows one phase of the actual inverter circuit. The number of levels in the n-level inverter is defined as the number of positive voltage levels including zero which appear in the inverter line voltage or by the number of DC voltage levels referred to the mid-point.

The output voltage of this configuration can assume any of the voltage levels V_1, V_2.....V_{n+1} by selecting appropriate nodes. For an example, the voltage level V_{J45}can be obtained at the output by turning the switches S_1 to S_n on and turning all the other switches off. The voltage level V_2 can be obtained by turning switches S_{-1} to S_{-n-1} on and turning all the other switches off [8]. When the current flowing out from the inverter leg is positive, only the switches corresponding to that voltage level are conducting. On the other hand, when the current is negative the anti-parallel diodes corresponding to the on-switches are conducting.

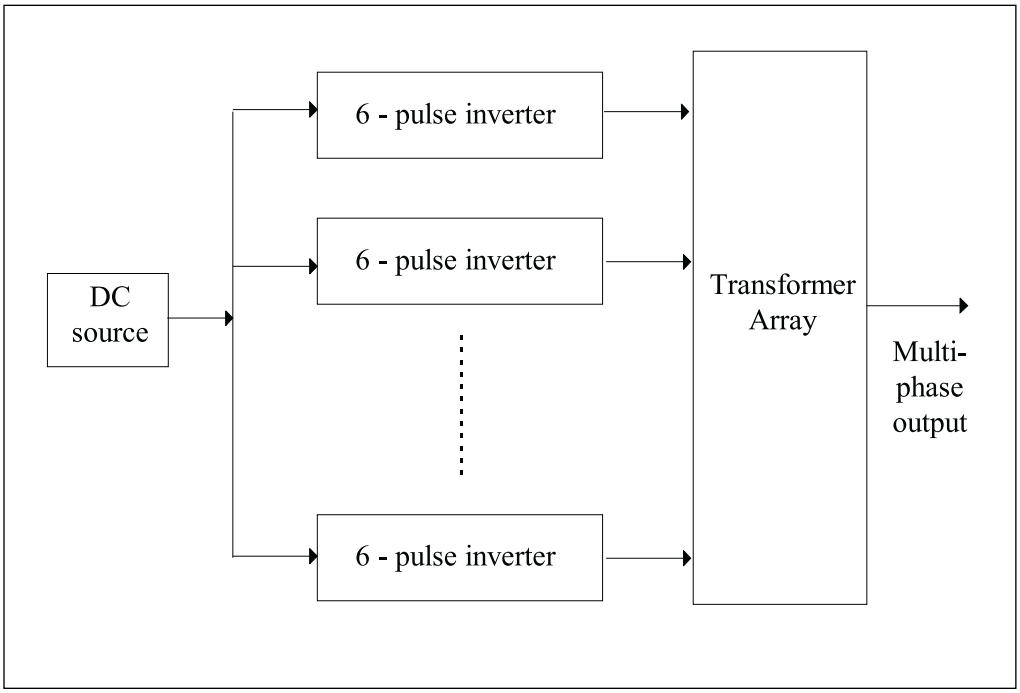

Fig 3.7: Schematic diagram of the multi-phase inverter.

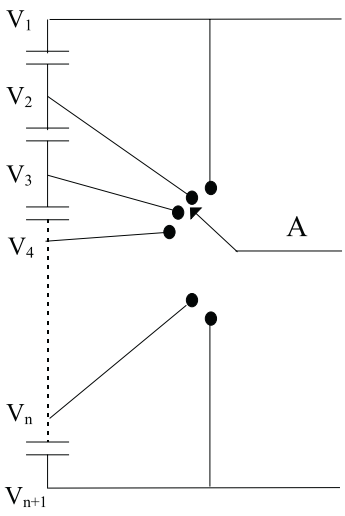

Fig 3.8(a)

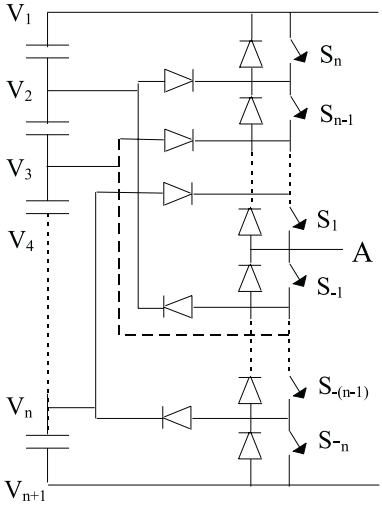

Fig 3.8(b)

Fig 3.8: Equivalent circuit and the real arrangement of one phase of a multi-level inverter.

The average voltage across each capacitor in the multi-level inverter should be identical. However, when establishing sinusoidal current waveforms, the currents flowing out from the inner capacitors (towards the mid point of the inverter) are higher than that from the outer capacitors, causing voltage unbalances in the string of capacitors. Various techniques, either based on a multi-level PWM method [9] or employing a regulator circuit [8], are described in the literature to overcome these unbalances.

An innovative approach is to use a cascaded inverter (sometimes known as a chain circuit). Figure 3.9 shows a simple representation of a 5 level cascade inverter. This uses a switching combination of the GTOs according to a preset switching scheme to obtain an output voltage of five levels per half fundamental period. PWM techniques may also be used in the inverter's switching scheme to further reduced the harmonic content.

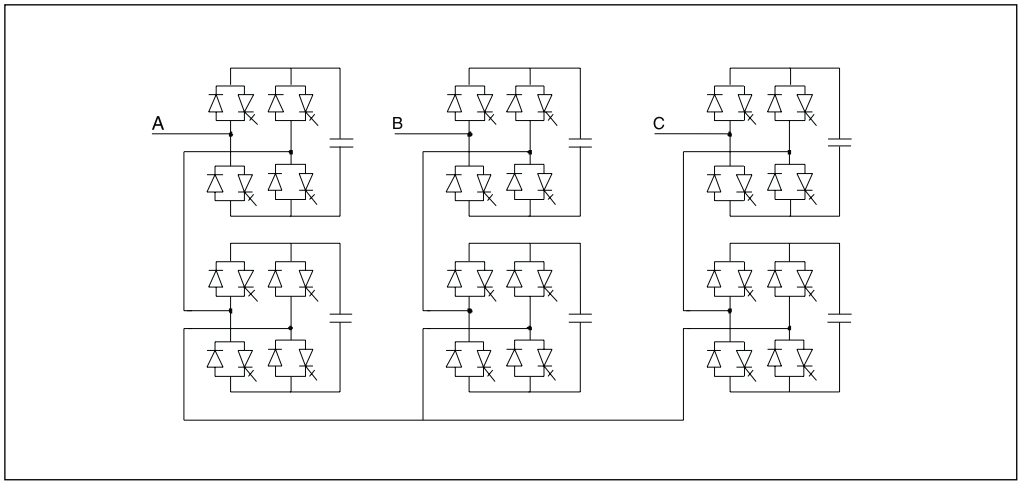

Fig 3.9: A 5-level cascade inverter.

3.4.6 PWM Technique to Improve the Performance of the Six-pulse and Multi-level Configurations

The six-pulse inverter and multi-level inverter can be operated with a higher switching frequency to eliminate some of the lower order harmonics appearing in the inverter output voltage. Two common switching strategies which can be used for ASVC applications are selective harmonic elimination modulation (SHEM) and overmodulated or optimum pulse width modulation (PWM) techniques.

In the SHEM technique, the basic square wave output produced by the six-pulse or multi-level inverter is chopped a number of times to eliminate some of the lower order harmonics. However the magnitude of some higher order har-

monics increases in this process. Fig 3.10 shows the voltage waveform corresponding to this case with an arbitrary number of chops per half a cycle. Assuming that the angle corresponding to the chop near to 90° is $ß_k$, the Fourier coefficient b_n can be found as [10]:

$$b_n = \frac{2V_d}{\pi n}\left[1 + 2\sum_{i=1}^{k}(-1)^i \cos(n ß_i)\right] \qquad \text{for odd n} \qquad (1)$$

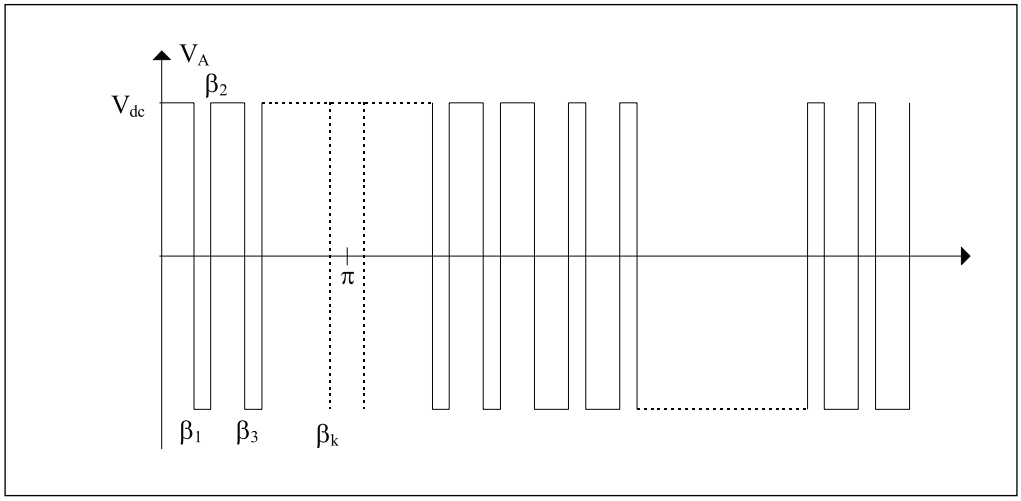

Fig 3.10: Waveform for SHEM operation.

By introducing m number of chops into the inverter output voltage as shown in Fig 3.10, any m number of harmonics can be eliminated from the output voltage. The angles corresponding to the m chops can be found by equating $b_n = 0$ for the m harmonic to be eliminated and solving those m simultaneous equations for $ß_i$ (for i = 1 to m). As an example, if two chops were used with $ß_1 = 16.3°$ and $ß_2 = 22.1°$, the 5^{th} and 7^{th} harmonic components can be eliminated from the output voltage waveform.

There are various PWM methods described in the literature [11, 12 & 13]. The sinusoidal PWM technique is the basic one and most of the other techniques are derivations of it. In the sinusoidal PWM technique, the angle of chops is determined by the intersection between a sine wave and a triangular wave. To obtain a three phase output the same triangular wave is compared with three sinusoidal signals that are 120° out of phase. The sinusoidal waveform is at the frequency which is required at the inverter output and the triangular waveform normally at a triplen multiple (m_f) of that frequency. If the magnitude of the sinusoidal waveform is less than that of the triangular waveform, then the inverter output produces harmonics around a multiple of m_f times fundamental frequency and no harmonics appear below that. However, the magnitude of the

fundamental is very low in this case and it becomes a limiting factor in determining the size of the component needed for the converter and its control requirements. Therefore overmodulation techniques, where the magnitude of the sinusoid is higher than the triangular waveform, or some optimum PWM pattern are often employed.

3.5 Power Electronic Devices for ASVC Inverters

The ideal power electronic device for an ASVC is a switch which can be turned on or off at any instant of time by a simple control signal. Since voltage source inverters are commonly used for the ASVC, these switches do not need to have reverse blocking capability [14]. The commonly used switches for the ASVC which satisfy the above specification are the Insulated Gate Bipolar Transistor (IGBT) and Gate Turn-off Thyristor (GTO). GTOs are available up to very large power levels such as 6 kV, 6 kA and IGBTs are available up to power level of 1500V, 1200A. The power rating of IGBTs is increasing constantly while their cost is decreasing.

3.5.1 Insulated Gate Bipolar Transistor

The IGBT is a hybrid switch which consist of a MOSFET in its gate side and a Bipolar Junction Transistor (BJT) in its conduction path as shown in Fig 3.11(a). Its circuit symbol is shown in Fig 3.11(b). This device combines the characteristics of both the BJT and MOSFET. The conduction losses at on state are less than that of a similar rated MOSFET and the switching on and off times are lower than that of a similar rated BJT. Unlike the BJT, the IGBT is a voltage driven device and can be easily switched on. The IGBT, turn-on process is similar to that of a MOSFET, and in the turn-off process the BJT plays a dominant role. Therefore during turn-off a long tail current flows, increasing the switching losses.

The IGBT has become a popular choice for medium power applications, because of its attractive characteristics. It would seem to be an appropriate choice for the smaller ASVCs which might be employed in future wind farms as their power level matches the reactive power requirement of the wind farm, i.e. in the order of few MVArs.

3.5.2 Gate Turn-off Thyristor

The GTO is a switch having a thyristor like p-n-p-n structure but with turn-off capability. In the case of the thyristor, once it is turned-on by a gate pulse, the gate no longer has control over the conduction of the device and can not be turned-off unless the conduction current is brought below a certain minimum. Therefore various structural changes are introduced into the thyristor structure to obtain the turn-off capability. First its p type anode is shorted by n^+ regions as shown in Fig 3.12(a) and cathode appears as n^+ type islands on the p type gate. The circuit symbol of a GTO is shown in Fig 3.12(b).

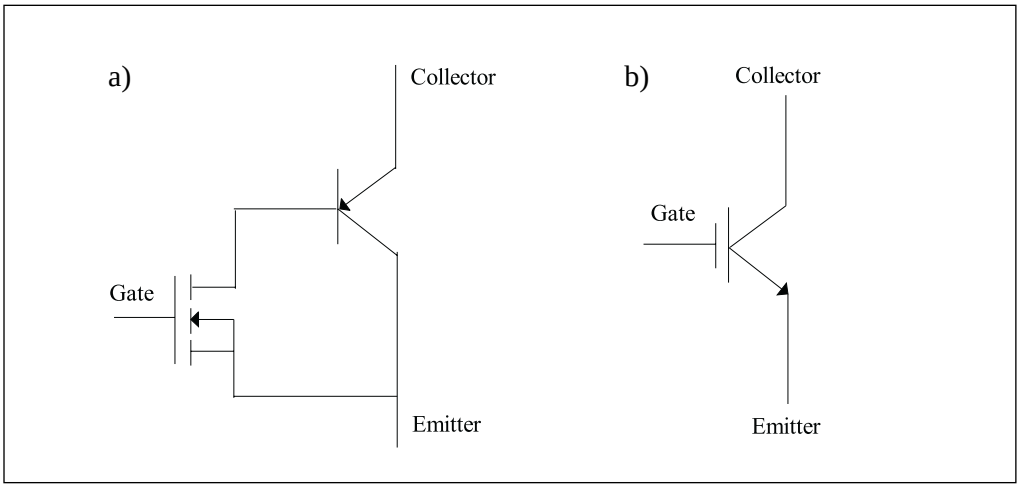

Fig 3.11(a): Equivalent circuit of the IGBT.
Fig 3.11(b): Circuit symbol.

The GTO can be turned on by applying a positive voltage to the gate with respect to the cathode. This creates a positive gate current pulse and the basic turn-on process is similar to that of a thyristor. The device can be turned off by applying a large negative gate current. This negative gate current must be very large, in the order of 20 - 30% or even higher of the anode current, but is required for only a short period of time. Therefore special drive circuits are required to turn the device off. The turn-on and turn-off times are longer than those of an IGBT.

This device is appropriate for large ASVCs whose rating is few MVArs to few hundred of MVArs. The application of GTOs to ASVCs are described in detail in reference [5].

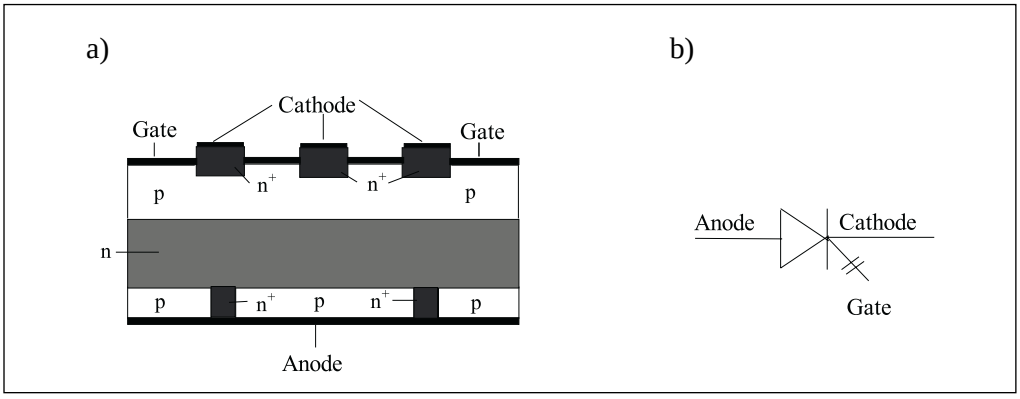

Fig 3.12(a): Structure of the GTO.
Fig 3.12(b): Circuit symbol of the GTO.

References

1. Miller, T.J.E., “Reactive power control in electric systems.”, (Book), John Wiley and Sons, 1982.
2. Weedy, B.M., “Electric power system.”, (Book), John Wiley and Sons, 1991.
3. Erinmez, I.A. Ed., “Static VAr compensators.”, Working group 38-01, Task Force No. 2 on SVC, CIGRE, 1986.
4. Miller, T.J.E., Chadwick, P., “An analysis of switching transients in Thristor Switched Capacitor compensated systems.”, IEE International Conference on Thyristor and Variable Static Equipment for AC & DC Transmission, London, Nov/Dec 1981, pp 104-107.
5. Gyugyi, L., Hingorani, N.G., Nannery, P.R., Tai, N., “Advanced Static VAr compensator using Gate Turn-Off thyristors for utility applications.”, CIGRE 23-203, 1990.
6. Mori, S., Matsuno, K., Takeda, M., Seto, M., “Development of a large static VAr generator using self-commutated inverters for improving power system stability.”, IEEE Tran. on Power Systems, Vol 8, No 1, Feb 1993, pp 371-377.
7. Newton C., Summer M., “Multi-level convertors: a real solution to medium/high voltage drives?”, Power Engineering Journal, February 1998, pp 21-26.
8. Choi, N.S., Cho, J.G., Cho, G.H., “A general circuit topology of multi-level inverter.”, IEEE Power Electronic Specialist Conference, USA, 1991, pp 96-103.
9. Choi, N.S., Cho, G.C., Cho, G.H., “Modelling and analysis of a static VAr compensator using multi-level voltage source inverter.”, IEEE Industrial Application Society 28th Annual Meeting, Oct 2-8, 1993, Canada, pp 901-908.
10. Petal, H.S., Holt, R.G., “ Generalised technique of harmonic elimination and voltage control in thyristor inverters, Part I - Harmonic elimination.”, IEEE Tran. on Industrial Applications, Vol IA-9, No 3, May/June 1973, pp 310-317.
11. Wuest, D., “Static reactive power compensator with self-commutated inverter at a low switching frequency.”, European Power Engineering Conference, Firenze, 1991, Vol 3, pp 70-75.
12. Boost, M.A., Ziogas, P.D., “State-of-the-art carrier PWM techniques: A critical evaluation.”, IEEE Tran. on Industrial Application, Vol 24, No 2, March/April 1988, pp 271-280.
13. Bowers, S.R., Midoun, A., “Sub-optimal switching strategies for microprocessor-controlled PWM inverter.”, IEE Proceedings, Vol 132, Part B, No 3, May 1985, pp 133-148.
14. Gyugui, L., “Reactive power generation and control by thyristor circuits.”, IEEE Tran. on Industrial Application, Vol IA-15, No 5, Sep/Oct 1979, pp 521-531.

Chapter 4

Basic Design of the ASVC

Frank Schettler
SIEMENS, Power Transmission and Distribution
Erlangen
Germany

4.1 Introduction

Figure 4.1 shows a single line diagram of the ASVC installed at the Rejsby Hede wind farm. It consists of the following major components:

- one three winding transformer
- two reactors, one connected to each transformer secondary
- two converter units with capacitive energy storage

A converter unit converts the DC-voltage of the energy storage into a three phase AC voltage. The converters used are of the three level type, i.e. the energy storage is separated into two series connected capacitors and one phase module of the converter connects sequentially the positive tapping, the negative tapping or the mid-point to the AC terminal. Therefore the generated AC voltage has a stair-step wave form. A typical wave form of a line to line voltage is shown in Figure 4.2. Wave forms like this are obtained if each GTO is switched on and off once a period of the system frequency (Fundamental Frequency Modulation - FFM).

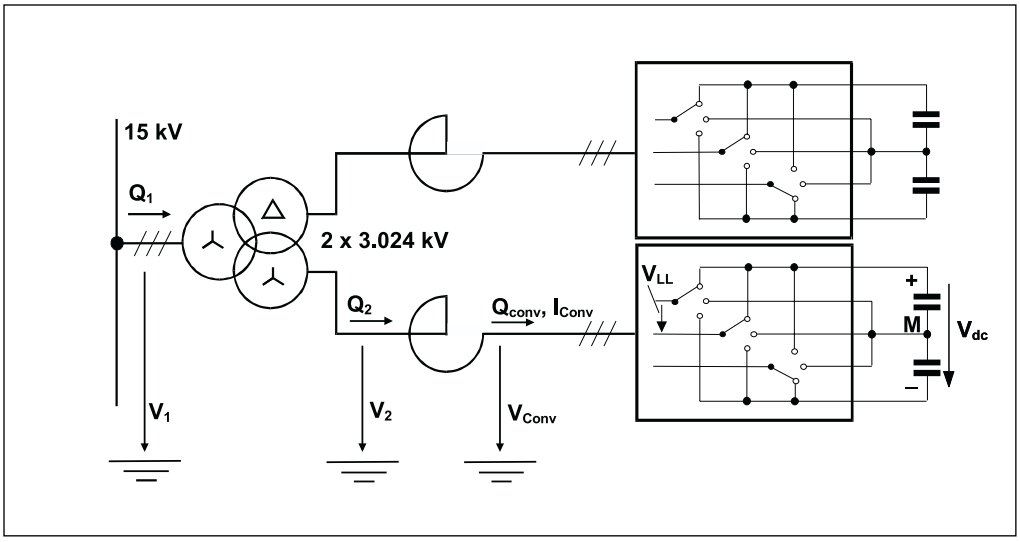

Fig 4.1: Single line diagram of the ASVC.

The magnitude of the fundamental component of the converter voltage wave in respect to the system voltage determines the reactive power output of the ASVC. Moreover, due to the stair-step wave form the ASVC voltage contains a higher harmonic voltage content. The ordinal numbers of the characteristic harmonics generated are

$$n = 6 \times k \pm 1 \quad (k=1, 2 \ldots n)$$

Besides these harmonics non-characteristic ones due to DC voltage ripple, system unbalances and switching tolerances appear.

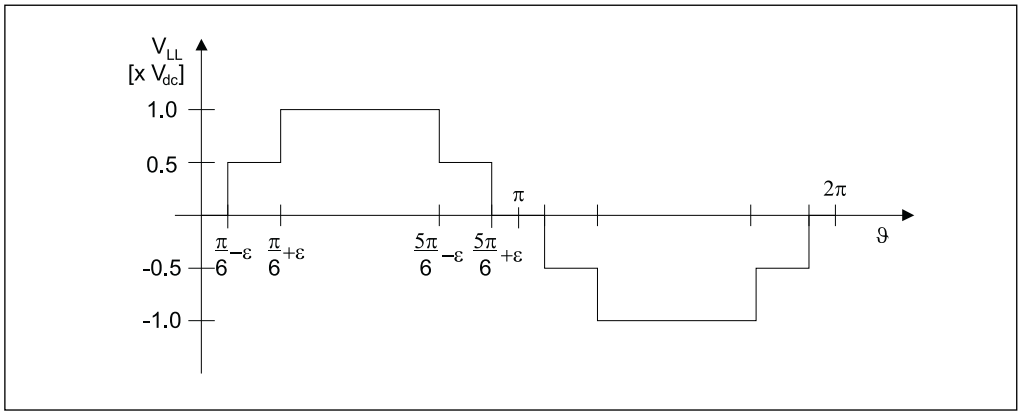

Fig 4.2: Line to line voltage at the converter terminals (Example using FFM).

Applying higher harmonic voltages results in voltage distortions in the surrounding network. These voltage distortions can be influenced by varying the pulse pattern of the converter and changing the transformer impedance. Connecting filters was not considered to be a possible solution. However, changing the harmonic content of the converter voltage as well as the variation of the transformer impedance also has an effect on the fundamental rating of the ASVC. That calls for a harmonic optimisation process.

4.2 Harmonic Study

4.2.1 General

The distortions in the system caused by the ASVC operation have to be below specified limits. Figure 4.3 shows a single line diagram of the wind park and the 60 kV network. The following harmonic requirements are to be met:

- Harmonics to be considered: 2nd to 50th
- Total Harmonic Distortion (THD): < 2.5 %

This values refer to the 15 kV bus where the ASVC is connected to (Point of Common Coupling - PCC).

- Individual Harmonic Content at the PCC: < 1.5 %

- The ASVC must not cause overloading of the reactive power compensation capacitors connected to the wind turbines and the 23 MVAr capacitor bank connected to the Bredebro 60 kV bus. The pre-load due to other sources of higher harmonics in the system is assumed to be zero.

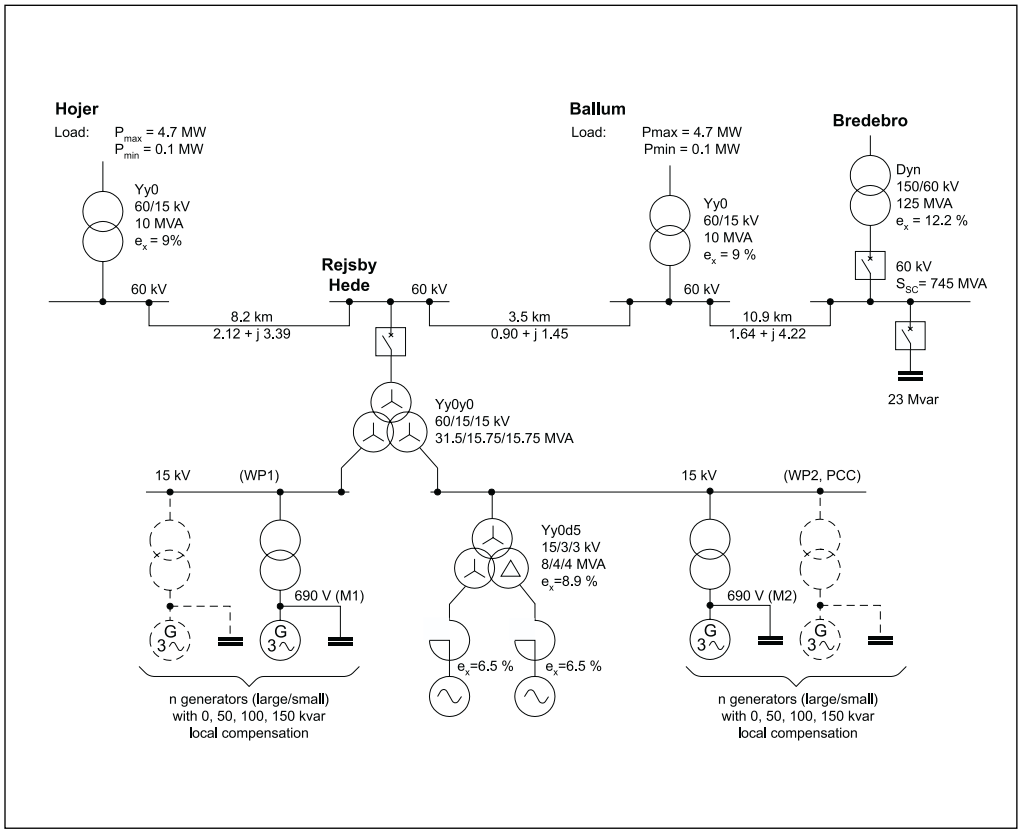

Fig 4.3: Single line diagram of the wind park Rejsby Hede and the 60 kV network. Only circuit breakers that have been important for the design of the ASVC are shown.

Figure 4.4 shows the equivalent circuit for harmonic distortion calculation at the PCC. The distortion depends on the impedances Z_T representing the transformer and series connected reactors and Z_N representing the system. Normally the system impedance Z_N can vary in a certain range due to various loading and connecting or disconnecting of capacitors. The following cases had to be investigated:

- The number of turbines in operation may vary between 0 to 40.

- Each turbine can operate either with its small generator (150 kW) or with its large one (600 kW).

- The reactive power compensation capacitors installed locally at each turbine are switched in 50 kVAr steps. Small generators are compensated by 50 kVAr, large generators are compensated by 150 kVAr. The total 150 kVAr are switched on by two intermediate steps of 50 kVAr and 100 kVAr lasting 6 seconds each.

- The loads connected to the 60 kV system may vary between 0.1 MW and 4.7 MW connected in Højer and between 0.1 MW and 4.7 MW connected in Ballum.

- The 23 MVAr capacitor unit in Bredebro might be connected or disconnected according to the requirements of the 150 kV system.

The harmonic study included variation of load and wind park generation based on small and large generators with the whole variety of operating cases.

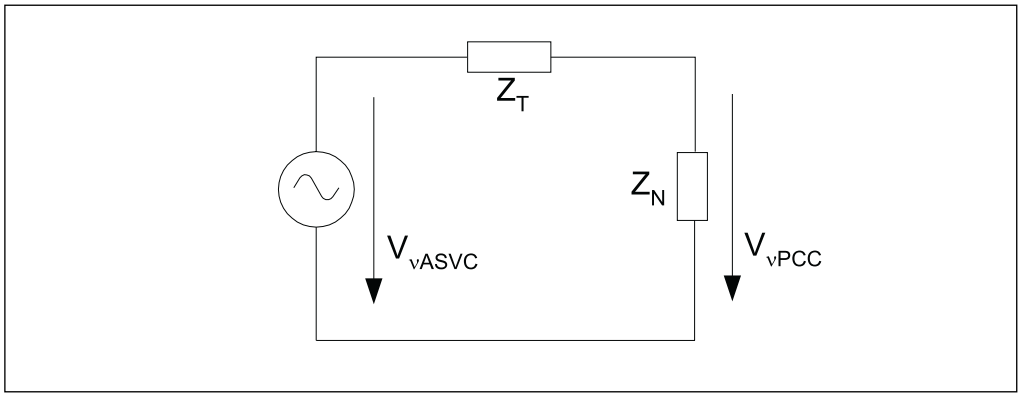

Fig 4.4: Equivalent circuit to calculate harmonic distortions at the PCC.

4.2.2 Results of the Harmonic Study

To calculate harmonic conditions the system as shown in Figure 4.3 was modelled in a harmonic load flow program. Static components of the system like transformers, transmission lines or capacitors were modelled by RX-branches. For the generators the negative sequence equivalent impedance was used. To a good approximation the R/X ratio of all inductive components can be assumed constant over the frequency range considered, e.g. the damping increases in direct proportion to the frequency.

The two GTO-converters are modelled by an equivalent voltage source. Realistic values for the characteristic and non-characteristic harmonic voltages generated were obtained from computer simulations using the Alternative Transients Program (ATP).

In a first approach to an optimised ASVC design regarding harmonics, the two GTO-converters were connected via separate transformers (one Y/Y, one Y/D) to each of the 15 kV busbars. The GTOs were controlled according to Fundamental Frequency Modulation (FFM). Different areas of interest were recognised:

The total harmonic voltage distortion in the 60 kV network remained below the specified value but single voltage distortion values were critical at the 11th and 13th harmonic order. The harmonic loading of the fixed compensation became critical when only a few wind turbines were in operation at the lower rated output.

The harmonic problems were resolved by:

- Developing a pulse pattern which eliminates the 11th and 13th harmonic voltages to the largest extent possible and minimises the 5th and 7th harmonics using three pulse Selective Harmonic Elimination Modulation (SHEM). Three pulse modulation means that each GTO is switched on and off three times a cycle of the fundamental. A comparison of the harmonic voltage content using FFM and SHEM is shown in Figures 4.5 and 4.6. Figure 4.5 shows the harmonic voltage content of the converter voltage at FFM. Figure 4.6 shows the harmonic voltage content using the optimised pulse pattern described above. The black bars show the theoretical values the white ones include effects due to unbalances, DC-voltage ripple and switching tolerances obtained by ATP simulations.

- Increasing the reactance between converter and 15 kV bus which changed critical resonance conditions. The transformer impedance was approximately doubled in respect to the optimum impedance calculated under reactive power rating aspects.

- Connecting the GTO-converters via a three winding transformer to one 15 kV bus. One converter is connected to a star the other one to a delta winding. In the case of parallel operation such an arrangement reduces harmonic distortion on the primary winding of a three winding transformer i.e. reducing six pulse harmonic orders 5, 7, 17, 19, etc.

Extensive harmonic load flow calculations verified the above measures. The results are presented in Figure 4.7. It shows the harmonic voltage distortion at the 15 kV busbar, where the 12 pulse ASVC is connected in the final design stage (see Figure 4.3).

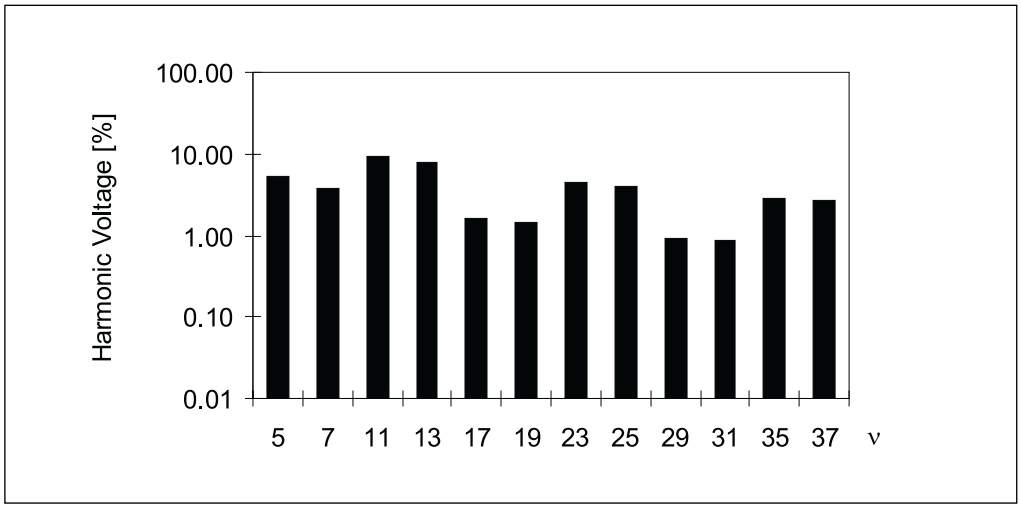

Fig 4.5: Harmonic voltage content of converter voltage in % using FFM.

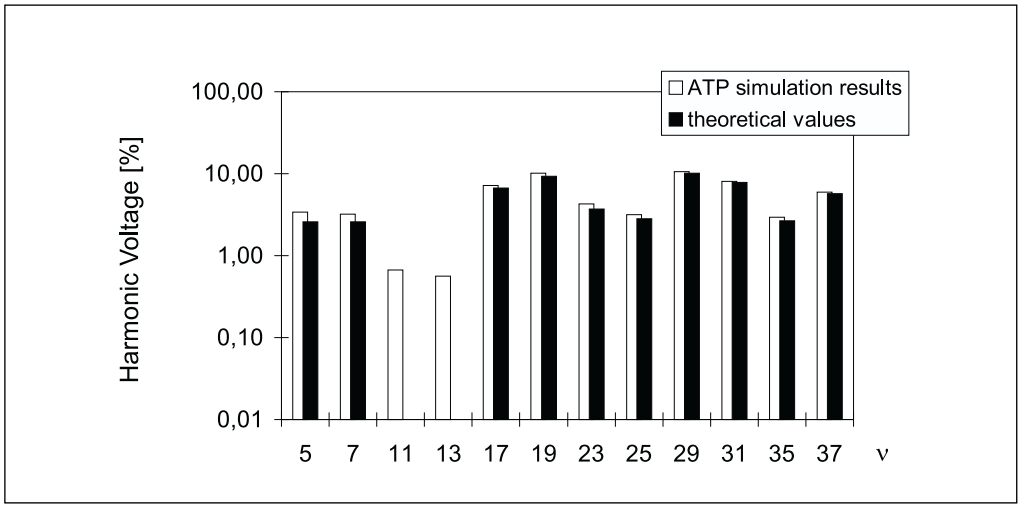

Fig 4.6: Harmonic voltage content of converter voltage in % using SHEM.

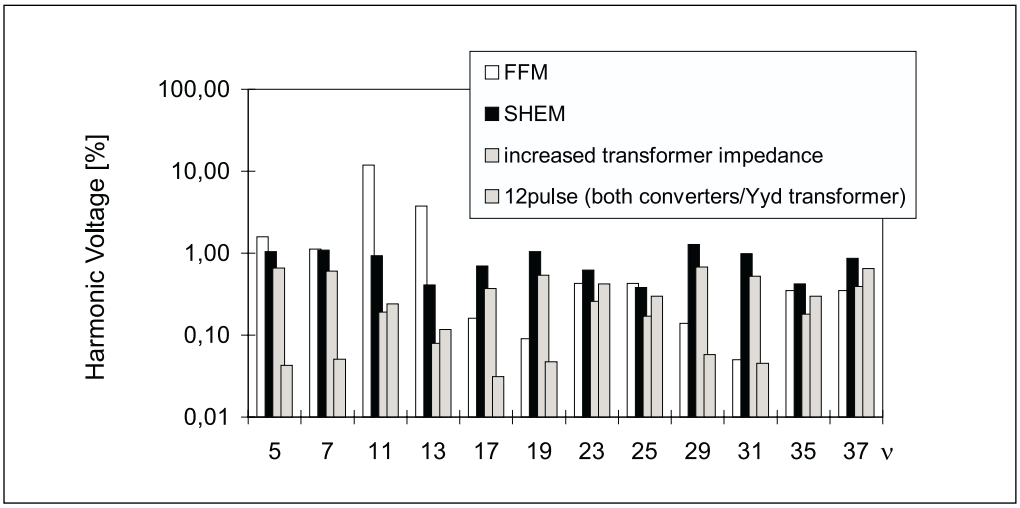

Fig 4.7: Harmonic voltage distortion of the 15 kV busbar (PCC) obtained during the design steps as described.

4.3 Load Flow Study

4.3.1 General

As a result of the harmonic study both converters have to be connected to one common 15 kV busbar forming a 12 pulse system.
Since the ASVC has to compensate the reactive power demand of the whole wind park, the reactive power for the second 15 kV side has to be transferred over the three winding wind park transformer (60/15/15 kV). Due to the leakage impedance of the transformer this causes a voltage drop from the 15 kV bus where the ASVC is connected to the other 15 kV bus. In order to determine the voltage conditions load flow calculations for the system shown in Figure 4.8 were carried out.

The ASVC is represented by a current source feeding in pure reactive current (phase shifted by 90° el. with respect to the node voltage at WP2). The magnitude of the reactive current depends on the reactive power demand of the wind park, measured at both 15 kV feeders of the three winding wind park transformer (60/15/15 kV).

For continuous operation the reactive current generated by the ASVC is limited to the nominal value.

4.3.2 Results of Load Flow Study

Load flow calculations were carried out for machine numbers varying from 0 to 18 at WP1 (n_{WP1}, see Figure 4.8) and 0 to 22 at WP2 (n_{WP2}) respectively. Table 4.1 summarises characteristic cases including maximum and minimum voltage values detected during the load flow calculations. The Table also shows the

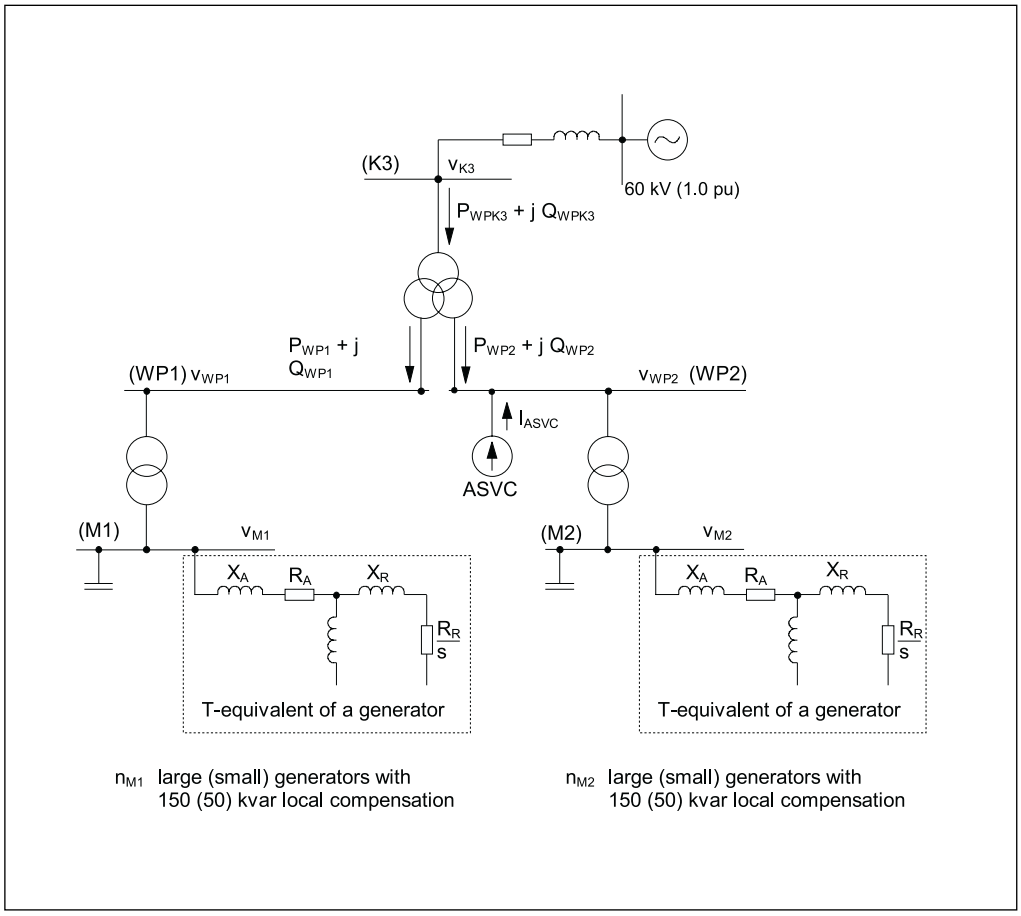

Fig 4.8: General circuit diagram for fundamental load flow calculations.

active and reactive power flow and the voltage at the other points of interest. With the exception of full load operation of the whole wind park (case 3), the reactive power demand of the wind generators is fully compensated by the reactive power output of the ASVC and the local phase shifting capacitors. The remaining reactive power demand of the wind park as seen from 60 kV side in Rejsby Hede (Q_{WPK3}) is determined by the reactive power consumption of the 60/15kV transformer. For case 3 the ASVC cannot cover the complete demand for compensation and reactive power has to be taken from the grid system. However, the cos φ at the 60 kV busbar is always very close to 1 (0.99).

The reactive power demand at WP1 is supplied by WP2, except for case 3 as discussed above.

The voltage drop between WP2 and WP1 depends on the number of generators connected to WP1. It is caused mainly by the transmission of reactive power.

case	n_{M1}	n_{M2}	v_{WP1} [pu]	v_{WP2} [pu]	v_{K3} [pu]	P_{WP1} MW	Q_{WP1} Mvar	P_{WP2} MW	Q_{WP2} Mvar	P_{WPK3} MW	Q_{WPK3} Mvar	v_{M1} [pu]	v_{M2} [pu]	i_{ASVC} [pu]
1	1	22	1.0	1.006	1.0	-0.6	0.218	-13.2	-0.218	-13.7	1.08	0.99	0.99	0.62
2	18	1	0.968	1.032	1.0	-10.8	4.063	-0.6	-4.063	-11.36	1.036	0.96	1.02	0.52
3	18	22	0.969	1.027	0.998	-10.8	4.058	-13.2	-3.547	-23.9	2.209	0.96	1.02	1.0
4	18	0	0.968	1.031	1.0	-10.8	4.064	0	-4.064	-10.77	1.05	0.959	...	
5	18	11	0.97	1.033	1.0	-10.8	4.055	-6.6	-4.055	-17.35	1.125	0.961	1.026	0.77
6	9	11	0.988	1.018	1.002	-5.4	1.986	-6.6	-1.986	-11.98	0.427	0.98	1.011	0.53

$n_{M1(,2)}$ = number of large wind generators connected

$v_{WP1(,2)}$ = absolute value of node voltage at the 15kV busbar

v_{K3} = absolute value of node voltage at the 60kV feeder

P, $Q_{WP1(,2)}$ = sum of the active / reactive power of one 15 kV busbar branch

P, Q_{WPK3} = sum of the active / reactive power of the whole wind farm seen at the 60kV side

$V_{M1(,2)}$ = terminal voltage of the wind generators

Table 4.1: Results of load flow calculations.

The maximum voltage difference amounts to 6.4% (case 2). The highest voltage occurs at WP2 (v_{WP2}, case 5) with 1.033 pu (15.5 kV), the lowest voltage at WP1 (v_{WP1}, case 2) with 0.968 pu (14.52 kV).
The voltages at the machines ($v_{M1,2}$) vary between -1 % to -4.1 % at M1 and -1 % to 2.6 % at M2.

This results in acceptable voltage conditions in the wind park.

4.4 Transient Study

4.4.1 General

Transient system conditions are a further important criteria for the design of the ASVC components. One of the worst cases to be considered for Rejsby Hede is islanding. Islanding means that the wind park becomes disconnected from the transmission system. This can be caused by opening either the circuit breaker connecting the 150 kV transmission system at Bredebro substation or opening the circuit breaker connecting the wind park at Rejsby Hede (see Figure 4.3).

Disconnecting the wind park means a sudden load rejection and change of the reactive power flow. Due to the drop of active power the slip of the induction machines becomes smaller. This results in higher system frequency immediately after the breaker has opened. Furthermore the phase angle of the system voltage changes. The reaction of the system regarding the change of the reactive power flow depends on the equivalent impedance of the remaining network as seen from the generator terminals. An inductive characteristic will result in de-excitation of the generators. In this case the terminal voltage will decrease, the generator rotors will accelerate and the system frequency will increase. The generator control will disconnect and brake the generators as soon as the corresponding setpoints are reached. In cases where the equivalent impedance is capacitive, the machines will become self-excited. This will result in a rapid voltage rise. Values of twice the nominal voltage could be reached within one or two cycles of the system frequency if no effective actions to limit the voltage are carried out. Effective actions would be disconnecting capacitors and dynamic reactive power compensation. Besides the rapid voltage rise the generator rotational speed will slow down and the system frequency will decrease.

To examine the system behaviour under islanding conditions with and without the ASVC, a transient study was carried out.

4.4.2 Results of the Transient Study

In an early stage of the project, the transient conditions were investigated by modelling the wind park and the surrounding high voltage system in the Alternative Transients Program (ATP). The results of these simulations formed

the basis for a first approach to the converter control design. As soon as the real control cubicles of the converter became available the development of the control algorithms and design of the control hardware continued in the Transient Network Analyser (TNA).
ATP allowed for a very detailed representation of the wind park and the 60 kV system. For the TNA-studies this model had to be simplified to reduce efforts to an economical optimum while providing all the functionality necessary for design and test of the control functions.

After the controller design was finished the ATP model was updated and the response of the ASVC to reference value steps and system transients was verified. Hence, the ATP model includes all control functions relevant for transient simulations up to a time constant of a few seconds in a manner corresponding to a digital control system.

The following cases had to be investigated:

- Opening the circuit breaker at the 60 kV side of the three winding transformer in Rejsby Hede

- Opening the circuit breaker to the 150 kV transmission system in Bredebro. The capacitor bank at Bredebro was taken into account. Large and small load respectively connected at Ballum and Højer were investigated separately.

The simulations have shown that there are no critical conditions to be expected in the case the wind park becomes disconnected from the 60 kV system directly in Rejsby Hede. The voltage or frequency deviations respectively will lead to braking and disconnecting the wind generators by the generator control if the corresponding setpoints are reached.

The behaviour of the island system after opening the circuit breaker at Bredebro mainly depends on whether the 23 MVAr capacitor bank is connected or not.

If the capacitor bank is connected, unacceptable overvoltages under islanding conditions will occur caused by self-excitation of the induction generators. One of the important results of the ATP simulations is that the capacitor bank has to be disconnected as fast as possible whenever the breaker to the 150 kV system receives a trip signal. Therefore a fast relay that provides co-ordinated tripping of both circuit breakers within 10 ms was installed at Bredebro.

Furthermore, it was seen that the ASVC would not react fast enough to limit the rising system voltage within the first couple of milliseconds after islanding. After the capacitor bank is disconnected the system behaves like it does without the 23 MVAr capacitor bank: After islanding the system voltage decreases and the system frequency increases. The load in Ballum and Højer leads to faster de-excitation of the generators.

The studies have shown, that islanding causes the ASVC to trip under worst case conditions, where the remaining load in the system is small compared to the generation of the wind park and the ASVC is at its maximum capacitive output. It stays connected in cases, when the generation is low or the remaining system is heavily loaded.

However, the transient simulations based on an equivalent circuit incorporating the fast relay for co-ordinated tripping of the capacitor bank in Bredebro have not shown hazardous system conditions due to islanding. In all cases the ASVC will be reliably protected by its protection schemes.

4.5 Basic Data of ASVC Design

4.5.1 General

As discussed in the sections above the basic design of the ASVC was determined by the results of the harmonic study. Keeping the harmonic distortions in the system below specified limits requires:

- a special switching pattern of the converter (eliminating 11th and 13th harmonics)

- a transformer impedance that is about twice the value calculated under optimum reactive power rating aspects

- 12 pulse arrangement of the converters.

These measures have an impact on the wave shape of the converter currents due to changes in their harmonic spectrum. Moreover, increasing the transformer impedance results in an increasing reactive power consumption of the transformer. Thus, the capacitive reactive power output of the converters had to be increased accordingly. Connecting both converters together to one of the 15 kV busbars has changed the voltage conditions in the wind park as calculated in the load flow study. The voltage operating range of the ASVC had to be extended towards higher values to cover all possible conditions of generation in the wind park and to avoid interaction with the tap changer control of the wind park transformer.

The results of the transient study are taken into account especially to define the transformer saturation characteristics.

The following paragraphs show the final design of the ASVC power components, that meets the requirements mentioned above.

4.5.2 Power Rating of the ASVC

The power rating of the ASVC for continuous operation at 1.0 pu is 2 x 4.0 MVAr capacitive and 2 x 4.0 MVAr inductive.

4.5.3 Network Conditions

Voltage

The voltage conditions at the 15 kV buses of the wind park are determined by the voltage regulating relay of the 60 to 15 kV step down transformer in Rejsby Hede. The design of the ASVC was based on the following assumptions:

- The relay controls the transformer tap changer to regulate the average voltage of both 15 kV systems to 1.01 pu.
- The relay will not change the tap changer position within a tolerance margin of ±0.013 pu.
- The operating time is set to 30 sec.

For the load flow calculations described above a system voltage of 1.0 pu at the Rejsby Hede 60 kV bus was assumed. This results in the following voltages at the 15 kV side where the ASVC is connected to

Maximum continuous voltage:	15.5 kV (1.033 pu) (see Table 4.1, case 5)
Minimum continuous voltage:	15.0 kV (1.0 pu) (see Table 4.1, case 1)

Together with the settings at the voltage regulating relay the operating range of the ASVC can be defined as follows

Nominal system voltage	15.0 kV (1.0 pu)
Maximum continuous voltage	15.85 kV (1.01+0.013+0.033=1.056 pu)
Minimum continuous voltage	15.0 kV (1.01–0.013=0.997 pu)

System Frequency

Nominal frequency	50.0 Hz

4.5.4 V/I Characteristic and Operating Points

The V/I characteristic of the ASVC as seen on HV side is shown in Figure 4.9. Figure 4.10 shows the V/I characteristic as seen at the converter terminals. Characteristic operating points are annotated. The corresponding electrical data for one converter branch are given in Table 4.2, Figure 4.1 shows the measuring points.

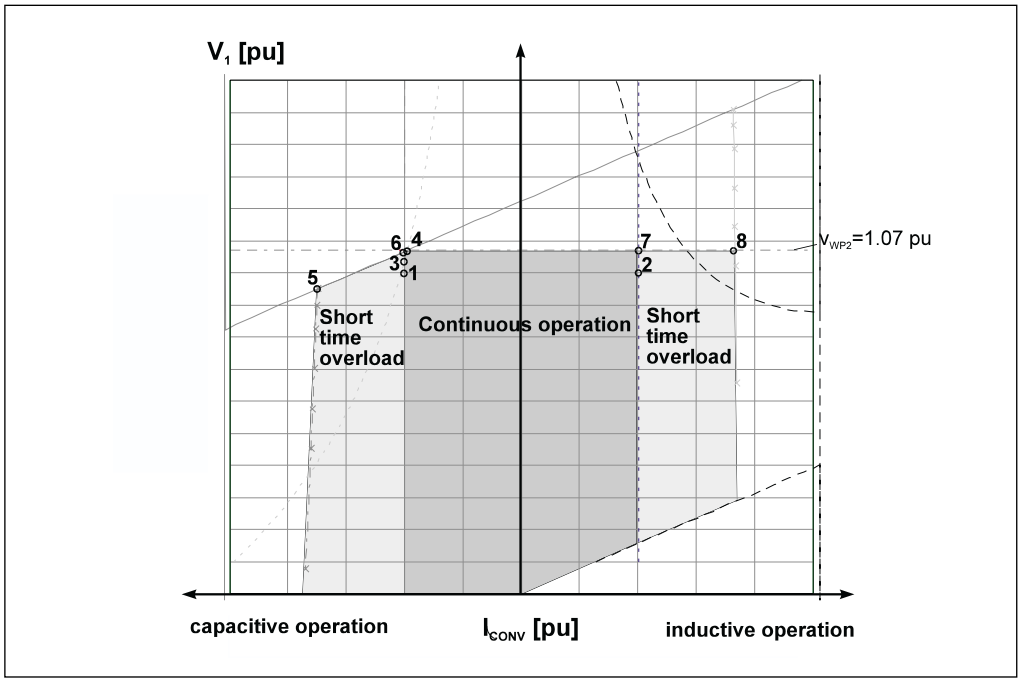

Fig 4.9: V/I characteristic as seen from HV-side.

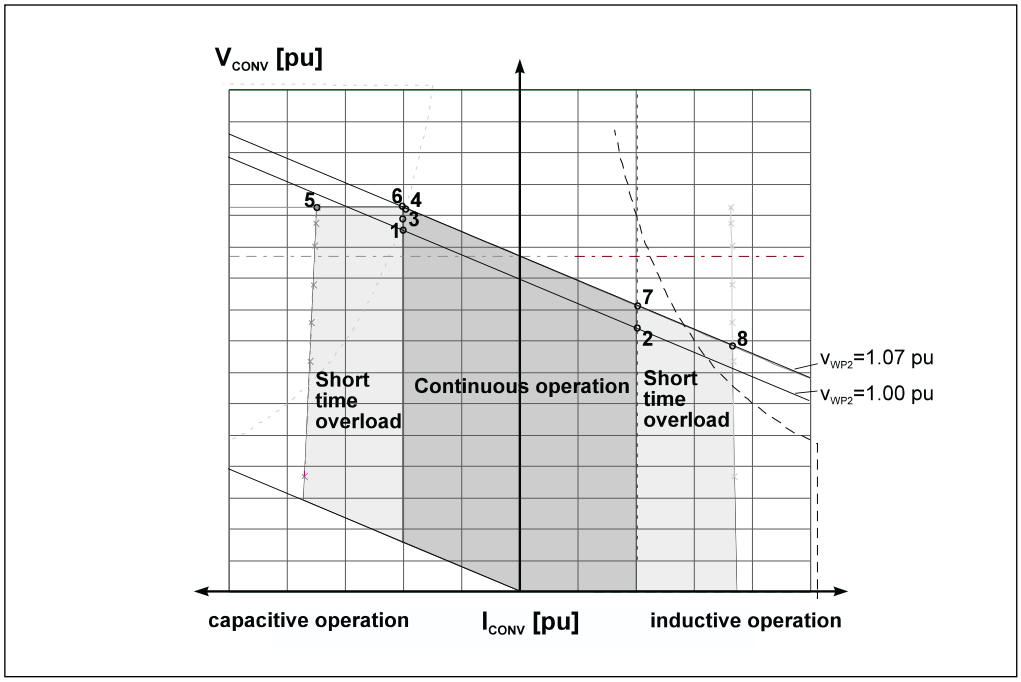

Fig 4.10: V/I characteristic as seen from LV-side.

The ASVC provides VAr-control for all operating points on the area labelled „Continuous operation“. This area is limited by the maximum converter current, which is 770 A both for inductive and capacitive operation and by a system voltage of 1.07 pu. Two control loops are incorporated to keep the operating point in the area for continuous operation: The current control limits the converter current to 770 A, the voltage control limits within the power rating of the ASVC the system voltage to 1.07 pu.

The setpoint chosen for voltage control (1.07 pu) is to prevent interference of the voltage regulating relay of the 60 to 15 kV transformer and the ASVC by means of voltage control.

The operating points given in Table 4.2 are now discussed in detail.

Operating points 1 and 2 show the voltages and currents at nominal inductive or capacitive reactive power output at 1.0 pu system voltage.

Operating point 3 is the capacitive design point.

Operating point 4 marks ASVC operation at converter output of 4.8 MVA and maximum average capacitor voltage of 5.0 kV.

Operating point 5 gives the maximum short time capacitive overload which is restricted to 10 s (Starting from 0 MVAr pre-load). The average capacitor voltage is 5.0 kV. The converter current is limited by a maximum instantaneous value of 2.7 kA. This overload range allows the ASVC control to reduce temporary over-currents caused by system transients to currents allowed during continuous operation. Instantaneous currents above 2.7 kA lead to pulse blocking triggered by the converter protection.

Operating point 6 is based on maximum average capacitor voltage (5.0 kV) and maximum converter rms current of 770 A. The converter output is 4.93 MVA.

Operating point 7 marks the inductive design point, i.e. maximum continuous reactive power output.

Operating point 8 gives the maximum short time inductive overload restricted to 3.0 sec (Starting from 0 MVAr pre-load). The converter current is limited by a maximum instantaneous value of 2.7 kA. This overload range allows the SVC control to reduce temporary over-currents caused by system transients to currents allowed during continuous operation. Instantaneous currents above 2.7 kA lead to pulse blocking triggered by the converter protection.

t (s)	OP	V_1 (pu)	Q_1 (Mvar)	V_2 (pu)	Q_2 (Mvar)	V_{CONV} (pu)	Q_{CONV} (Mvar)	V_{dc} (kV)	I_{CONV} (A)	Remarks
∞	1	1.0	-4.0	1.089	-4.36	1.157	-4.63	4.727	763.8	nominal reactive power capacitive
∞	2	1.0	4.0	0.911	3.64	0.843	3.37	3.446	-763.8	nominal reactive power inductive
∞	3	1.04	-4.16	1.129	-4.52	1.197	-4.79	4.89	763.8	capacitive design point.
∞	4	1.07	-4.2	1.157	-4.54	1.224	-4.8	5.0	749.1	
10.0	5	0.95	-6.64	1.105	-7.73	1.224	-8.56	5.0	1336.0	short time overload capacitive
∞	6	1.066	-4.30	1.155	-4.66	1.224	-4.93	5.0	770.0	
∞	7	1.07	4.32	0.980	3.95	0.912	3.68	3.727	-770	inductive design point
3.0	8	1.07	7.83	0.907	6.64	0.783	5.73	3.201	-1397.3	short time oveload inductive

t	time allowed for operation
OP	number of operating point
V_1	Voltage at HV-side (node WP2)
Q_1	Reactive power output of one converter branch as seen from HV-side (node WP2)
V_2	Voltage at transformer LV-side
Q_2	Reactive power of one converter branch as seen from transformer LV-side
V_{CONV}	Voltage at converter terminals
Q_{CONV}	Reactive power of one converter as seen from converter terminals
V_{dc}	DC capacitor voltage of one converter (both capacitors connected in series)
I_{conv}	Current flowing into one converter

Table 4.2: Operating points referring to one converter branch.

4.5.5 ASVC Components

The design requirements for the ASVC power components as shown in Figure 4.1 are given in detail in the following chapters.

- Converter data

Type of converter:	Air cooled three level converter
AC Side	
Rated voltage:	3.7 kV
Rated current:	763.8 A
Rated power:	4.9 MVAr
Terminal voltage ratio (Three pulse modulation):	0.949
Switching angles:	a1=12.2 ° a2=19.5 ° a1=23.9 °
Overload: according to Table 4.2, operating points 5 and 8	
DC Side	
Capacitors:	2 x 5 mF ± 10 %
Rated voltage:	2 x DC 2.5 kV
Max. voltage (instantaneous value)	2 x 2.9 kV
Rated current (rms value):	AC 800 A

- Transformer data

Type of transformer:	3-phase, oil-insulated
No. of windings:	1 primary, 2 secondary
Insulation levels	
Highest System Voltage, prim.:	24 kV
Lightning Impulse Withstand Voltage, prim.:	125 kV (Cable Connection Box)
Power Frequency Withstand Voltage, prim.:	50 kV
Highest System Voltage, secondary:	7.2 kV
Power Frequency Withstand Voltage second.:	20 kV
Nominal Power	±2 x 4 MVAr at 1.0 pu system voltage
Nominal Voltage, primary side	15 kV
Nominal Voltage, secondary side	3023 V
Nominal Frequency	50 Hz
Leakage Impedance	8.9 % (on 8 MVA basis)
Vector Group	Ynyd5
Saturation knee-point above	1.3 pu
Maximum fundamental current for each low voltage side (continuous) $I_{(1)rms}$:	771,0 A

- Reactor data

Type of reactors:	three phase iron-cored reactors
Inductance 0.471 mH	
Tolerance on inductance	± 2 %
Maximum total current (continuous) I_{rms}:	771.0 A

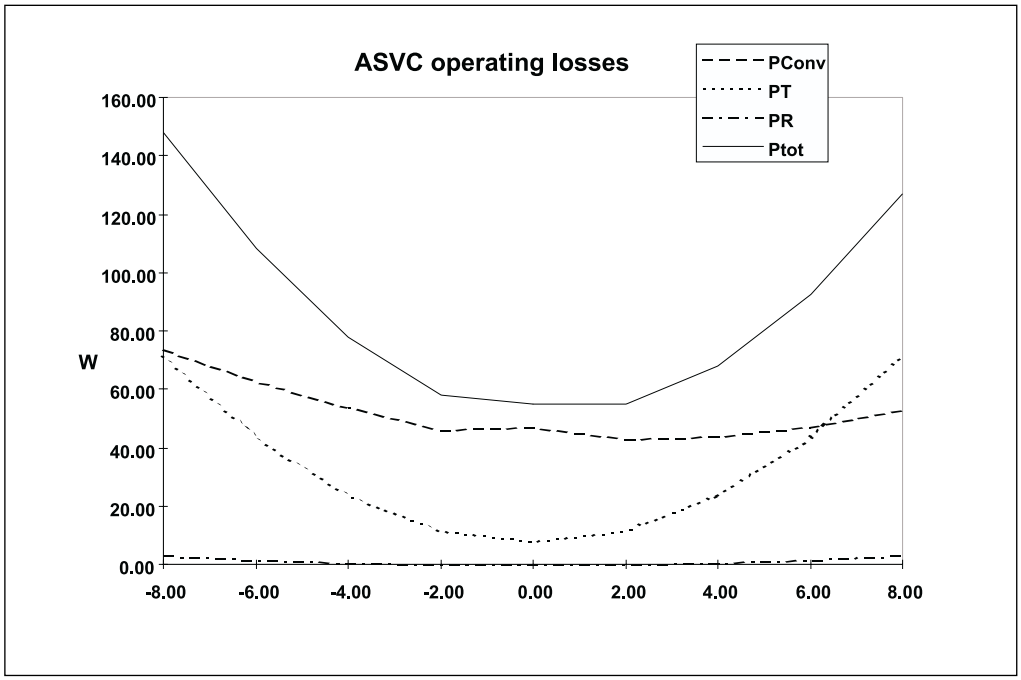

Fig 4.11: Operating losses of the ASVC.

4.5.6 ASVC Losses

Losses depend on the operating point of the ASVC. Figure 4.11 shows the fundamental losses of the main components of the ASVC for the continuous operating range from 8 MVAr capacitive to 8 MVAr inductive referring to 1.0 pu system voltage at the PCC.

Chapter 5

Detailed Design of the ASVC

Klaus Bergmann
Ralf Stöber
SIEMENS, Power Transmission and Distribution
Erlangen
Germany

5.1 Component Arrangement

The ASVC is connected to one busbar of the wind farm. Potential transformers, current transformers and the 15 kV circuit breaker are located in the switchgear building at Rejsby Hede Substation. From there 15 kV single core cables lead to the three winding converter transformer which is positioned outdoors, at one end of the ASVC building (Figure 5.1).

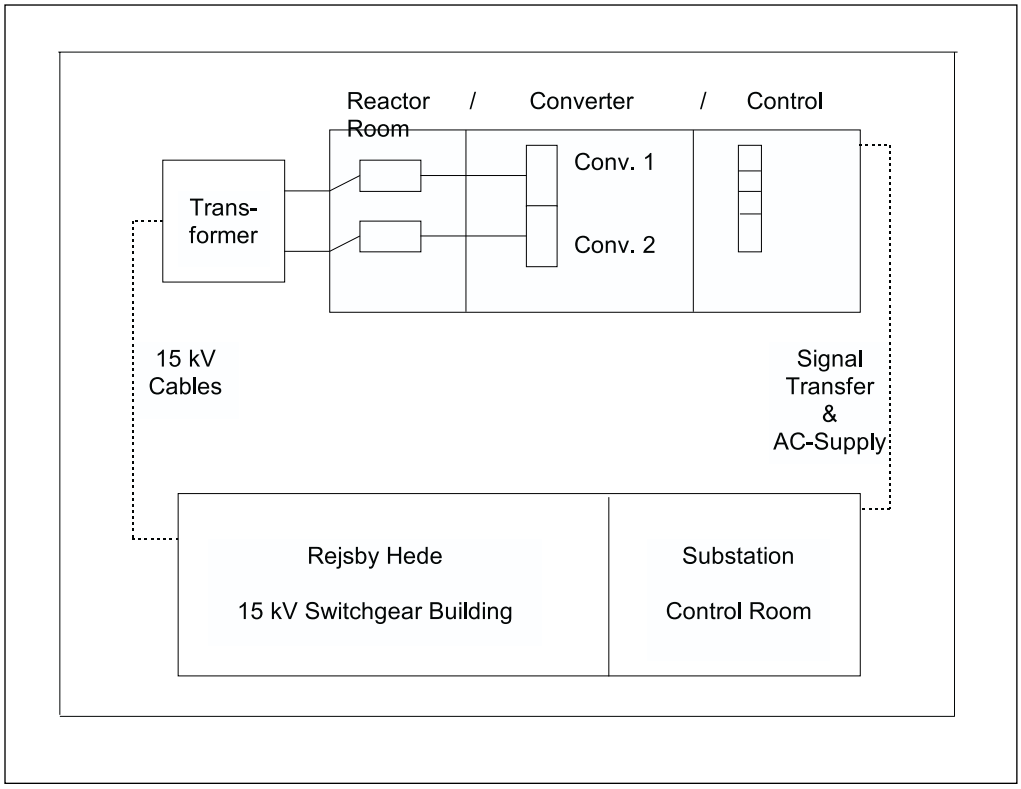

Figure 5.1: Component Arrangement.

To double the transformer short circuit impedance, one 3-phase iron core reactor per secondary winding is connected via 3.6 kV cables. The reactors are placed in a separate room for safety reasons, since their terminals are open.

Finally, the two air-cooled GTO-converter cubicles are connected to the power circuit, again via 3.6 kV cables. They are also located in their own room to reduce the noise of the cooling fans and to provide the necessary air flow through the room for cooling purposes.

The ASVC Control Cubicle, the Uninterruptable Power Supply (UPS) System and the AC-Distribution are located in the control room. Furthermore, the measurement equipment developed by DTU was installed in this room.

To allow for remote control and monitoring, a selection of signals and alarms is transferred from the Control Cubicle to the Remote Terminal Unit (RTU), which is placed in the Rejsby Hede switchgear building and provides the parallel interface to the EASV signal transmission system.

The electrical interconnections are shown in the Single Line Diagram, Figure 5.2.

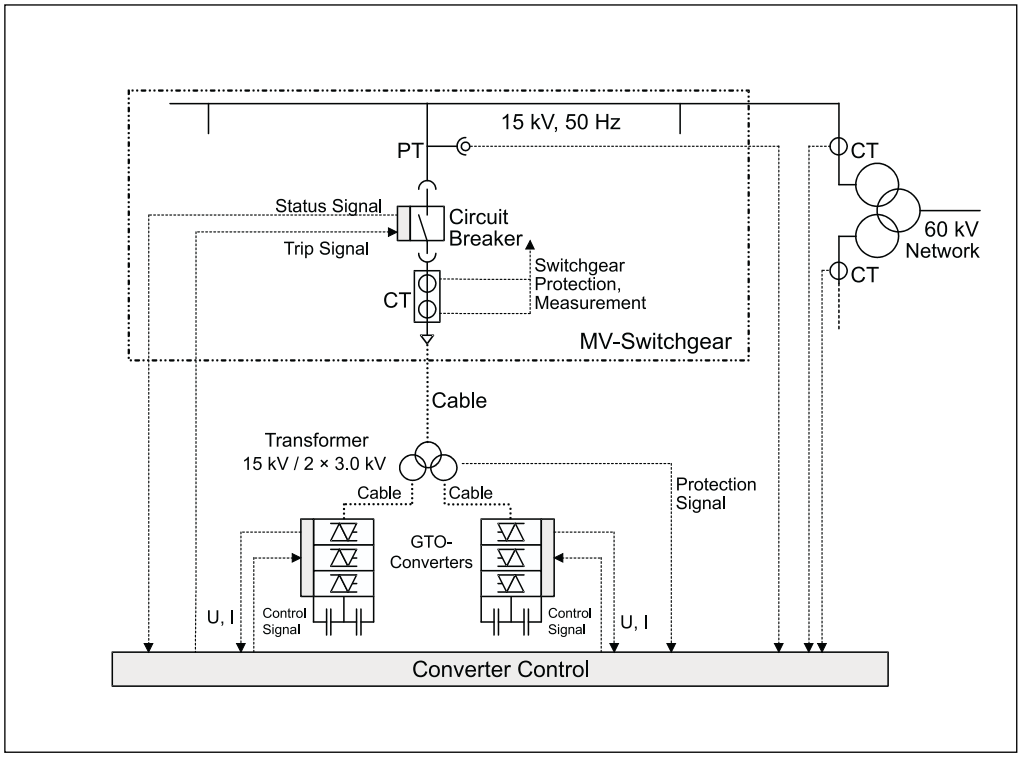

Figure 5.2: Single Line Diagram.

5.2 GTO-Converter Cubicles

One converter cubicle, as shown in Figure 5.3, contains three vertically arranged GTO-thyristor stacks with gate units and snubber circuits, the two DC-link capacitors with short circuit device and pre-charge circuit, converter control system, power supplies and grounding facilities. Since the converters are air-cooled, two top mounted fans per cubicle have to provide the necessary air flow. Cooling air is sucked in at the bottom front side of the cubicles and blown out on top.

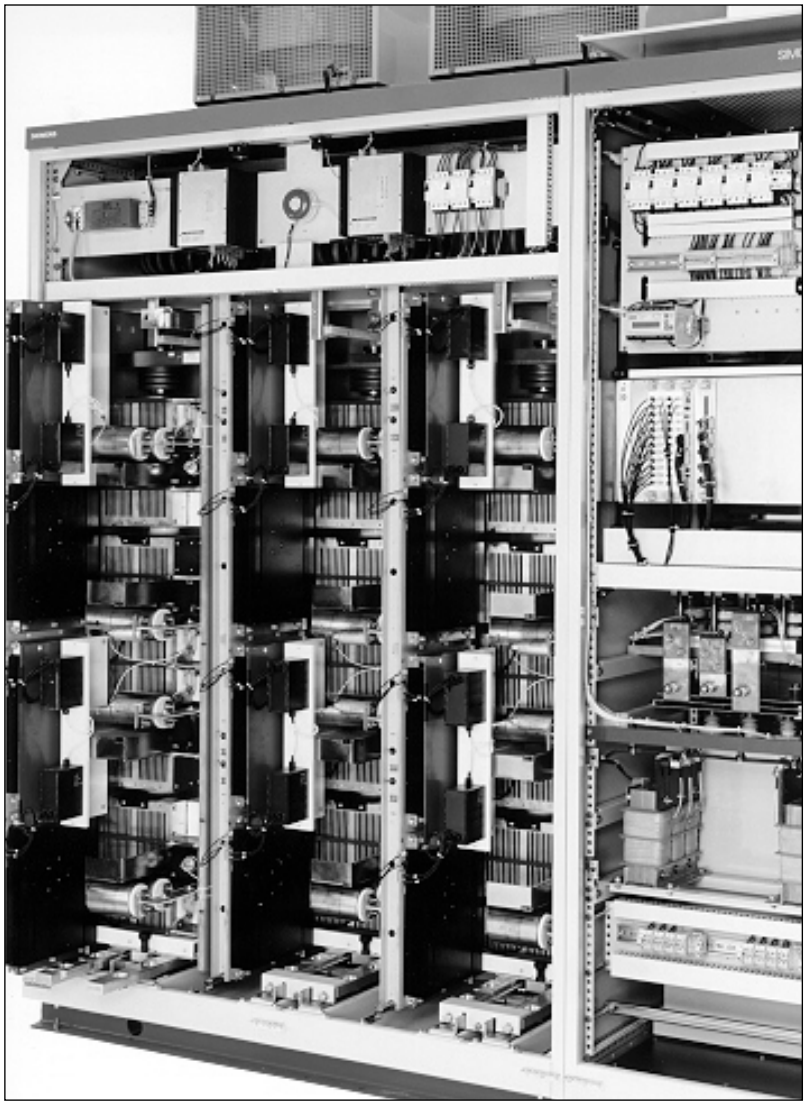

Figure 5.3: GTO-Converter Cubicle.

The converter used for the wind farm application is a Three-Level Converter with a maximum continuous reactive power output at the cubicle terminals of ± 4.6 MVAr at 770 Amps.

Further technical details:

- Type of operation:	three-pulse operation
- Converter connection voltage:	3 kV, 50 Hz
- GTO-thyristor:	
reverse conducting (RCGTO)	
electrical data:	3000 A / 4500 V
size (contact area / overall):	80 mm / 120 mm
- Size of one converter cubicle:	L: 2100mm / H: 2800 mm / W: 1200mm
- Weight of one cubicle:	2700 kg

Further data is given in Chapter 4, Basic Data of ASVC Design.

Fast overcurrent and overvoltage protection functions are located in the converter cubicle including the necessary current and voltage transformers. The current transformers are also used for DC-current monitoring and control.

Furthermore, each converter cubicle contains a thyristor switched short circuit device for the DC-capacitors, which is triggered by the fast overvoltage protection and absorbs the capacitor energy in a resistor.

The converter cubicles are equipped with the thyristor control set, which provides the interface between the converter and the ASVC controller. The control set generates control pulses for the gate units which then produce the actual firing pulses for the GTO-thyristors. There is one gate unit for each thyristor.

Before initial start-off, the DC-link capacitors have to be charged via the 230 V auxiliary supply system. During operation the capacitor voltages vary according to the operating conditions.

5.3 Control Cubicle

The ASVC controller is based on SIMADYN D, the Siemens multiprocessor digital control system. The system is fed with the actual voltage and current values of the wind farm busbars. It contains all functions and software to operate and protect the ASVC within the required operating range. A more detailed description is given in the later section “Control System Design and Implementation”.

Settings and parameters can be implemented and changed via the door mounted Operator Interface OP2 which can also display several parameters, like busbar voltages, reactive power generated, alarm messages, status of plant, etc. Furthermore, there is a mimic panel at the front door of the control cubical

which indicates the status conditions of the 15 kV circuit breaker (CB), disconnector and ground switch (Figure 5.4). The 15 kV CB is switched by the ASVC controller automatically, according to operational needs.

The controller also collects alarms and trip signals which are then shown on the alarm panel at the cubicle front door. The detailed alarm statements are available on the OP2 display or in form of a printout.

Various push buttons and current / voltage indicators provide the necessary facilities for the start-up and close-down sequence of the ASVC.

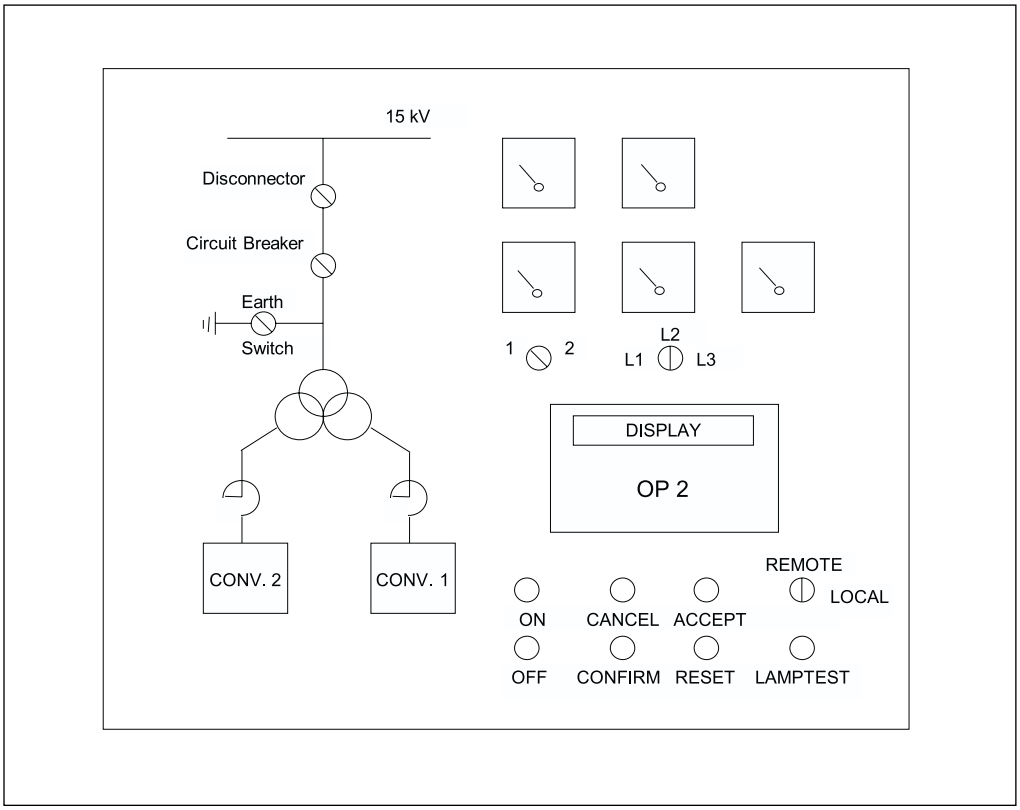

Figure 5.4: Mimic Panel.

5.4 Protection of Plant

This paragraph describes the conventional protection system, i.e. protection relays. There is one overcurrent relay installed in the switchgear building which provides Overcurrent/Time and Instantaneous Overcurrent Protection for the feeder bay and the 15 kV cables.

From the same set of current transformers one signal (3-phase) is taken for the differential protection of the converter transformer. The other two current values (3-phase) for the differential protection relay are taken from bushing current transformers at the secondary windings of the converter transformer (please refer to attached Figure 5.5). Additionally, the differential protection provides the back-up function for the overcurrent /time protection. Furthermore, this relay contains an overload function for transformer protection which uses an integrated current technique.

The protection signals generated by the relays initiate the trip of the feeder vacuum circuit breaker. The signals are also sent to the ASVC controller to initiate alarms. In addition to the conventional protection, the ASVC controller can send trip signals to the circuit breaker, generated by overcurrents, overvoltages or ground faults in the converter cubicles.

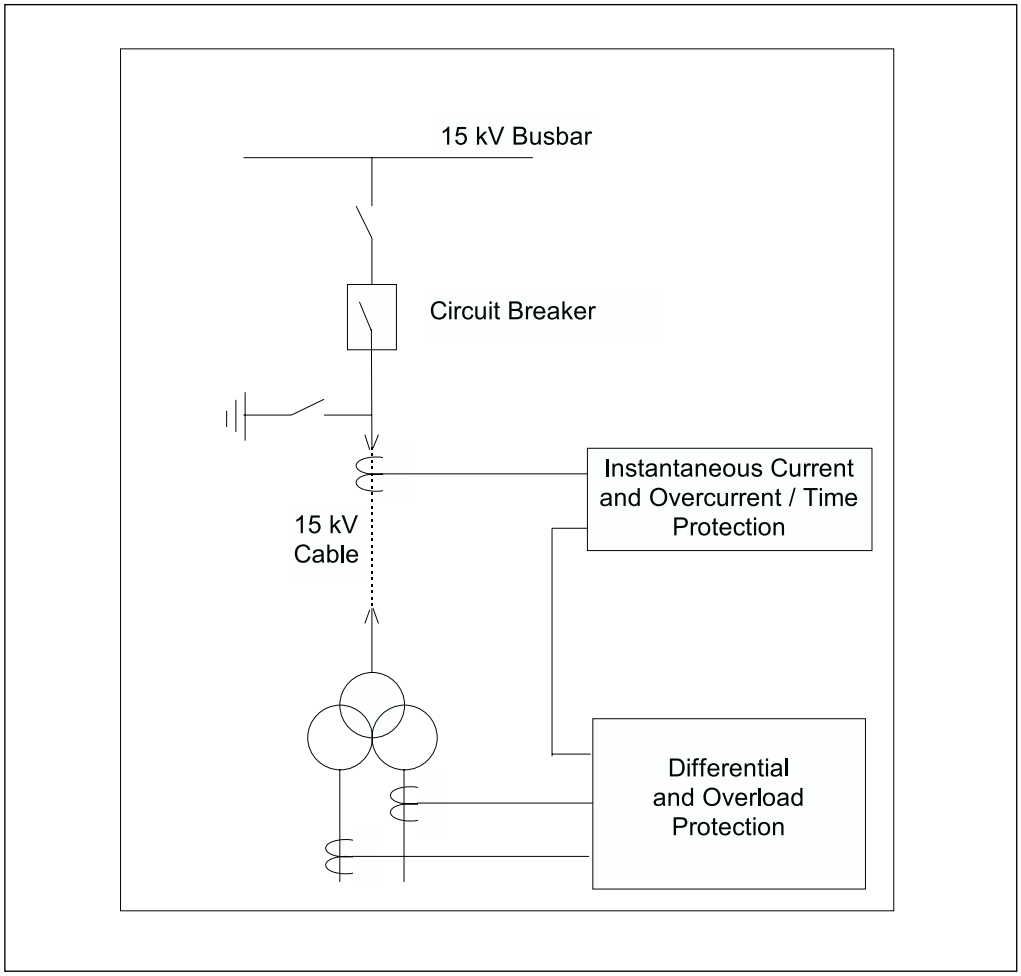

Figure 5.5: Protection Scheme.

5.5 Transformer

The natural cooled converter transformer is of double stack, three winding design, with star-star-delta connection. The rated voltage at the primary winding is 15 kV, and at the secondary windings is 3 kV. The short circuit impedance amounts to 8%. The transformer is designed for cable connection at the primary and secondary sides.
It weights 33 tons with an overall height / width / length of 3.8 / 3.6 / 4.5 meters.
Each phase of the secondary windings is equipped with one bushing current transformer for connection of the differential protection relay.

The transformer protection consists of Oil Temperature and Oil Level Monitoring and of Rapid Pressure Rise Detection. Furthermore a Pressure Relief Device protects the sealed tank transformer against overpressure.

5.6 Iron Core Reactors

The first task of the iron core reactors is to approximately double the short circuit impedance of the converter transformer from 8% to 16%. To design the transformer itself for 16% would have been very expensive and technically difficult.
The second task is fine tuning of the transformer plus reactor inductance within a tolerance of ±2%. This is achieved by manipulating the gap in the iron core after having the measured values of the transformer inductance available.
The windings of the three-phase reactors are vacuum-pressure-impregnated using Polyester resin.

5.7 Auxiliary Supply

The auxiliary transformer located in the 15 kV switchgear building also supplies the ASVC equipment.
The auxiliary supply cable is connected into the AC distribution cubicle from where the loads are fed. All loads are protected with miniature circuit breakers (MCBs).
In case of loss of the AC-Supply the ASVC is switched-off. Then the control and protection system will be powered from an Uninterruptable Power Supply (UPS) for two hours, so that status and alarm signals can be transmitted to the area control centre and a remote controlled re-start of the ASVC is possible when the auxiliary supply voltage returns.

5.8 Control System Design and Implementation

5.8.1 Introduction

The following section gives a description the closed loop control of the Rejsby Hede ASVC for Eltra/Denmark.
The control is based on the SIMADYN D®, digital control system. This control system is a multiprocessor configuration that provides a sampling time of 1 ms. For special applications, e.g. filtering, digital signal processors with shorter sampling times are used. The digital control system SIMADYN D®, covers a wide range of sophisticated power engineering applications, e.g. AC and DC motor drives, HVDC, SVC and ASVC.
It offers the following main advantages:

- User-configurable and user-friendly operation
- Flexible configuration of control functions
- Expansible to suit growing user requirements
- Self diagnostic routines
- Remote diagnostics
- Error-free self documentation directly in block diagrams
- Worldwide support
- Normal production line equipment

5.8.2 Interfaces

The ASVC control has several interfaces for measurements and data exchange. Figure 5.6 gives an overview of the layout and the main components of the ASVC in conjunction with the interfacing of the control.

System Measurements

The controller takes voltage and current measurements from both 15 kV busbars. The conversion of the CT and VT measurements into values suitable for the controller is carried out in a number of steps. Beyond the terminals and miniature circuit breakers (MCB) overvoltage protection devices and interference suppression filters to guard against HF voltage components are fitted. The signals are then converted by galvanically isolated V/V or I/V – converters into signals at control circuit potential with voltage limitation and interference suppression. Calibration facilities are provided for each input.
The input interface and signal conditioning is realised with analogue devices. This adapts the input signals to the subsequent digital and analogue control circuits.

The following input signals are used:

- 15 kV line to line busbar voltages ($V_{Line\_1/2}$)

- 15 kV busbar currents ($I_{Line\_1/2}$)

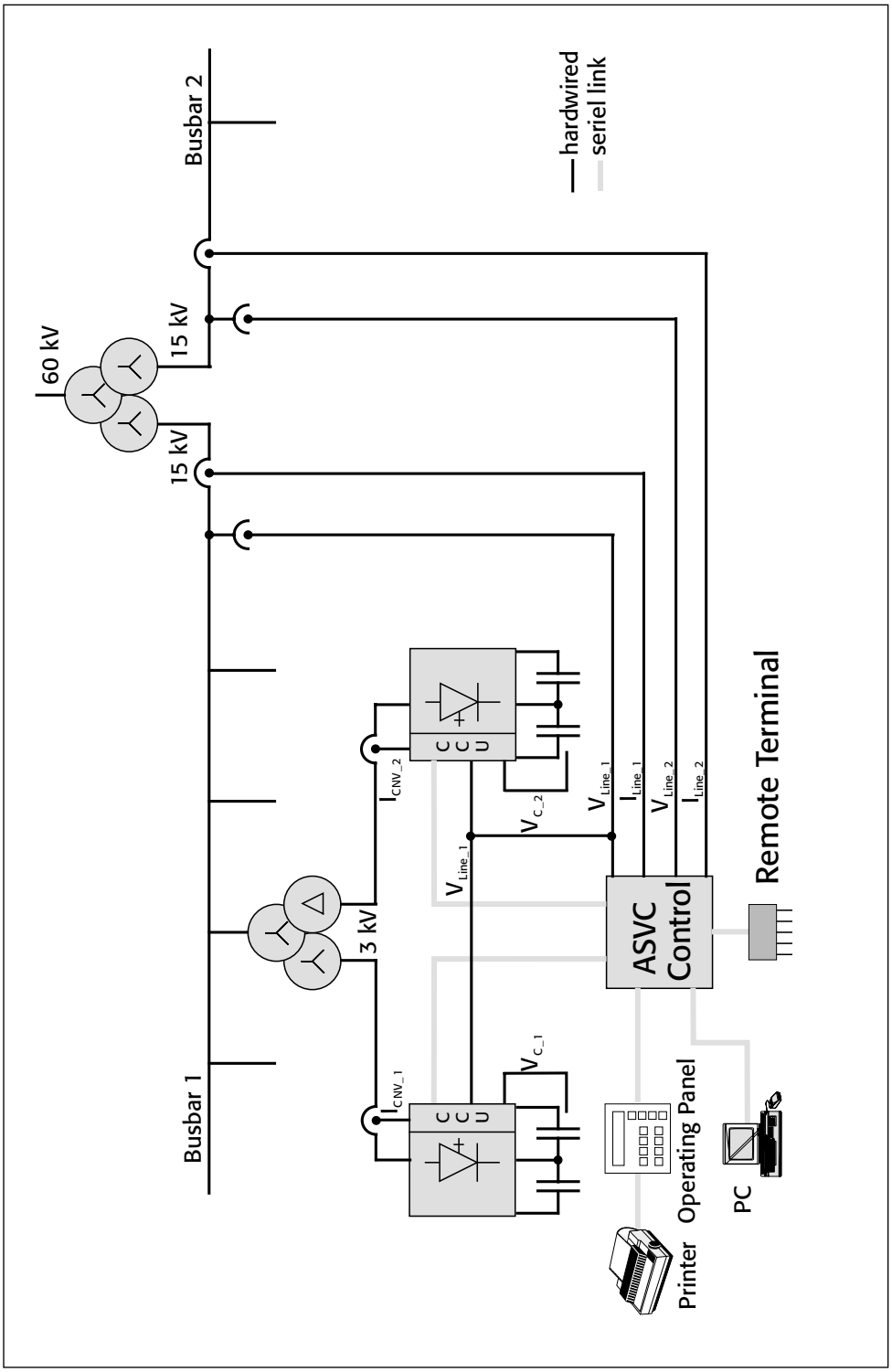

Figure 5.6: ASVC Layout.

Converter Measurements and Converter Control Signals

The converter currents ($I_{CNV\_1/2}$) and the DC-link voltages ($V_{C\_1/2}$) are measured with electronic transducers and are digital processed in the converter control unit (CCU), located in the DC-link cubicle. Additional the voltage measurement of busbar 1 (V_{line_1}) and binary signals are transferred to the CCU. All measured signals are digitally transferred to the controller (via a high speed optical bus).
Converter control signals are digitally transferred via the same bus from the ASVC control to the CCU. These signals are processed to generate gate signals for Gate Drive Units (GDU).

Operating Panel

For operating purposes, service and diagnostics an operating panel is connected with a serial link to the control system. An optional printer can be connected to the operation panel.

Remote Terminal and Switchgear Control

Under normal condition the ASVC will be controlled from the control centre at Skaerbaek. The data exchange for ASVC remote control and the swichgear control are handled with an ET200® interface which is connected via an optical serial link to the ASVC control.
The trip circuits of the switchgear control are hardwired.

PC

For commissioning, service and diagnostics a standard PC can be connected to the control system. This can be done directly in the local control room or from remote using the remote diagnostic tool (Telemaster) and a standard phone line.

5.8.3 Control Scheme
The control scheme is composed of several main function blocks shown in Figure 5.7.
Double framed function blocks are indicate, that this function exists twice, once for each converter.

Actual Value Sensing

This function processes the input quantities of the ASVC control and provides calculated actual values for the subsequent space vector based control. The main steps are:
- A/D conversion of the measured analogue values
- Transformation of 3-phase measurements into space vector quantities using the rotating orthogonal a,b coordinate system

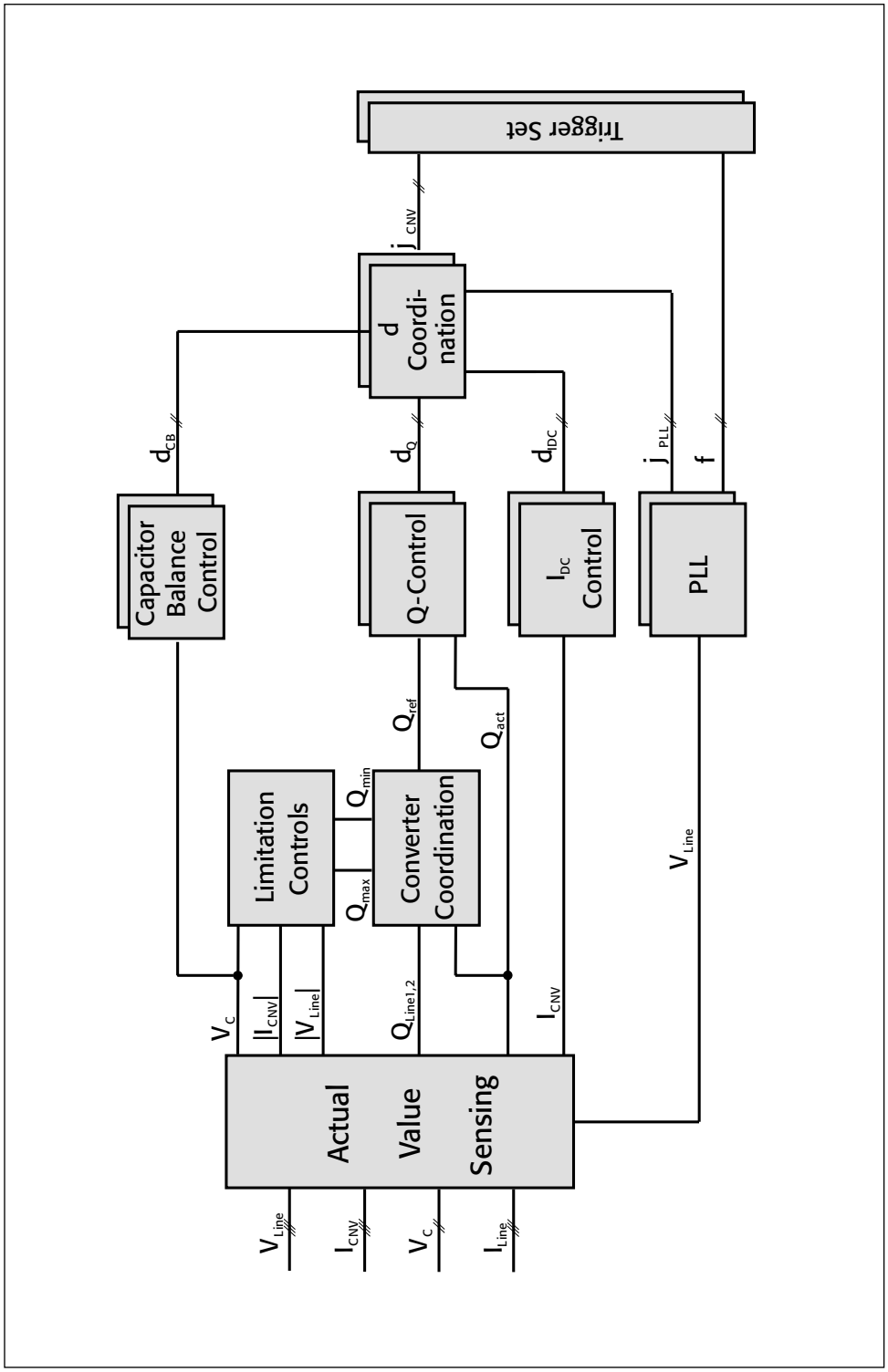

Figure 5.7: ASCV Control Scheme.

- Calculation of the actual instanteneous active and reacvtive power of both busbars
- Calculation of the actual instanteneous reactive power of both converters
- Calculation of the phasor magnitude of the converter current and the line voltage
- Single phase calculation of the magnitude of the 15 kV line to line voltages
- Filtering of measured and calculated values.

Converter Coordination

The converter coordination calculates the actual reactive power demand of the wind park (Q_{Line}) and determines the reactive power reference value (Q_{ref}) for both converters. The reference value is limited by the maximum capacitive (Q_{max}) and inductive (Q_{min}) reactive power, which is dynamically determined by the limitation control. The maximum rate of change of the reference value is limited to 100 kVAr/ms. If, under extreme conditions, fast control action is required the reference value will be modified instantaneously.

Q-Control

The Q-control determines the required reactive power output of the ASVC. Input quantities to this control unit are the reference value Q_{ref} and the actual value Q_{CNV} of the converter instantaneous reactive power. The difference between both values is controlled to zero by a proportional/integral PI controller. The output of the PI-controller defines the phase delta d_Q between the fundamental network voltage space vector and the fundamental converter voltage space vector.
Under steady state conditions this value is close to zero. Changing this value causes an active power exchange of the converter with the power system and an increase or decrease of the dc capacitor voltage. The capacitor voltage determines the magnitude of the converter ac voltage and therefore the reactive power exchange with the system (Figure 5.8).
To achieve a constant and operating point-independent step response the nonlinear control loop is linearized. This is covered with a linearization characteristic forming the output signal $d_{Q,lin}$.
The step response as shown in Figure 5.9 is approximately 20 ms.

Phased Locked Loop (PLL)

The PLL circuit calculates the phase and frequency information of the fundamental, positive sequence component of the 15 kV busbar voltage V_{line_1}.
Input quantities are the a,b-components of the 15 kV busbar voltage V_{line_1}.
Under steady state conditions the speed of response is very slow to get well filtered and noise-free output signals. At system transients the PLL controller is speeded up to achieve a fast resynchronization.

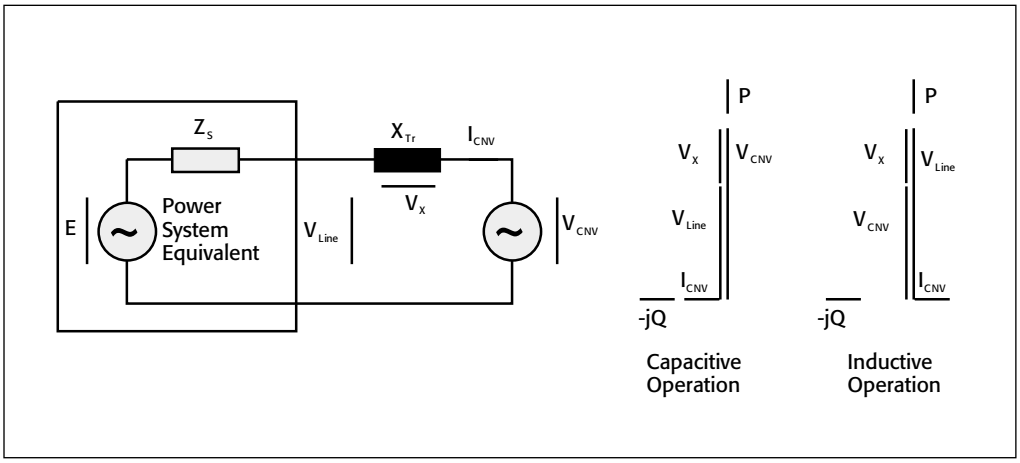

Figure 5.8: ASCV Space Vectors.

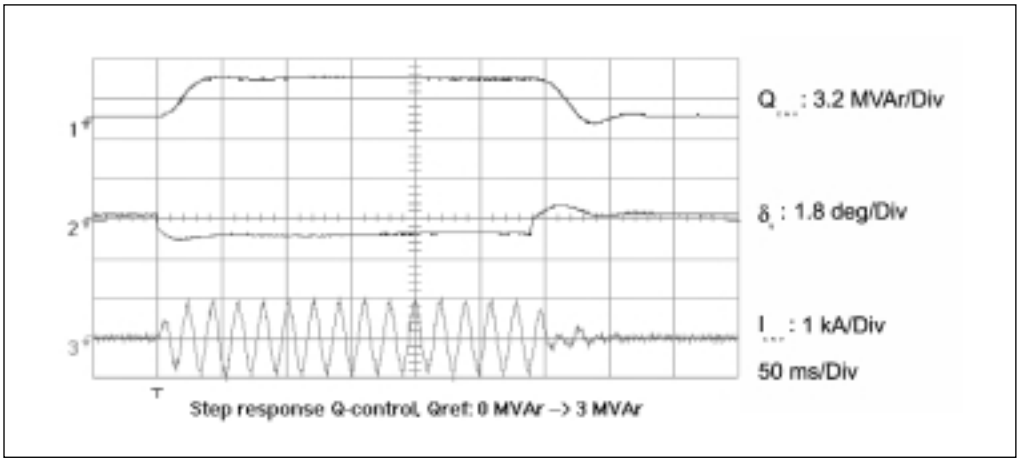

Figure 5.9: Step Response Q-Control.

d-Coordination

The δ-coordination forms the angle j_{CNV} of the required converter voltage space vector for the trigger set by combining various input angles. These are:

- the actual power system phase angle j_{PLL} given by the PLL

- phase angle difference $d_{Q,lin}$ between the converter and the power system voltage

auxiliary modulation angles from capacitor balance control (150 Hz modulation) and dc-current control (50 Hz modulation).

Trigger Set

Depending on the required converter voltage phase angle jCNV and the actual system frequency f the switching signals for the GTOs are generated in the trigger set. They are derived using an optimised pulse pattern with 3 pulse modulation (150 Hz switching frequency), which is stored in a lockup table. The off-line calculation of the pulse pattern has taken the basic design of the ASVC as well as the harmonic requirements into consideration.
Since the trigger set operates with this fixed pulse pattern, the modulation depth (ratio between dc capacitor voltage and the magnitude of the converter voltage) is constant.

Limitation Controls

The maximum capacitive and inductive MVAr limits Q_{max} and Q_{min} are determined by dynamic limitation controls. These controls take the line voltage as well as the internal dc capacitor voltage V_C and the converter currents I_{CNV} into consideration to avoid overload situations of the converters and of the power system.

V_{Line} - Limitation

The V_{Line} - limitation controls the 15 kV line voltage of busbar 1 to suitable values in case of system faults or extreme system conditions. Two levels are implemented:

- V_{Line} > 1.07 pu: Decrease of the capacitive MVAr output (or increase of the inductive) to limit the system voltage to the threshold with a response time of 100 ms -200ms. The threshold is coordinated with the slow acting tap changer control of the local 60 KV/15 kV transformer and should also be coordinated with already existing overvoltage alarm levels.

- V_{Line} > 1.20 pu: Instanteneously switchover of the Q_{ref} value to full inductive operation (-8 MVAr) with a subsequent slow increase to the initial value. Reduction of the first threshold level to 1.0 pu.

Capacitor Voltage Limitation

The capacitor voltage limitation protects the GTO-thyristors and the dc capacitors against excessive voltage stresses. Because the ASVC is operated with a fixed pulse pattern, the dc capacitor voltages V_C depend on the magnitude of the system voltage and the amount of reactive power being exchanged. Capacitive operation increases and inductive operation decreases the voltage compared with no load conditions. Two levels are implemented:

- V_C > 2.5 kV: The maximum value of the four capacitor voltages is controlled to the 2.5 kV threshold by reducing the capacitive MVAr output (Q_{ref} reduc-

tion). Filtered V_C measurements are used to suppress the harmonic ripple generated by the switching operation of the converter. The response time is 100 ms - 200ms.

- V_C > 2.7 kV: Instanteneously switchover of the Q_{ref} value to no load operation (0 MVAr) with a subsequent slow increase to the initial value.

I_{CNV}-Limitation

The GTOs can only carry a device dependent maximum current. The I_{CNV}-limitation lowers the amount of reactive power when excessive currents occur. The ASVC converter can exchange twice the rated power for a few seconds, depending on the pre-load conditions. Two levels are implemented:

- I_{CNV} > 1pu: The maximum magnitude of the current space vectors of both converters is controlled to the nominal current by reducing the MVAr output (Q_{ref} reduction). The response time is 100 ms - 200ms.

- I_{CNV} > 1.5pu: Instanteneously switchover of the Q_{ref} value to no load operation (0 MVAr) with a subsequent slow increase to the initial value.

Capacitor Balance Control

In the case of 3-level converters, care must be taken that the individual capacitor voltages of every converter are balanced. Otherwise capacitor overvoltage and current distortion may result. If the voltages differ above a certain limit (ΔV_C > 75 V), the control is activated and switching is modified such, that the capacitors with the higher voltages inject energy to the network and capacitors with the lower voltages receive energy at the same time and an equalisation is thus affected.
For this the control provides an auxiliary modulation signal d_{CB} which is added to converter voltage phase angle via the d-coordination.

I_D-Control

Non-ideal operation of the ASVC converter can cause a DC voltage in the line-side converter voltages. This in turn causes a DC current and can lead to saturation of the ASVC transformer resulting in highly distorted ASVC currents. The dc components in the converter currents therefore is detected and controlled to an acceptable minimum level. The control determines the modulation of the phase angle by adding the auxiliary signal d_{IDC} via the d-coordination. Additional a dc current supervision circuit is implemented in the control, tripping the ASVC in the case of unacceptable DC components.

Auxiliary Controls

The auxiliary controls have to detect extreme power system and ASVC conditions and have to re-act rapidly to support the main controls and – if possible – to avoid unnecessary tripping of the ASVC.
In the case of tripping, these circuits coordinate the shutdown sequence of the ASVC due to the requirements (fast or slow shutdown), if possible the main circuit breaker will be opened at 0 MVAr.

5.8.4 TNA testing

The AC/DC Simulator (TNA) is designed for transient real time AC and DC system studies, as well as for tests of control and protection equipment for HVDC, SVC and ASVC systems. The simulator components are high-quality R-L-C elements combined with microelectronic components, a digital real time simulator (RTDS) and a powerful digital data acquisition system.
RTDS models can be used both for fully digital real time simulations and in combination with the analogue simulator as a hybrid simulator extension. Controlled electronic sources can be used as system infeed. Any voltage, phase angle or frequency variation including unbalances or harmonic injections can easily be generated to test control systems even under extreme system conditions. Thus, with a simple network representation, complex system disturbances can easily be simulated.

The ASVC representation includes a detailed modelling of all components together with measuring circuits needed for the closed loop control and additional signals for the data acquisition system.

Figure 5.10 shows the test set-up for the TNA testing including a digital real-time simulation of the windfarm.

For the verification of the ASVC performance under transient conditions, additional power system elements are provided. These are saturable transformers for the simulation of inrush-effects, controllable variable loads and line models for generation of higher frequency harmonics.

With variable line impedances tuned to any system fault level it is possible, to test the dynamic response and the controller stability, even under extreme system situations (weak network). By these means, the complete spectrum of system transients from 0 Hz (TCR-DC currents causing transformer saturation and second harmonic voltage) up to 1 kHz for line switching and above 5 kHz for valve transients including protective firing can be simulated.

Simulator test were carried out to develop and optimise the ASVC control, to verify the performance of the each individual control loop and of the complete ASVC.

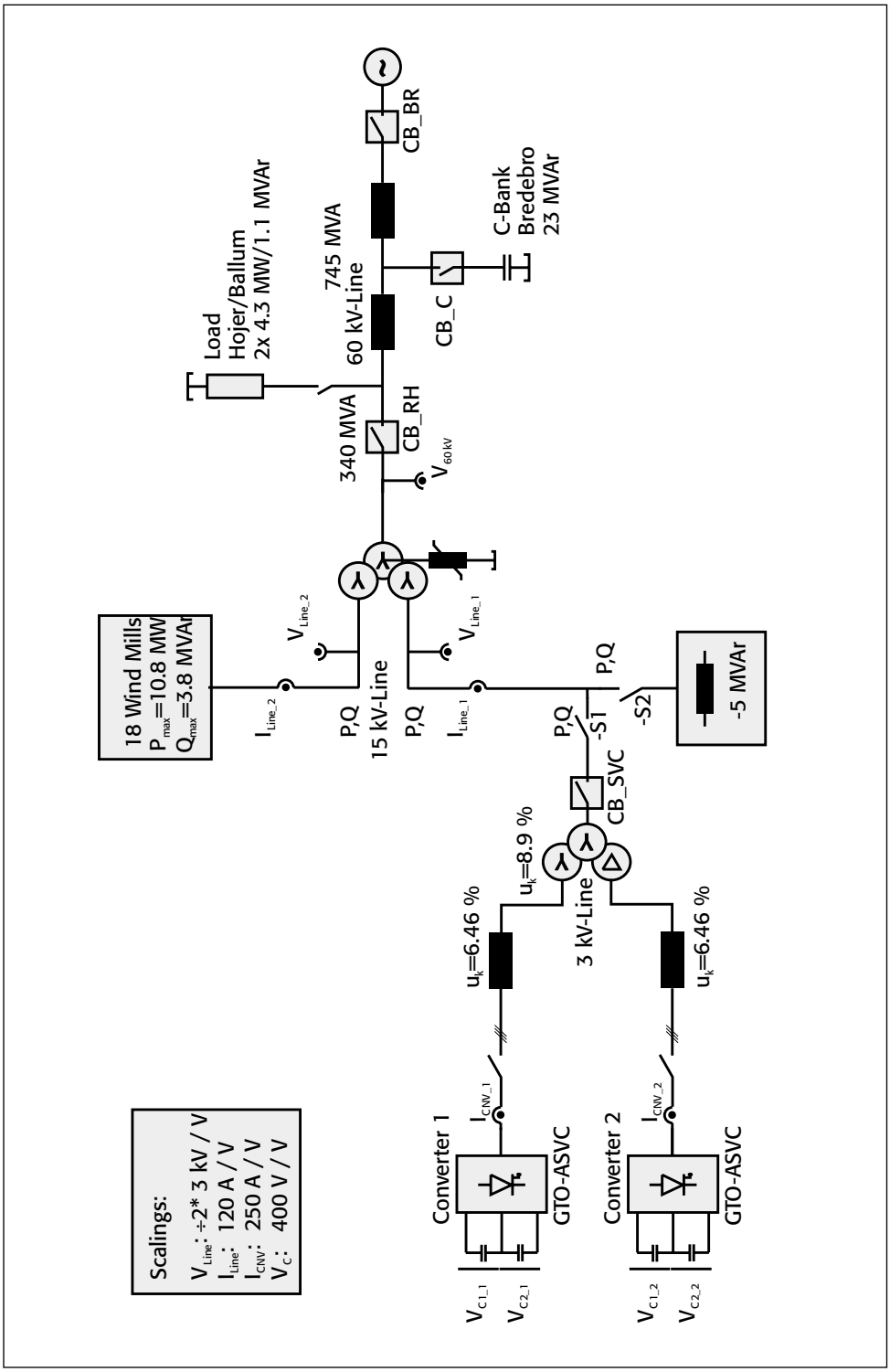

Figure 5.10 : TNA Set-up

The following test program was performed:

- Verification of Controls
  - Actual Value Sensing
  - Phase Locked Loop (PLL)
  - Reactive Power Control
  - Capacitor Balance Control
  - IDC Control

- Verification of Protection Features
  - Voltage and current limitation
  - Converter crest-current protection
  - Capacitor crest-voltage protection
  - AC Under/Overvoltage protection

- ON/OFF Sequence
  - Pre/Discharging
  - On/Off - Control
  - Trip/Emergency Off
  - Standby Mode

- Load Variation at 60kV
  - Symmetrical loads
  - Unsymmetrical loads
  - Energization of external transformers and capacitors

- System Fault Behaviour
  - Symmetrical faults
  - Unsymmetrical faults
  - System faults with load rejection (variation of system phase angle)
  - System faults with variation of system frequency

- Windfarm Load Variations
  - Windmill startups
  - Variation of power generation
  - Windmill shutdown

- Windpark Islanding
  - Islanding at Rejsby Hede
  - Islanding at Bredebro

Figure 5.11 gives an example of the TNA simulations. It shows the fast shut-down (tripping) of 18 windmills at busbar 2 and the response of the ASVC.

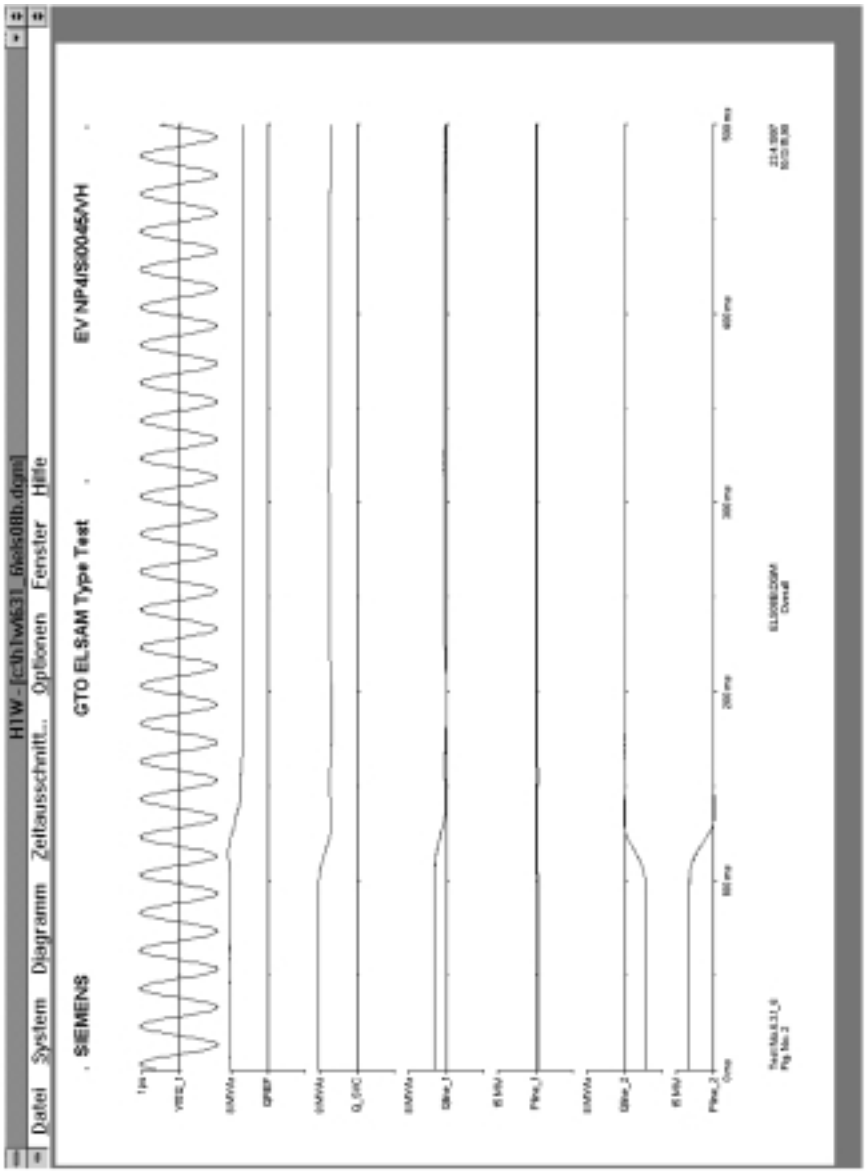

Figure 5.11: TNA Simulation, Windmill shut-down.

Chapter 6

Installation at Rejsby Hede

Kent H. Søbrink
I/S Eltra
Fjordvejen 1-11
P.O. Box 140
DK-7000, Fredericia
Denmark

6.1 Introduction to the Rejsby Hede Wind Farm Site

The Rejsby Hede wind farm site is situated in the south western part of the Danish peninsula of Jutland – the mainland. It is a good windy site close to the coast and it is a typical post-glacial flat area with sandy soil – a moor which has been reclaimed. The area has been protected from shifting sand by wind-breaks of trees and in between the windbreaks the area is cultivated with corn.

Figure 6.1: Wind turbines (Micon 600/150 kW) in the Rejsby Hede wind farm.

It is a very sensitive and peculiar landscape, a part of the marshland which covers several countries from Denmark in the north over Germany to the Netherlands in the south. The location of technical equipment, such as a wind farm and an electrical substation, has a great visual impact on the landscape and is therefore a very delicate matter. Environmental considerations were therefore important at the planning stage of the project in order to fit in the equipment with as little impact on the landscape as possible.

6.2 Civil Works

The ASVC installation can be divided into four main parts; the converter cubicles which contain the power electronic system, the control system, the output reactors and an output power transformer. The transformer is an outdoor, oil-cooled transformer, whereas the other equipment is installed indoors, in a building close to the existing 15 kV substation in the wind farm.

The local authorities required that the building for the ASVC should look like the existing switch-gear building. The building is therefore a red brickwork construction with red tile roof, like the existing building, see Figure 6.2.

Figure 6.2: The ASVC building and the ASVC transformer.

Figure 6.3: Control room

The building is separated into three rooms; the control room, the converter room and the reactor room, Figure 6.9.

The control room contains the control cubicles, the AC distribution system and an Uninterruptible Power Supply (UPS) unit. The measuring system and an event recorder are also placed in the control room as well the variable speed control for ventilation systems in the converter and the reactor room.

The converter room contains the two 4 MVAr ASVC units which are encapsulated in metal clad cubicles on top of which two radial ventilators are placed for cooling the converter cubicles. Moreover, the converter room is provided with a ventilation system in order to obtain an ambient room temperature below 35 deg. C; the heat dissipation from the converters is up to 2 x 40 kW. The converter room is depicted in Figure 6.4.

Figure 6.4: The converter room.

The reactor room contains the two output reactors, see Figure 6.5. The reactor room is a restricted area with high voltage (3 kV), the door to the room is properly marked in accordance with the regulations and only authorised personnel have admission to the room. The reactor room is also provided with a ventilation system; because the heat dissipation from the reactors is up to 15 kW.

The three rooms are separated by fireproof walls which go up to the roof so that roof fire cannot spread.

In the building an earthing system of copper bars (3 x 40 mm), for potential equalisation and protection, goes through all three rooms in the cable trench.

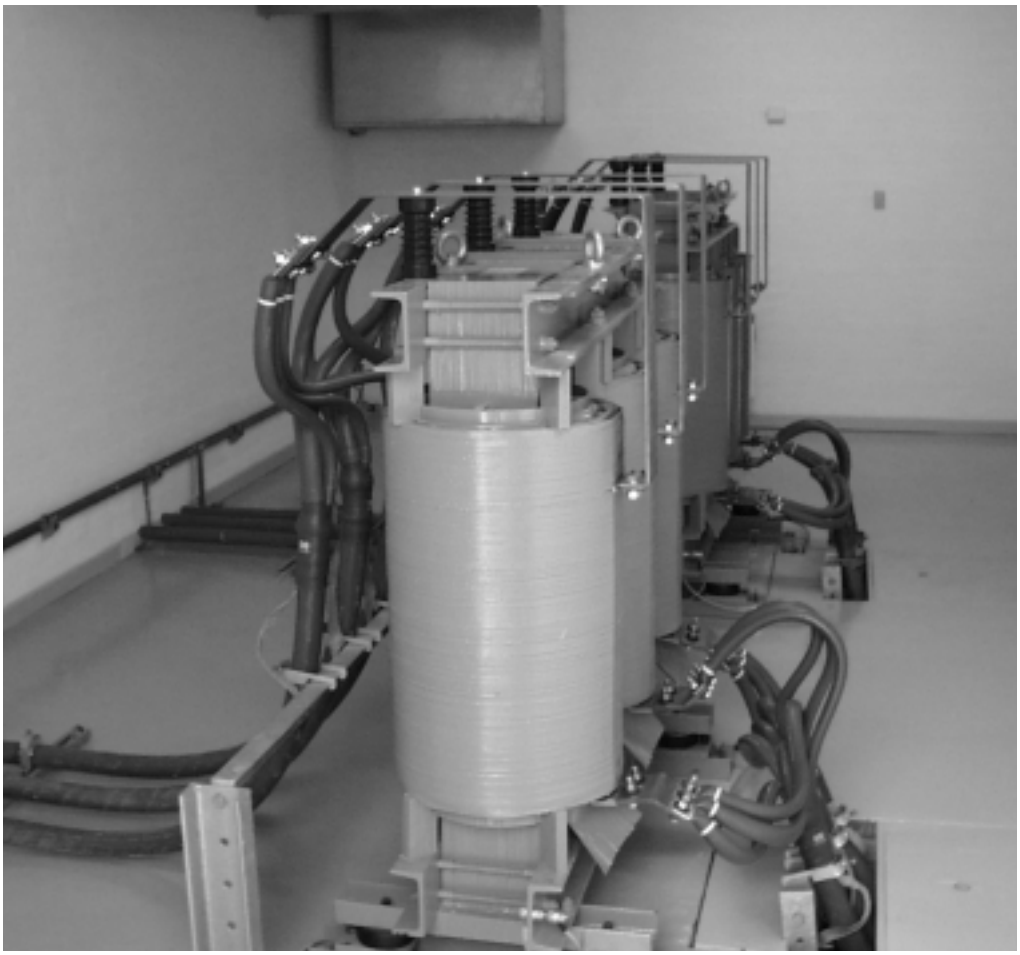

Figure 6.5: The reactor room.

Metal parts of the equipment as well as the reinforcement steel in the building are connected to the earthing system, which is connected to a grid buried in the ground surrounding the building.

Besides, the electrical installation for the ASVC building is provided with ordinary electrical wiring for socket outlets, light and heating.

At the end of the converter building, a concrete transformer foundation with integral oil sump was cast. The oil sump is designed in such a way that it can contain all the oil of the transformer in case of a leak. In order to damp the transfer of vibration from the transformer, two planks of oak are placed between the concrete foundation and the transformer.

The basic consideration for the civil work was:
- Regulations
- Requirements from the local authorities
- Requirements from the distribution company
- The visual impact of the building
- The audible noise level (max. allowed is 45 dB at the boundaries of the lot)
- The physical size of the electrical equipment
- Requirements for interconnection of the electrical equipment
- The ventilation requirement from the manufacturer
- The physical size of the ventilation systems
- Interface to the existing installation.

The design of the building was carried out in close co-operation with all relevant parties.

An access road was established in connection with the construction work, and after it was finished, plants similar to the existing vegetation were placed around the building.

The building project was carried out on the basis of invitation to submit tenders for three different contracts for the building, the electrical installation and the ventilation systems respectively. Each of the different contracts was awarded to the lowest bid.

The construction works started in August 1996 and were finished in January 1997, followed only by some minor follow-ups.

The ASVC building layout is depicted in Figure 6.9, and the site plan is depicted in Figure 6.10.

6.3 Interface with the Existing Plant

The interface with the existing plant relates to the 15 kV system, the protection, measurements and to remote control. Besides, it was necessary to co-ordinate the ASVC on one side with the capacitors for no-load compensation in the wind turbines as well as a 60 kV, 23 MVAr shunt capacitor battery in the Bredebro 150/60 kV substation from where a radial line supplies the Rejsby Hede wind farm.

In order to limit the short-circuit level, the 15 kV switch-gear has been split up on two busbars of which 22 wind turbine generators are connected to bus 1 whereas 18 are connected to bus 2.

6.3.1 Interface with the 15 kV Rejsby Hede Substation

The ASVC is connected to a vacuum circuit breaker on bus 1 (22 wind turbine generators). The circuit breaker is provided with one shunt release and one

undervoltage release. In order to avoid improper switching of the ASVC circuit breaker, it is not provided with a local on/off switching mechanism. The circuit breaker can only be controlled electrically from the ASVC control panel in a sequence determined by ASVC control system. The interface signals for operating the circuit breaker are provided with opto couplers with an insulation voltage of 3.5 kV.

For control and protection the two 15 kV busbars are provided with current transformers (CTs) and voltage transformers (VTs) which are interfaced to the ASVC control system. The ASVC is connected to bus 1, a voltage difference therefore arises between the two buses, because of reactive power flow from bus 1 to bus 2 via the 60/15/15 kV three winding infeed transformer. In order to determine a mean voltage between the two busbar voltages, a special connection between the VTs on bus 1 and bus 2 was implemented. The ASVC controls the busbars voltages in such a way that they are lying on the opposite side of the mean voltage. This means that if the voltage difference between the two busbars is 1 kV, one busbar voltage is 0.5 kV above and the other busbar voltage is 0.5 kV below the mean value of the voltages between two busbars.

For overcurrent and transformer differential protection the ASVC circuit breaker is provided with CTs.

The wind turbines are each provided with three 50 kVAr capacitors for no-load compensation of the dual asynchronous generators (150/600 kW). When the wind turbines are operated with their 150 kW generators, one capacitor (50 kVAr) is switched in, and when they are operated with their 600 kW generators, three capacitors (150 kVAr) are switched. The switching of the capacitors is controlled by the wind generator control system. The capacitors are switched in steps with a defined time span between each step. Harmonic analyses revealed that the time span between switching the 50 kVAr capacitors was critical and that it should be as short as possible. The time span of 200 ms was found to be an acceptable compromise, which was implemented in the generator control system. The wind generator control cubicle at the bottom of a wind turbine tower is depicted in Figure 6.6.

The wind farm is supplied from the Bredebro substation where a shunt capacitor battery of 23 MVAr for reactive compensation is provided. An islanding situation may occur if the transformer breakers the in Bredebro substation trip. Transient simulations revealed that overvoltage at islanding of the wind farm is critical if the 23 MVAr shunt battery is switched in. In order to prevent this critical islanding situation, a fast intertrip relay (10 ms) was installed with the purpose of tripping the 23 MVAr shunt battery if the Bredebro transformer trips. The Bredebro substation is depicted in Figure 6.7.

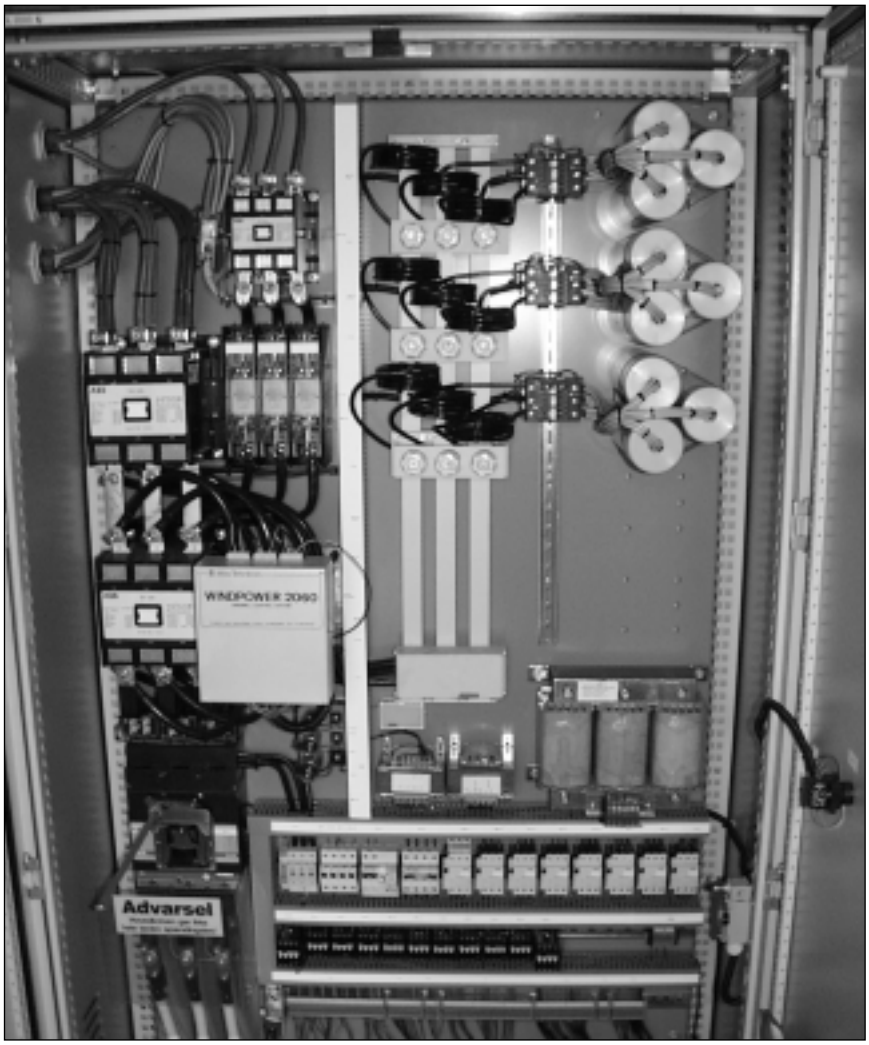

Figure 6.6: The wind generator control cubicles.

6.3.2 ASVC Control

Figure 6.8 shows a photo of the ASVC control cubicle front, which is provided with push buttons for start and stop commands as well as buttons for confirmation or cancellation of the same commands. For shifting between local/remote ASVC control a key lock switch is also provided. Furthermore, there is a control panel with a display provided, where set points for automatic start/stop can be changed and where the set points together with various measured values and fault messages can be displayed. On the front are meters installed for showing the output currents and the 15 kV busbar voltages and the total reactive power from the ASVC.

The ASVC can be operated in manual mode, remote mode and in standby mode. In local mode the ASVC can only be operated locally, whereas in remote mode it can only be operated from the regional control centre.

In standby mode the ASVC starts and stops automatically in accordance with reactive power set points in the control system and the reactive power demand of the wind farm. It has been experienced that proper set points for automatic stop are 0.5 MVAr and that for automatic start it is 1.0 MVAr. A dead band of 0.5 MVAr between automatic start and automatic stop seems to be a reasonable value in order to prevent on/off jitters.

Figure 6.7: 23 MVAr shunt bank in Bredebro substation.

A Remote Terminal Unit (RTU) for interface between the ASVC, the 15 kV switchgear and the regional control room is installed in the wind farm substation. The interface signals comprise digital signals for control and check back and an analogue signal representing the ASVC reactive power output. The various types of control and status signals are summarised in Table 6.1.

The ASVC installation was successfully commissioned in August 1997.

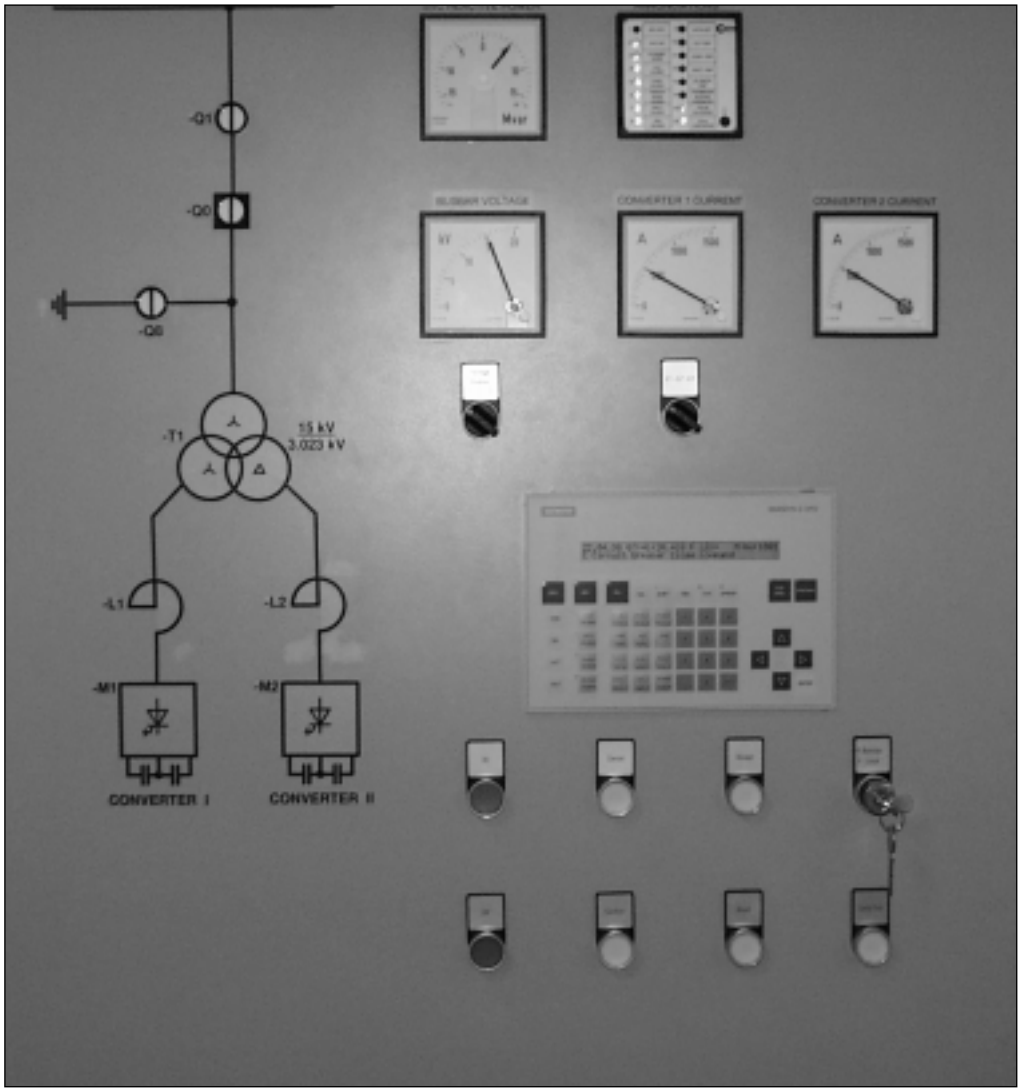

Figure 6.8: The ASVC control panel.

Switch gear control/status	ASVC status	ASVC local control	ASVC remote control
Circuit breaker on/of	Local/remote	Local/remote	
Earth switch closed/open	On/off	On/off	On/off
Current relay indications	Standby mode	Standby mode	Standby mode
	Trip/alarm	Confirm/cancel	Confirm/cancel
	+/- 8 MV Ar (0 - 20 mA)	Output control by change of controller setting	No output control

Table 6.1: Summary of control and status signals.

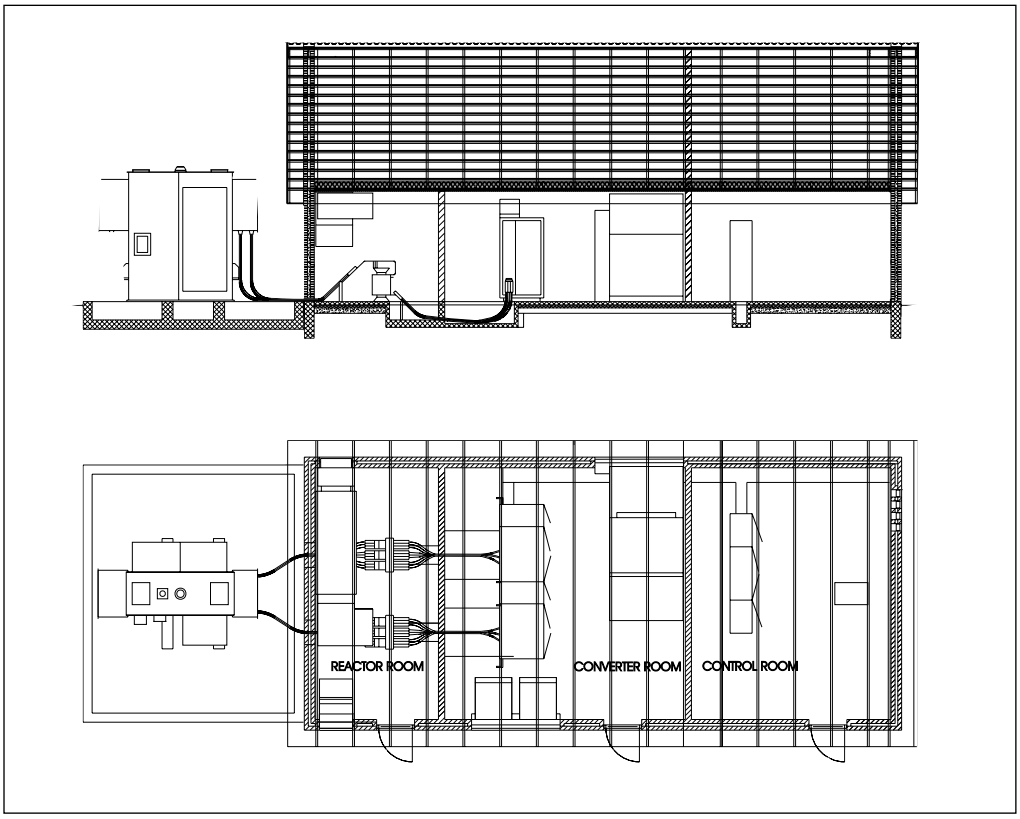

Figure 6.9: The ASVC building layout.

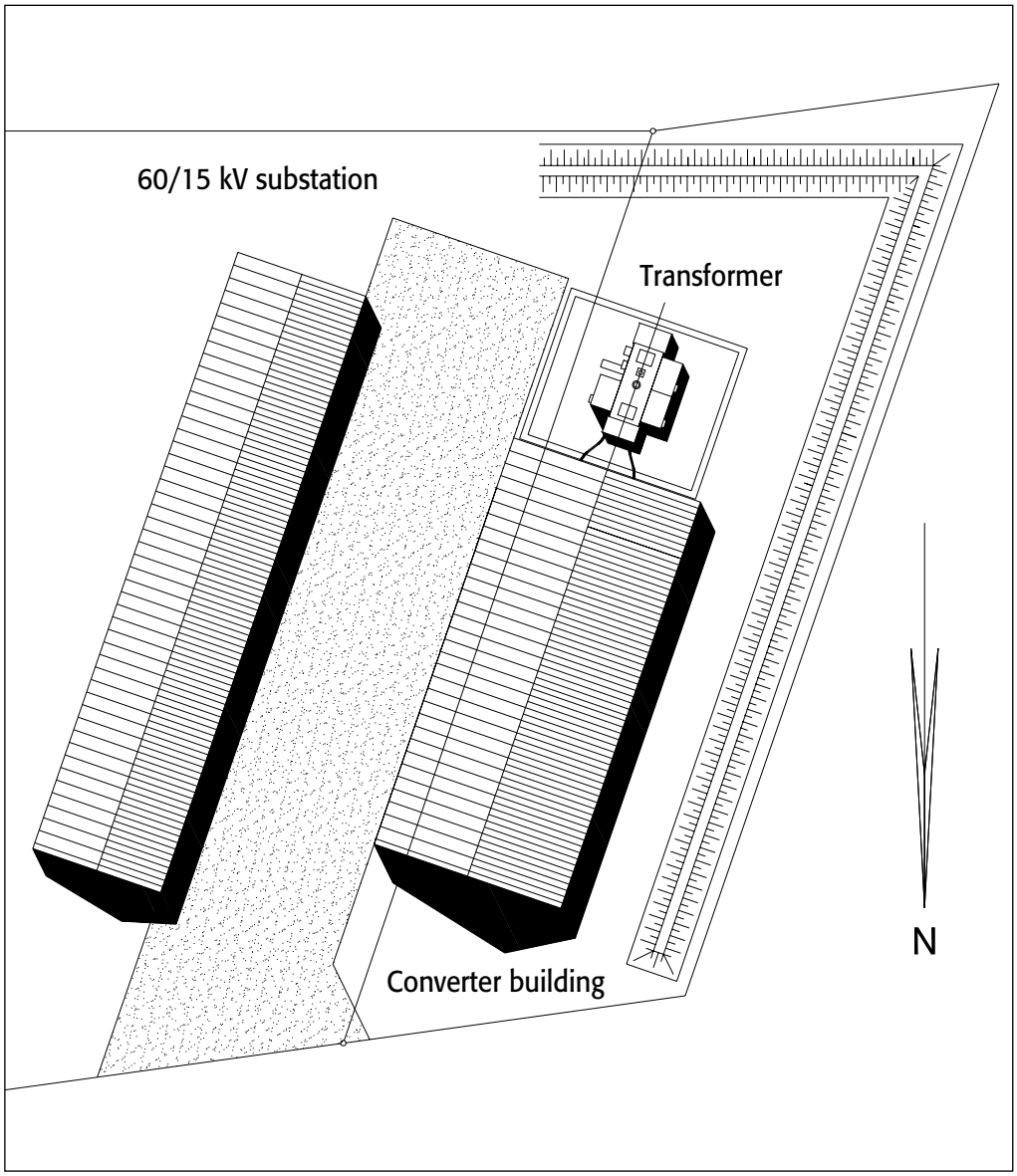

Figure 6.10: The substation site plan.

Chapter 7

Description of the Measuring Equipment

Jørgen Kaas Pedersen
Technical University of Denmark
Department of Electrical Power Engineering
DK-2800 Lyngby

Knud Ole Helgesen Pedersen
Technical University of Denmark
Department of Electrical Power Engineering
DK-2800 Lyngby

7.1 Introduction

It was the task of the Technical University of Denmark, DTU, to carry out the measurements. The type of equipment which may be used for these measurements was investigated and two alternatives were considered. The first alternative was to purchase ready-to-use components capable of producing, from instantaneous signals, rms values of voltage and current, power and reactive power to be logged into a PC (Personal Computer). However, this approach was discarded as it produces a large number of measurements in a very short time and requires additional sampling of the instantaneous signals in order to calculate higher harmonics.

The second alternative was to sample all instantaneous signals with a sufficiently high sampling rate before feeding them to a PC. The PC would then be used to generate the desired rms values of voltage and current, power, reactive power and to calculate higher harmonics. This type of equipment produces large amounts of data and therefore reducing the amount of data without loosing vital information is required. This option was chosen for the measurements, using National Instruments equipment; even though it requires more hardware and software equipment as compared to the first one.

7.2 Network Connection of the Wind Farm

A schematic representation of the wind farm is shown in Figure 7.1. The wind farm consists of two groups of wind turbines (18 and 22 in number) connected to different 15 kV busbars. Both busbars are connected to the 60 kV network via a three phase three winding transformer. The Advanced Static VAr Compensator (ASVC) is connected to the busbar with 22 wind turbines. The measuring transducers are installed on both 15 kV busbars where the wind turbines are connected.

7.2.1 The Signals

Instantaneous values of the network's voltages and currents were measured. Figure 7.2 shows the connection of all 15 signals (2x3 phase voltage signals and 3x3 phase current signals) used for these measurements. A sampling rate of 256 per 50 Hz period was employed. This led to a tremendous amount of data generated, i.e. 192,000 values per second. Storing data sets of such size was a

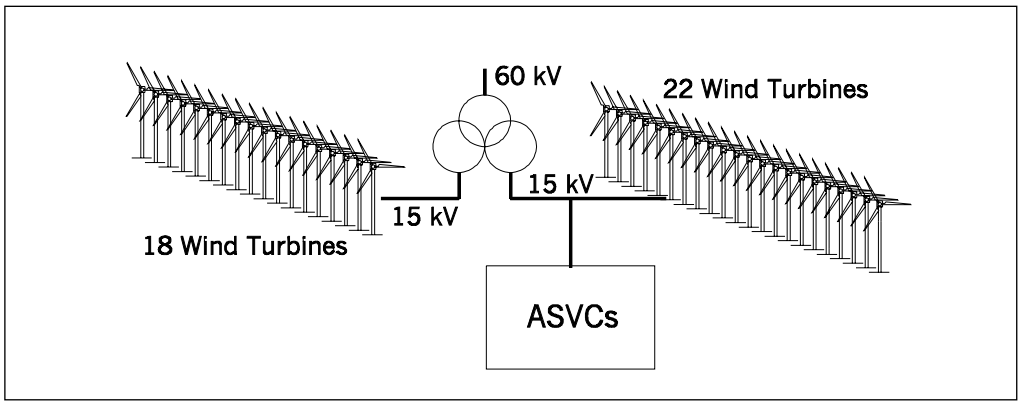

Figure 7.1. Schematic drawing of the windfarm and its associated ASVC.

problem and a reduction in the amount of data was necessary during normal operation. The full storage of data should only be performed for extreme conditions and for very short periods of time. The following procedure was adopted for measurement and data storage.

Over each interval of 8 cycles, rms-values of all the 15 signals, the power, and reactive power of each busbar and the compensator's output are calculated. After each 8 cycles interval, the harmonics and Total Harmonic Distortion (THD) for every signal are determined. Then, every 2 minutes, the results are reduced to mean, maximum and minimum value of each signal. This explains why the time taken by calculations is much greater than that of the sampling procedure. The sampling and calculations were simultaneous and therefore only the results from two 8 cycle intervals per second were possible.

To limit the number and size of data, only the harmonics of interest are calculated. Harmonics which theoretically should not be in the network's voltages and currents, such as even harmonics and third harmonics components, were excluded. However, the second and third harmonic, which may be used for control purposes, were considered. The number of harmonics was initially chosen to be 40. Following suggestions that harmonics greater than 40 were also important, the number of harmonics has been increased to 80. Capturing all this data during a 24 hour period would require 4.8 Mbytes and therefore a software tool for analysing the data of interest was developed.

7.3 The Hardware

7.3.1 The Connection of the Transducers

Figure 7.2 shows the way in which the 15 transducers were connected. The voltages are measured using a capacitive voltage divider which gives an alternative voltage to the signal which is otherwise be obtained by using a conven-

tional voltage transformer. Measurements carried out on a wound type voltage transformer indicated a resonant frequency around 1.5 kHz in the transfer function, which may lead to some difficulties when measuring higher harmonics. Therefore, for a safe operation of the ASVC, the four wound type voltage transformers were not used although they were already installed. Nine current transformers were used to measure current signals. A short description of each component in the measuring equipment is described in the following sections.

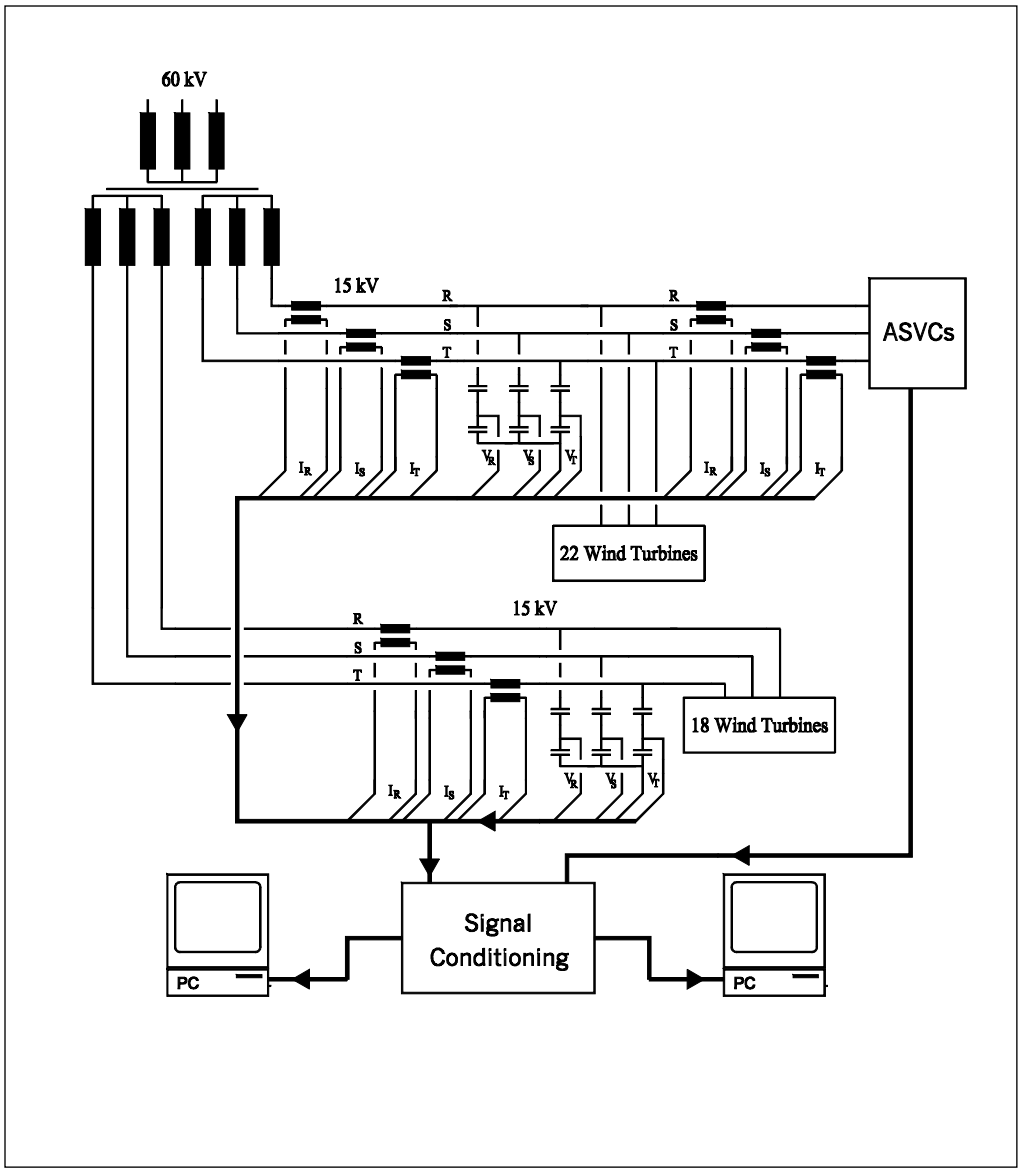

Figure 7.2. The connection of the transducers to the two 15 kV two busbars.

Figure 7.3. A photo of the three capacitive voltage dividers mounted on one of the busbars. The top dark cylinders are high voltage fuses and the light grey cylinders below them are the high voltage capacitors. The low voltage capacitors are seen at the bottom.

7.3.2 The Capacitive Voltage Dividers

They consist of high voltage capacitors with oil/paper isolation with a maximum voltage of 42 kV rms. Under normal conditions, they operate at 9 kV which gives a safety margin. The high voltage capacitors have a capacitance of 8 nF. The low voltage capacitors have a capacitance of 30 µF plus some much smaller capacitors for adjustments. All the six capacitive voltage dividers were adjusted to give a voltage ratio of 1: 3733 ± 0.2 %. The connection of each of the capacitive voltage dividers to the signal conditioning circuit results in a phase shift of 0.5 to 0.6 degrees (leading).

7.3.3 Signal Conditioning

The transducer signals were scaled to approximately 125 mV rms before being fed to the signal conditioning unit, during normal conditions. The input ports of the signal conditioning circuit were galvanically isolated from the output circuit as shown in Figure 7.4. This was done both to minimise noise in the signal and to prevent earth currents from running into the unit. The digital filter used was a 6th order Butterworth filter with a 3 dB cut off frequency at 5 kHz. The sampling frequency was 12.8 kHz and the harmonics of interest were up to 80 which is equal to 4 kHz. The sample/hold circuit was used to allow all 15 channels to be sampled simultaneously as the data acquisition card can only read one channel per 3 µs.

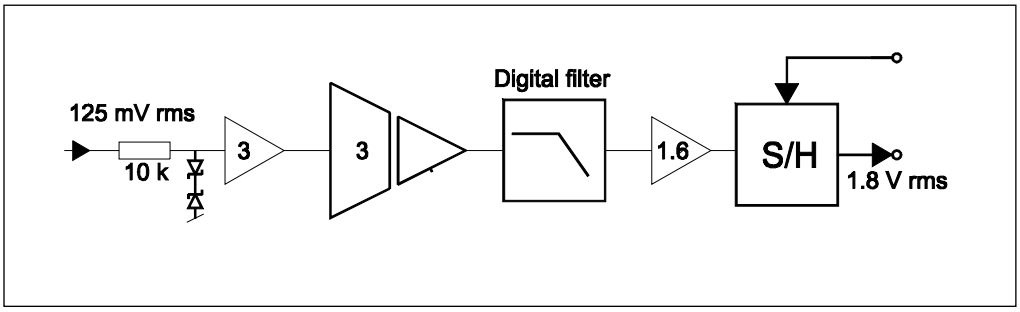

Figure 7.4. Principle of the signal conditioning circuit.

7.3.4 The Personal Computers

Two PCs (HP 166 MHz, 64 Mbytes RAM and 2 Gbytes HD) were installed at the Rejsby Hede wind farm site. One was used for receiving signals from the transducers whereas the other was employed for analysing data and capturing control signals from the ASVC. Both computers were equipped with a National Instruments data acquisition cards “NI-DAQ” (type AT-MIO-64E-3) with 32 differential inputs. Both cards have a maximum sampling rate of 300 kHz which is more than 15 channels multiplied 12.8 kHz. The A/D-converter used measures each signal as a 12 bit digital value. One bit is reserved for critical situations, another one is for the sign and the remaining 10 bits give the preci-

Figure 7.5. The signal conditioning unit with its auxiliary circuits.

sion of the A/D converter during normal operation. Figure 7.5 shows the signal conditioning unit with its auxiliary circuits and the connections from the control cubicle of the ASVC. Figure 7.6 shows how the PCs are placed as near as possible to the signal conditioning unit to avoid noise.

7.3.5 Noise

All the transducers were placed on busbars located in one substation building.

Figure 7.6. The location the PC's and the cabinet with the signal conditioning circuit.

The ASVCs were located in another building together with all the control cubical and measurement equipment. This led to long cable connections, between the transducers and the signal conditioning cards, which resulted in additional noise in the transducers' signals. In an attempt to eliminate such noise, filters and galvanic isolation were installed both on the signal input side of the signal conditioning unit and on the power supply side of network.

The uninterruptible power supply of the ASVC, also supplies power, containing noise, to all the measuring equipment. A total of about 4 mV rms noise, which was some 0.3 % of the signal, was present in the signal input ports of the DAQ cards. However, the rms values of currents and voltages would be more accurate than this since a noise contribution to an rms value averaged over 8 cycles is negligible.

7.4 Calibration of Measuring Equipment

7.4.1 The Capacitive Voltage Dividers

These were calibrated with a voltage of 10 kV but were tested up to 20 kV. On the high voltage side, the voltage was measured with a voltage transformer 20 kV/100 V, 50 VA class 0.5. Two voltmeters HP 3478A, with an accuracy of about 0.5 %, were used. The high voltage was generated by a 100 kV high voltage transformer supplied from a variable transformer connected to the network. Because of small variations in the network voltage and as it was difficult to read two voltmeters at the same time, three measurements were taken and an average value was calculated. Preliminary measurements were performed to determine adjustments in the capacitance to be added, in parallel, to the low voltage capacitor. Then, the voltage dividers were connected to the 20 kV circuit for 24 hours and measured again. These measurements were carried out to determine the calibration constant. No work was done concerning the variation of this constant with temperature as all voltage dividers operated indoors and at room temperature. Figure 7.7 shows the results of calibration of the 6 capacitive voltage dividers.

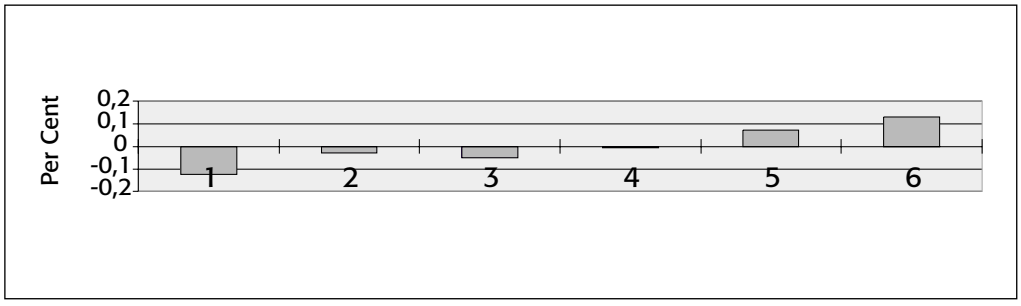

Figure 7.7. Results of calibration of the voltage dividers.

7.4.2 Calibration of the Signal Conditioning Unit

A 50 Hz AC voltage, which is obtained from the network's voltage using a step down transformer, was connected to the input ports of the signal conditioning unit where the transducers were to be connected. The input signals were measured with a HP voltmeter 3457 with a 0.3 % accuracy. The instrument was set up to calculate an rms value of the signal over 8 cycles after being triggered each time. At the same time, a PC was used to calculate the rms value of the

signal taken over 8 cycles with a sampling rate of 256 per cycle. The triggering of the voltmeter and the PC was done manually and simultaneously. Calibrations were carried out for different input signals. The following three figures show their corresponding results. The small variation in the network voltage and the trigger time is not exactly the same and so may explain some of the variations in these figures.

Figure 7.8 shows the measurement of the signals from the capacitive voltage dividers. The bars show the deviations, in %, of the desired gain from input to screen of the PC. Each grey scale represents a different input voltage. The desired gain is 1.1126. The ratio from busbar to screen may be calculated as 1.1126/3733=3355.2 .

Figure 7.9 shows the current measurements of all 9 channels. The current was determined as a voltage across a calibrated resistor with a resistance of 0.968555 Ω. The gain from input to screen is fixed at 0.6800 V/A.
Figure 7.9 shows the deviation, in %, from this value. Each grey scale represents a different current. From busbar to screen, the ratio is equal to (800/5)/06800=235.29 A/V.

Figure 7.10 shows measurements of the 4 channels for the existing voltage transformers which were in use only for a very short time during the commissioning stage. From input to screen, the gain is fixed at 0.023384 V/V. Figure 7.10 shows the deviation from this value, in %, and where each grey scale represents a different input voltage. The ratio of voltage from busbar to screen is 5830.7 which is equal to (5000/110) / 0.023384.

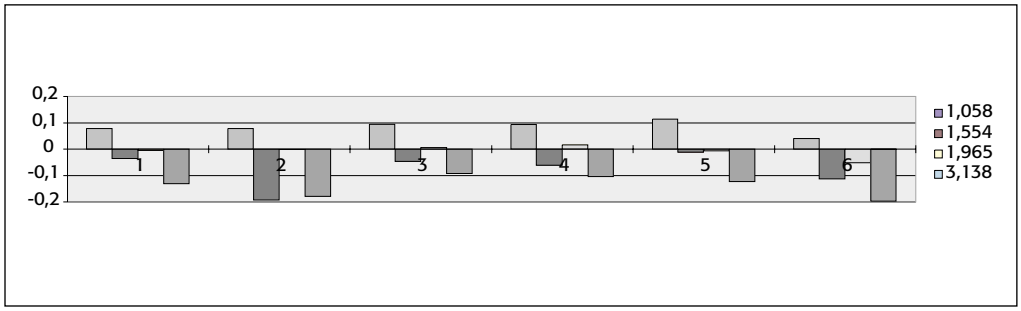

Figure 7.8. Results of calibration of the total signal path from transducers to reading on the screen for the voltage signals from the capacitive voltage dividers.

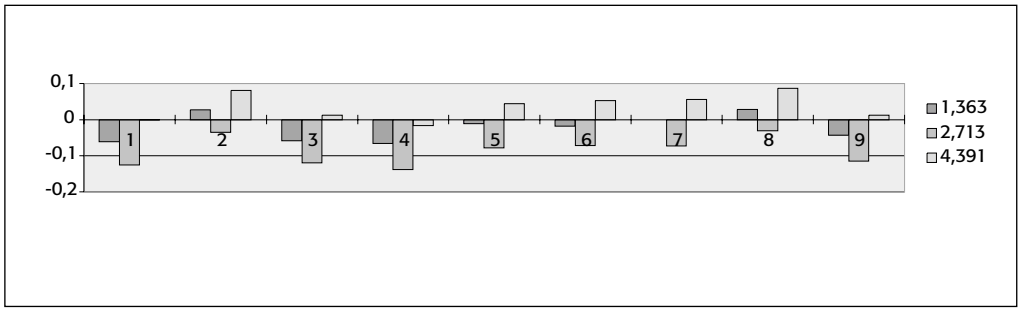

Figure 7.9. Results of calibration of the total signal path from transducers to reading on the screen for the voltage signals from the CTs.

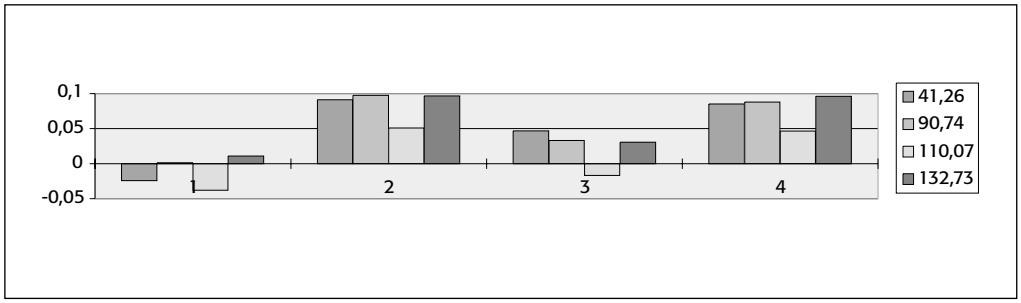

Figure 7.10. Results of calibration of the total signal path from transducers to reading on the screen for the voltage signals from the VTs.

7.5 Software

7.5.1. Goals

The acquisition of measurement data from the network and the ASVC of the Rejsby Hede wind farm, was performed using the following software developed by DTU for the project:

a) Continuous monitoring of the power quality and the power generation from the wind farm.
b) Continuous monitoring of the operation of the ASVC combined with a detection of any abnormal events.
c) Fast acquisition of measurements to be used for example in connection with 'islanding' tests.
d) Conversion of data into suitable formats, such as EXCEL and MATLAB, to facilitate detailed analysis of the data.
e) Creating a WEB-page with an animated picture of the power production.

7.5.2 Hardware Configuration

The measurement system was based on PC-techniques. Two 166 MHz Pentium PCs were installed in the control room at the wind farm site – one used for measurements of voltage and current in the network, and the other used for measurements of control signals from the ASVC. Both PCs were equipped with a 32 channels, 12 bit, 300 kHz ADC-board from National Instruments. Signals from the measurement process were then connected to the ADC-boards through transducers and the signal conditioning equipment.

The two PCs were connected to their own private LAN, which through an ISDN-line was linked to the LAN at DTU – as shown in Figure 7.11. This meant that the two PCs were part of the DTU-LAN and therefore could be accessed from DTU. This configuration was beneficial in many ways as listed below:

a) The PCs in Rejsby Hede can be remotely controlled from DTU through the program CarbonCopy, which has been a great advantage in program development and program testing.
b) Data stored on disk in Rejsby Hede can be transmitted to DTU.
c) A WEB-page with automatic updating of production data can be designed.

7.5.3 Basic Specifications

A complete picture of the state of the network and its associated wind farm can be obtained from measurements of 15 signals, i.e the voltages and currents

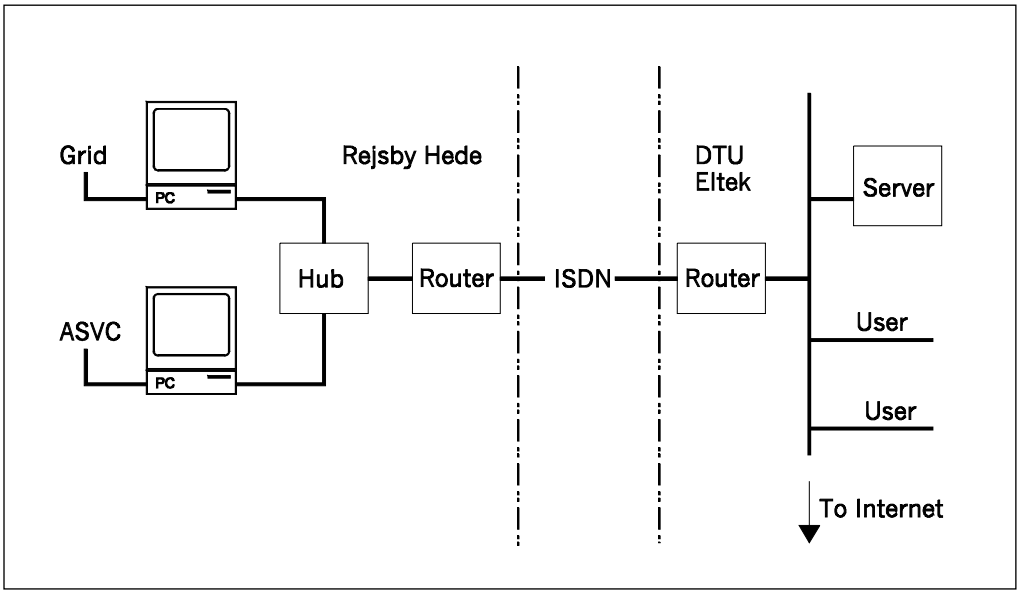

Figure 7.11. PC configuration.

in all three phases of the two busbars where the wind turbines are connected, and the currents in all three phases of the ASVCs, as was shown in Figure 7.2. The harmonic content, up to a certain frequency, of these signals is also important. The IEC-norms recommend calculation of harmonics up to the 40th, evaluated over a window width of at least 8 cycles (i.e 160 ms) at 50 Hz. Following preliminary tests, it was decided that 40 was not enough and an increase in the range of harmonics up to the 80th was considered. The cut-off frequency in the signal conditioning equipment and the sampling rate were chosen accordingly. The sampling rate was set to 12.8 kHz giving exactly 256 measurements per signal at 50 Hz, which was suitable for performing FFT analysis. The 15 signals sampled at 12.8 kHz, plus an FFT-analysis over 8 cycles (2048 points) required a lengthy and complex process on the PC. Therefore, it was not possible to carry out continuous real time analysis without missing any information. An alternative approach was to use a computer platform with a DSP-based system. However, due to time constraints on the project (WPQI-project), the PC system combined with the available software tools were used.

A continuous monitoring of 5 out of the 23 different internal signals in the control system of the ASVC device was required by Siemens. In addition, any specific event on 4 of the control signals should be traced at any given time. Furthermore, in case of such an event, all 23 control signals should be recorded a few cycles before and after the event at a sampling rate of at least 6 kHz. A sampling rate of 6.4 kHz was chosen.

A separate PC was installed specifically so that in case of any event, every single sample in the 23 control signals is recorded. The use of this PC system was satisfactory in capturing every single data needed but has put a severe limitation on the calculations, which should be performed in real time.

7.5.4 Programming Tools

LABVIEW, which is a software package from National Instruments compatible with the measuring equipment, was used. LABVIEW was chosen because of its speed since it can acquire and store real time measurements on a disk very fast. It works in a Windows environment and it is a multitasking system. It includes a variety of drivers for PC peripherals and dedicated measurement boards. LABVIEW is very flexible, it is equipped with a special graphical programming language and has a number of effective algorithms for creating user interfaces.

7.6 Programs

7.6.1 Monitoring the Wind Farm

The connection of an ASVC to a wind farm influences the power quality of its associated network and introduces harmonics in the network's voltages. Therefore, it was important to study and analyse the effects of the ASVC on the network during data acquisition. A program has been specifically developed

for this purpose. Changes in the network were continuously monitored through measurements of relevant 3-phase voltages and currents – in all 15 signals sampled at 12.8 kHz (see Figure 7.2). Parameters characterising each single signal and the power production were calculated every 160 ms, i.e. 8 periods at 50 Hz, and with a total of 2048 samples per signal. The voltage and current signals are described as follows:

1) RMS — both the total RMS value with all harmonics and the RMS value of the 1st harmonic
2) Phase — of the 1st harmonic – one signal is defined as reference, and the phases of all other signals are specified as the deviation from this reference
3) Harmonics — up to the 80th or 4 kHz – derived from a FFT over 2048 samples
4) THD — calculated on the basis of the 80 harmonics
5) Frequency — of the reference signal, estimated from detection of phase changes between cycles of the 1st harmonic

The power is divided into the following categories:

1) Apparent power — calculated from RMS values of voltage and current signals – in 3 phases.
2) Active power — calculated by multiplying simultaneous measurements of voltage and current signals – in 3 phases.
3) Reactive power
   a) calculated as above, but with the currents displaced a quarter of a period.
   b) calculated using the space vector method.

Alternatively the same power categories may be determined using the positive sequence components of the system found by a 1st harmonic analysis. This analysis makes it possible to verify the symmetry of the network, which is a basic assumption for the method used in controlling the ASVC. Thus, the introduction of a final parameter defined as:

4) Asymmetry — the ratio between the negative sequence component and the positive system component.

The capacity of the PC is not sufficient for calculation of all these parameters in real time without loosing parts of the signals, notably the FFT algorithm which is a time consuming process. To reduce the load on the PC, the harmonics of just one signal were evaluated each time a set of parameters is calculated, then at the next time another signal is evaluated and so on. In this way, new parameters can be obtained twice a second, covering 16 cycles or around one third of the content of the signals.

A huge amount of data was produced and therefore effective ways of reducing this data into files of manageable sizes, to be stored on disk, was necessary. The

chosen procedure was based on storing data at 2 minutes intervals. At each interval, the mean, maximum and minimum values of all parameters are derived. A file, approximately 4.5 Mb for a 24 hours recording period, is then written to the disk. A new file, with a date dependent name, is created each midnight (i.e, at 00:00). The files may be transmitted, on demand, to DTU via the ISDN link.

The performance of the Rejsby Hede wind farm-network was analysed using these data files. Experience has shown that the data gave an adequate description of the operation of the network and allowed the effects of the ASVC on the network to be investigated.

A simple user interface was build into the program. It presents the values of most of the parameters on the screen and updates them each time new parameters are calculated. It also allows plotting of pre-selected signals and parameters.

7.6.2 Monitoring the ASVC

The internal functions of the ASVC were observed using the 23 signals, accessible from the outside as +/- 15 V signals. Five of these signals have to be monitored continuously. The mean, maximum and minimum values of each of the signals are calculated every 2 minutes and saved on disk.

In case of specific events, the recording of all 23 signals was performed. The recording consisted of a few cycles of pre-event and post-event data. This has lead to a continuous scanning of every single sample measurements from all 23 signals without missing any measurements. A sampling rate of 6.4 kHz was used, as suggested by Siemens.

A program performing both tasks have been developed. The 2-minute values are stored in files on a daily basis whereas each event is stored in a separate file. Since the recording function is very demanding on the PC, no further online analysis can be carried out.

7.6.3 Fast Data Acquisition.

There was a need for a data acquisition system which can collect measurements and store data on disk as fast as possible. Such a system was constructed. Its performance was only limited by the capacity of the ADC-board (i.e. approximately 300,000 measurements a second).

An additional program which reads the measurements from disk and plots selected signals has also been developed. It has been applied in an experiment in Rejsby Hede, where the wind farm was disconnected from the network to run in an ‘islanding’ mode. The analysis of data from this experiment is not yet completed.

7.6.4 Conversion of Data

LABVIEW stores data in a special format meaning that a conversion must be made before the data can be used by standard PC-programs. A number of DOS-programs, and which are compatible with all three types of data acquisition methods mentioned above, have been developed for this purpose. Data can be translated into ASCII CSV-files, which is the format used in spreadsheets (EXCEL), or can be transformed into binary MAT-files allowing the use of the advanced mathematical analysis of MATLAB. To facilitate the data analysis, a simple user interface was also made available, so that parameters of interest could be selected and analysed.

7.6.5 WEB-page

A WEB-page showing the production of power in Rejsby Hede is featured on the Internet with the address: **http://www2.eltek.dtu.dk**. The WEB-page is accessible through standard Internet browsers from Netscape or Microsoft. The system is set to manage a large number of Internet users simultaneously. The Internet connection is established via a http-Server at DTU. The generation of the data and plotting of curves are made by two JAVA-programs, one running on the Server and the other running on the Internet user's – the client's – machine. The client receives the JAVA program through a JAVA- applet included in the html-page.

Three curves are plotted on this page. Two of the curves display the total active and reactive power produced by the wind farm, and the third shows the reactive power produced by the ASVC over the past 24 hours. The curves are updated each 15 minutes. The power data from Rejsby Hede is created and stored in a special data file by the PC, which monitors the wind farm performance. The server reads the files and transfers the necessary data to DTU over the ISDN link.

7.7 Measuring Results

After commissioning of the ASVC measurements were recorded.

Figure 7.12 shows the measurements of the mean values over a 2 minutes period of power, ASVC's reactive power and the resulting reactive power from the network to the wind farm. The ASVC was started on the 22nd of October at about 9 o'clock. After a test with maximum VAr-production, it was capable of supplying all the reactive power requirement of the induction generators in the wind farm. On midday of the 23rd of October, the ASVC was operating at its maximum reactive power output of 8 MVAr. This meant that some of the wind farm's reactive power demand was supplied from the network.

Figure 7.13 shows the measurements in more detail from the 23rd of October. This figure shows the power, the reactive power exported to the network and

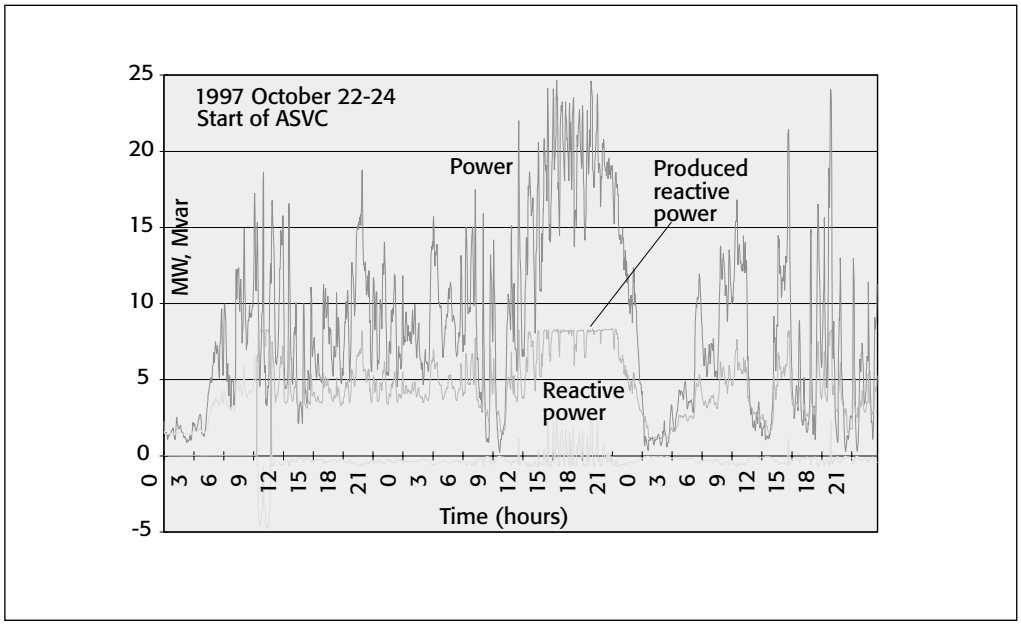

Figure 7.12. 72 hours measurements of generated power, generated reactive power and resulting reactive power to the network. All points are mean values over a 2 minutes period.

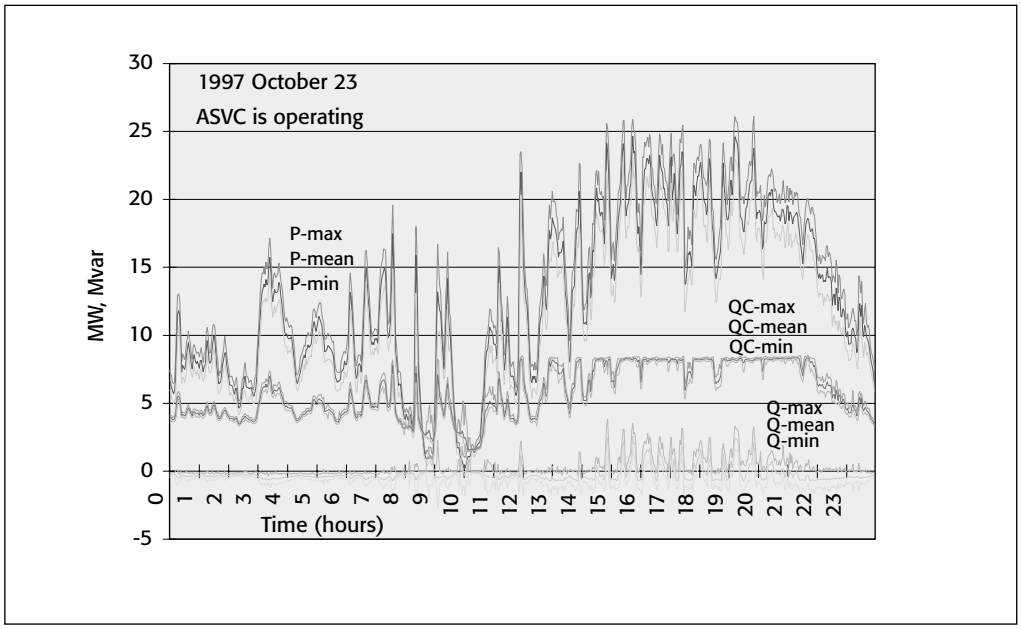

Figure 7.13. 24 hours measurement of generated power, generated reactive power and resulting reactive power to the network (Maximum, mean and minimum values over a 2 minute periods).

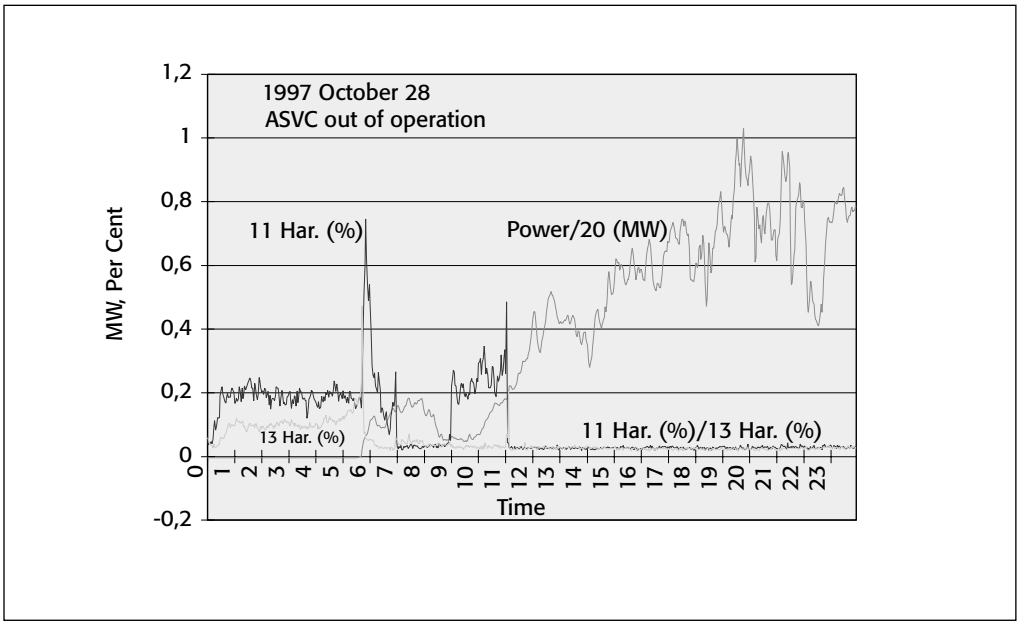

Figure 7.14. 11th and 13th harmonics in network voltage related to the power output from the windfarm with the ASVC out of service.

the produced reactive power from the ASVC. The curves show the maximum, the mean and the minimum value over a 2 minutes period for each of the variables.

During certain conditions, the wind farm was shown to be sensitive to the 11th and 13th harmonics, as shown in Figures 7.14 and 7.15. In Figure 7.14, the ASVC was out of operation and disconnected from the network. This figure contains the power curve (red) which was conveniently scaled, and curves representing the 11th and 13th harmonics. Figure 7.15 shows the same plots as in Figure 7.14 but with the ASVC in operation. The ASVC was carefully designed to eliminate 11th and 13th harmonics and therefore it was concluded that these harmonics may have been generated by the network.

It was also noted that 11th and 13th harmonics increase dramatically when the power decreases to a level of 1 MW or less. When the power is less that 1 MW, it means that all wind turbines are operated at low speed (6-poled state) with the smaller or even no power factor capacitors. This condition leads to a resonance condition for frequencies about 600 Hz in the wind farm. Unfortunately, this condition could not be further investigated since it was not possible to monitor the performance of each single wind turbine.

In Figure 7.16 the amplitudes of most of the largest harmonics are shown.

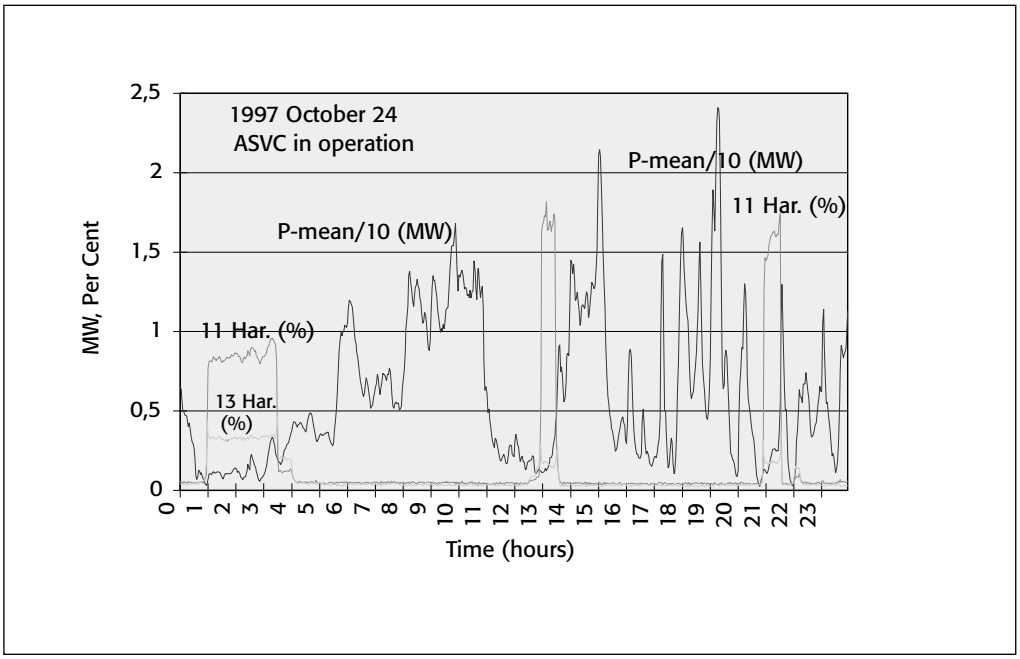

Figure 7.15. 11th and 13th harmonics in grid voltage related to the power output from the windfarm with the ASVC in service.

There are no critical harmonics at higher frequencies in the data (recorded between the 22nd and the 24th of October 1997). A comparison between this figure and Figure 7.12 shows that there is no visible correlation between wind farm generation and harmonic amplitude.
The data material is still to small for doing any conclusions about conditions under which special harmonics occur, but the measurements continue.

Figures 7.17 and 7.18 show the deviation of the phase voltage in phase R on bus 2 and bus 1 respectively.

The ASVC, connected to bus 2, was in operation from about 9 o'clock. During the first one and a half hour, the ASVC was working with full reactive power which explains the increase in the voltage (4 %) at bus 2 and the decrease of approximately the same percentage in bus 1 voltage. The power and reactive power at each bus are plotted individually in two separate figures. To obtain the total power and reactive power, the two curves from bus 2 and bus 1 must be added.

Figure 7.19 shows the three phase voltages (designted R, S, T) on bus 1, which is the bus without the ASVC. Figure 7.20 shows the three phase voltages on bus 2, which is the bus with the ASVC and this explains the variations observed in these waveforms. The power generated when the measurements were carried,

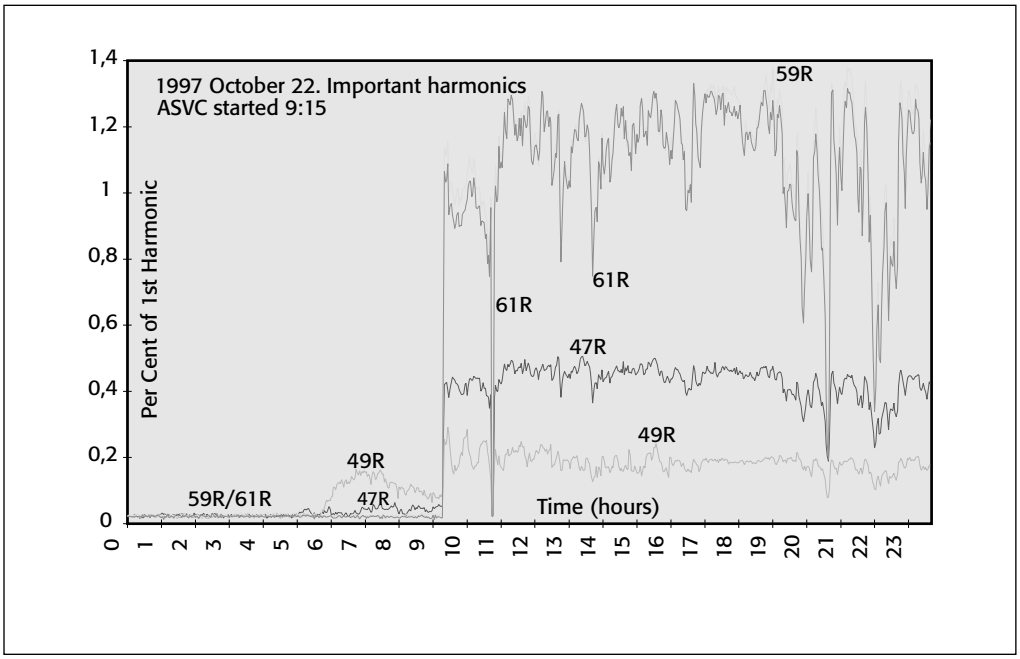

Figure 7.16. Harmonics 47, 49, 59 and 61 in the network voltage before and after connection of the ASVC.

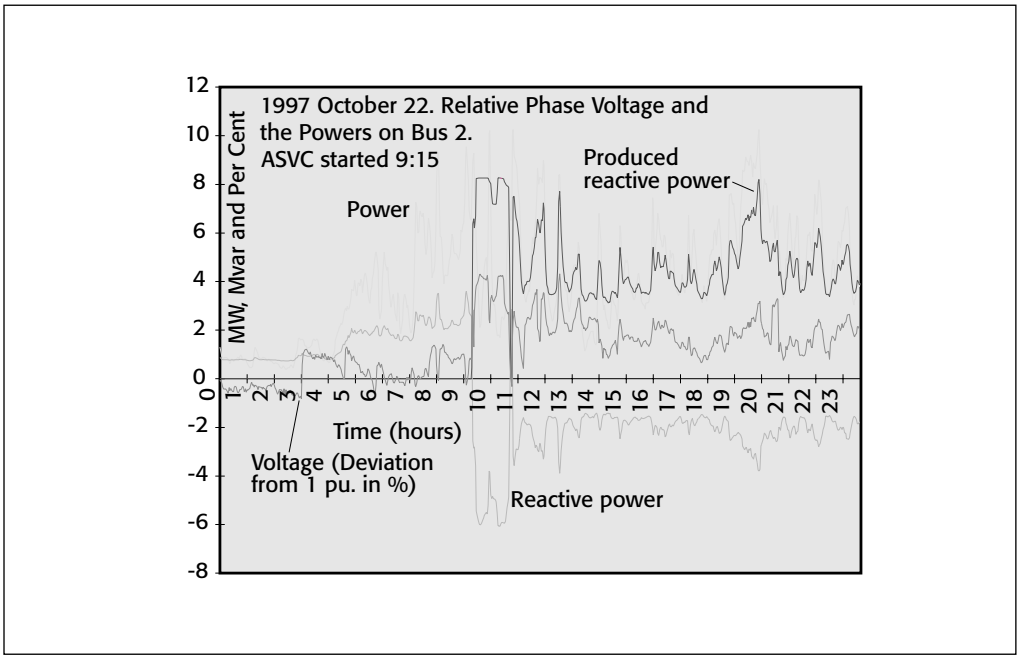

Figure 7.17: Relationship between phase voltage and reactive power on bus 2.

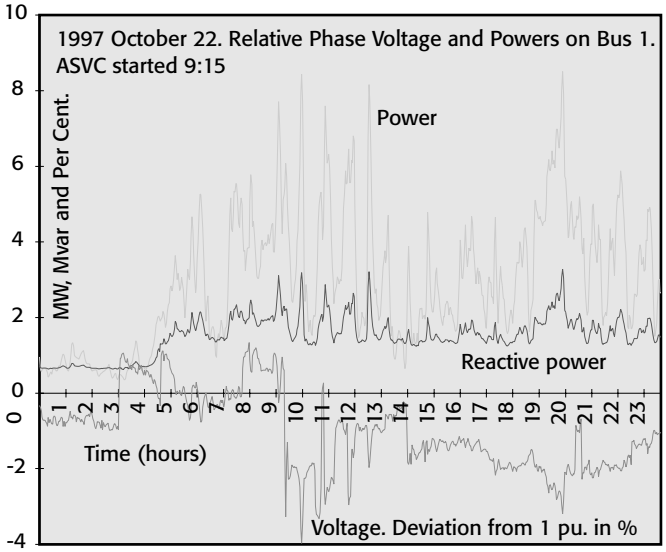

Figure 7.18. Relation between phase voltage and reactive power on bus 1.

approximately 17 MW, is far beyond the power level which may give rise to 11th and 13th harmonics. The disturbance observed in these waveforms may be caused by higher harmonics as shown in Figure 7.16.

Figures 7.21 and 7.22 show the currents at bus 1 and bus 2 respectively. The currents from the ASVC are shown in Figure 7.23. This waveform contains oscillations generated as a result of the switching of the power electronics. The combination of delta/delta and delta/star for the connection of the two units of the ASVC and the appropriate choice of the firing angle for the GTO-thyristors have resulted in mitigating these oscillations and bringing the curve to a near pure sinusoidal waveform.

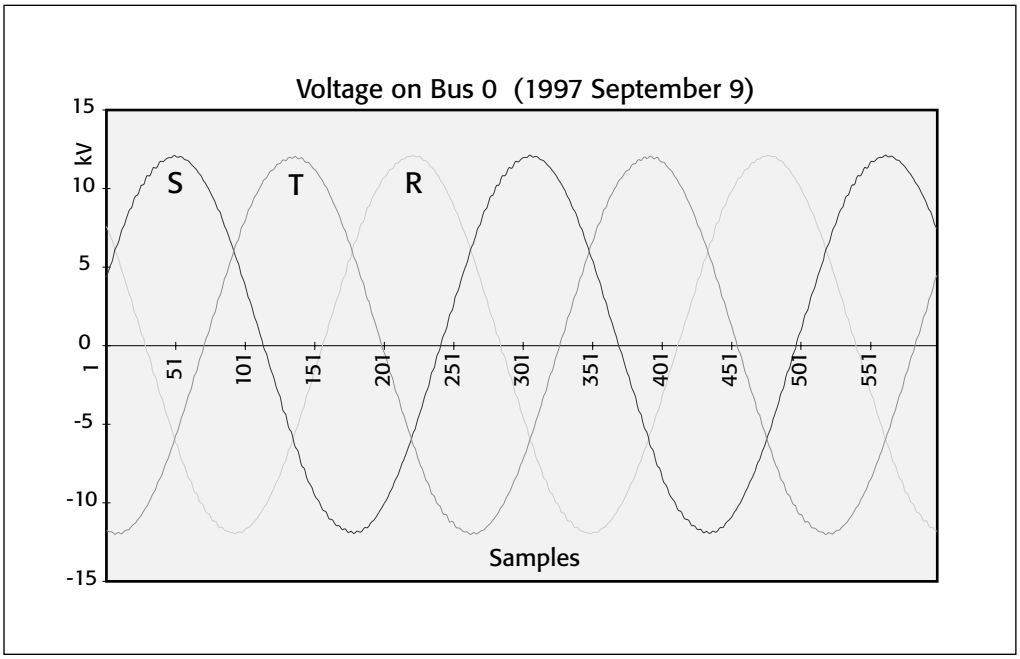

Figure 7.19. Phase voltages on bus 1.

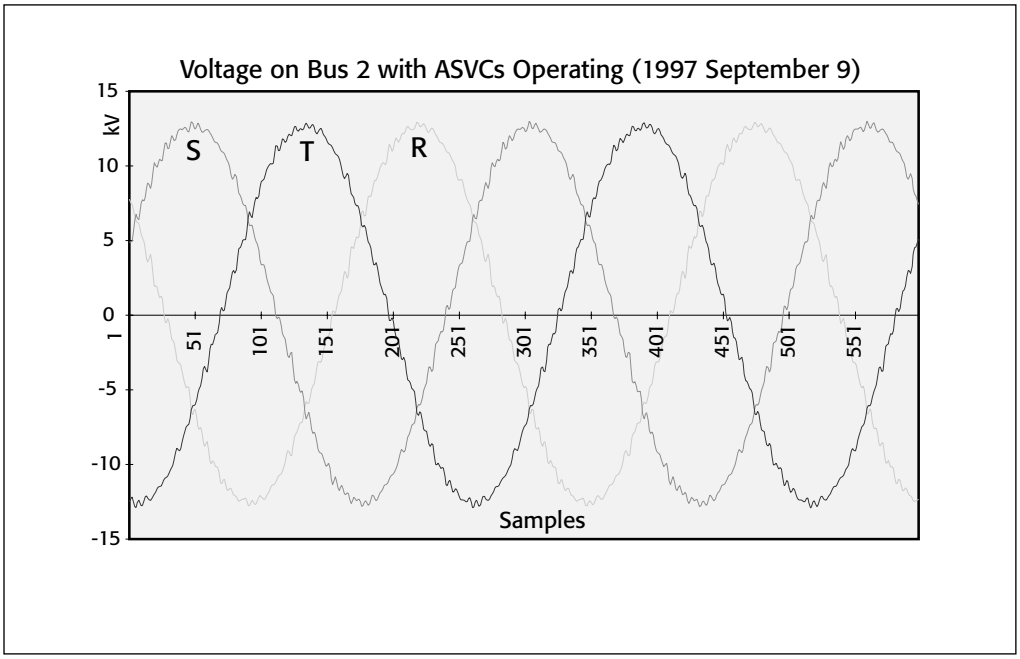

Figure 7.20. Phase voltages on bus 2.

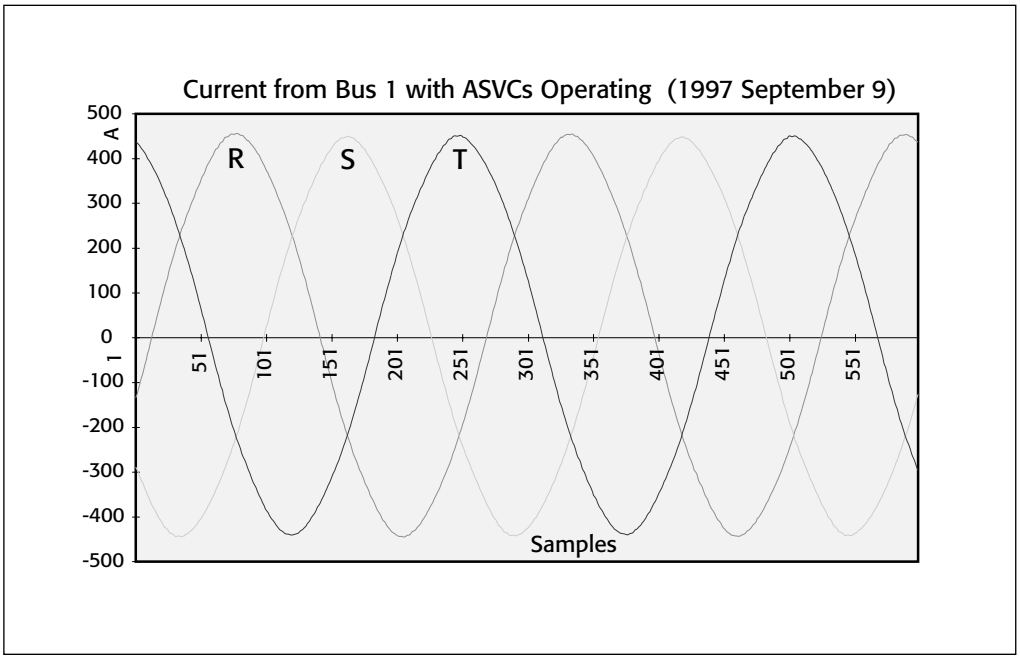

Figure 7.21. Current at bus 1.

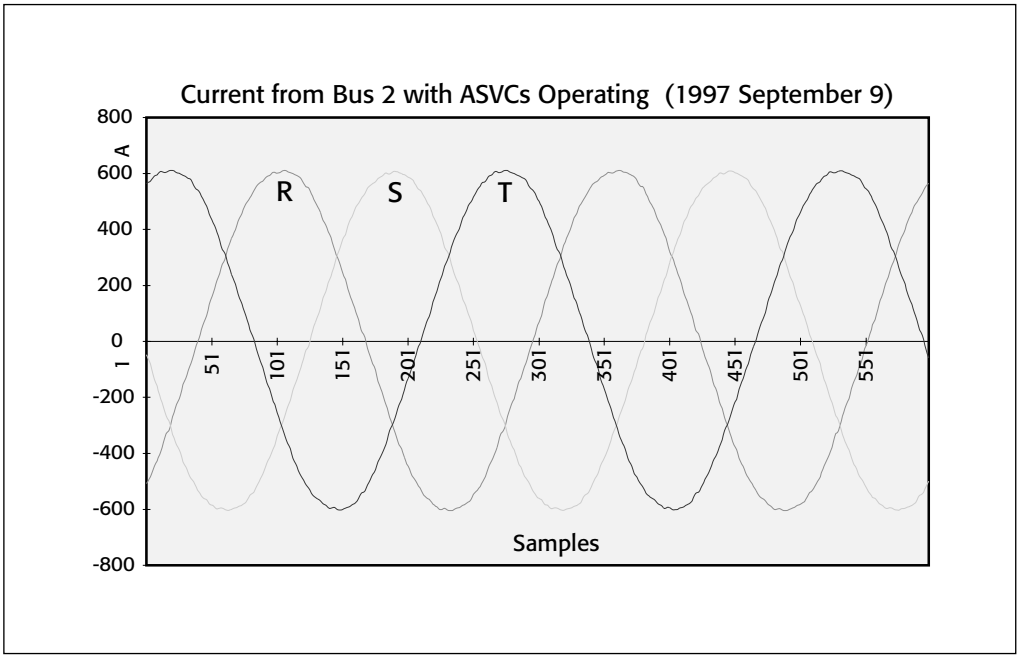

Figure 7.22. Current at bus 2.

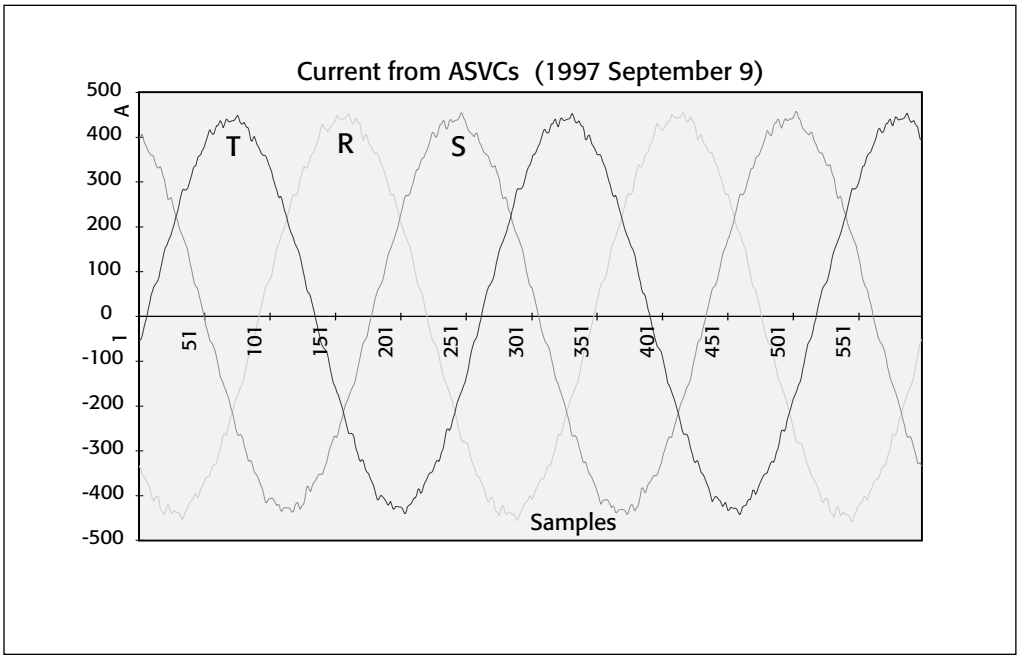

Figure 7.23. Current from the ASVC.

Chapter 8

The Application of Advanced Static VAr Compensators (ASVCs) to Other Wind Farms

Zouhir Saad-Saoud, Maria Luiza Lisboa, Nicholas Jenkins, Goran Strbac
Department of Electrical Engineering and Electronics
UMIST
PO Box 88
Manchester
M60 1QD
ENGLAND

Janaka Ekanayeka
Department of Electrical and Electronic Engineering
Faculty of Engineering
University of Peradeniya
Peradeniya
SRI LANKA

8.1 Introduction

The economic and technical aspects of connecting wind generation into distribution networks are of significant interest to both wind farm developers and network operators [1] and effective reactive power control and voltage regulation can have an important influence on the level of embedded generation which is acceptable and on the costs of its connection [2-4].

Therefore, a comprehensive set of studies was undertaken to investigate the use of Advanced Static VAr Compensators [5-8] to improve both the steady state and dynamic impact of wind farms on the networks to which they are connected. The application of ASVCs to three different wind farms was investigated and their effects on networks' power losses, on the voltage profile and on the amount of the active power that can be injected were examined.

8.2 Study Case 1

Study Case1 was that of a large (21.8 MW) wind farm connected to a rural 33 kV network with a low short circuit level. The size of the wind farm is similar to that of Rejsby Hede but the distribution network is at a lower voltage level (33 kV rather than 60 kV) and with a much lower short circuit level.

A simple representation of the electrical network is shown in Figure 8.1. The wind farm consists of 36 x 600 kW fixed speed stall regulated wind turbines. Each wind turbine is connected to the wind farm power collection network by a 630 kVA, 0.69/33 kV transformer. Power factor correction capacitors of 175 kVAr are connected at the terminals of each wind turbine generator. The wind farm is connected to the 33 kV network at B5 by mainly an overhead line with a small section of underground cable. The reactive power demand of the induction generators at rated output is 10.5 MVAr. This leads to a reactive power deficit of 4.2 MVAr which, unless supplied by an ASVC, will be obtained from the network.

Under normal operating conditions, the three phase short-circuit level at the boundary of the wind farm (B6) is 121 MVA with an X/R ratio of the source impedance of 2.24. In the event of a fault on one of the 33 kV circuits between B2 and B5, the fault level at the wind farm 33 kV connection will drop to 85

MVA with an X/R ratio of 2.18. Therefore, the ratio of fault level to embedded generation rating for this network is 5.6 under normal conditions, dropping to 3.9 under outage conditions.

8.2.1 Steady State Performance

Unity Power Factor and Optimal Power Flow Control (UPF)

At Rejsby Hede, a Unity Power Factor based control strategy was adopted. The UPF based control strategy makes the power factor of a wind farm equal to one ($\cos \alpha = 1$), resulting in a zero reactive power flow between the distribution network and the wind farm at all times. With this control scheme, the wind farm's reactive power requirement is locally supplied and so the impact of embedded generation on the network losses is minimised.

In order to analyse the performance of the UPF control strategy, a simple load flow simulation model was developed. The procedure was based on successive iterations between the AC load flow and a simple algorithm that determined the set voltage point of the ASVC at the wind farm busbar which leads to zero reactive power flow between the wind farm and distribution system for a given operating point. After the new ASVC voltage is determined, a load flow is performed and a new overall system solution determined. This iterative process between the two programs converges when the set point of the ASVC results in a load flow solution with no reactive power flow between wind farm and the distribution system.

The UPF control strategy does not explicitly take into consideration the network's active power losses. Therefore, an Optimal Power Flow (OPF) model which minimises losses explicitly was also developed and implemented. This model optimises the ASVC's set voltage to minimise network power losses for a given loading condition of the system. As minimisation of power losses in distribution networks is a non-linear optimisation problem, the OPF problem was solved by implementing a successive linear programming (SLP) technique, which iterates between an incremental load flow model and a linear programming algorithm. The process converges when no further improvement (reduction) in active power can be achieved: power losses are minimised by adjusting the voltage of the ASVC taking into consideration its reactive power capacity.

The UPF based control and OPF model were compared using the wind farm illustrated in Figure 8.1. The simulation results show that the UPF control leads to larger power losses than the loss minimisation based control (Figure 8.2(a)). However, the maximum difference of 51 kW, recorded for the maximum power output of the wind farm, is not very significant. By minimising the reactive power flow between the wind farm and the system, active power losses may be close to minimum, particularly if there is no load connected close to the wind farm. It is important to note that this small improvement in losses would require a significant increase in ASVC capacity (an additional 5 MVAr) as shown in Figure 8.2(b) which would be difficult to justify commercially.

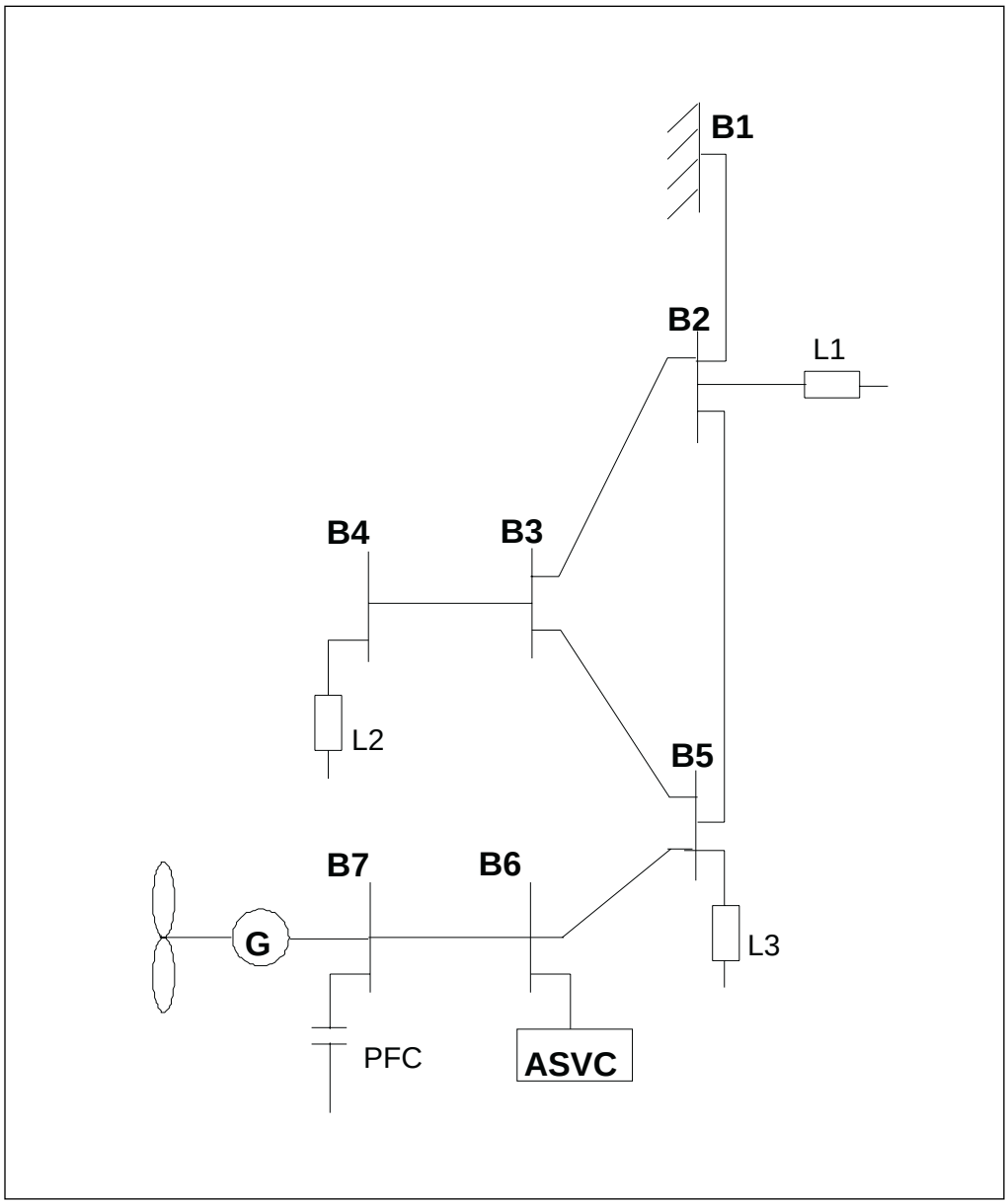

Fig 8.1 : Wind farm and network representation - Study Case 1.

For "weak" distribution systems, one alternative reactive power compensation strategy would be to increase the amount of active power that can be injected. The appropriateness of such strategy was examined by considering the voltage profile and reactive power flows under extreme, but realistic, operating conditions: light loading of the network with high levels of active power output of

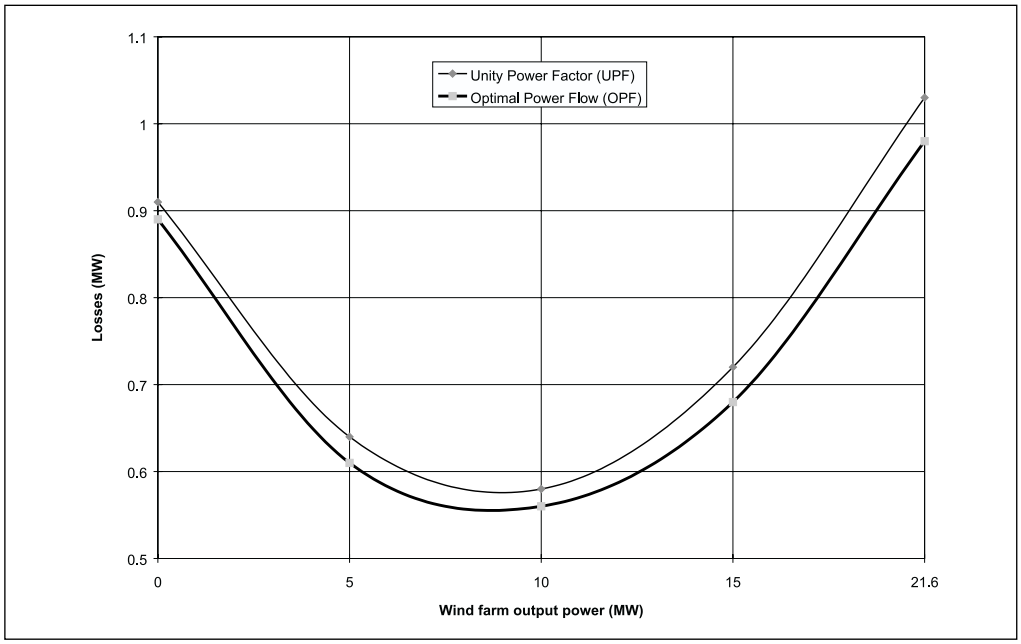

Fig 8.2(a): Comparison between Unity Power Factor (UPF) and Optimal Power Flow (OPF) control in terms of network power losses (maximum network load).

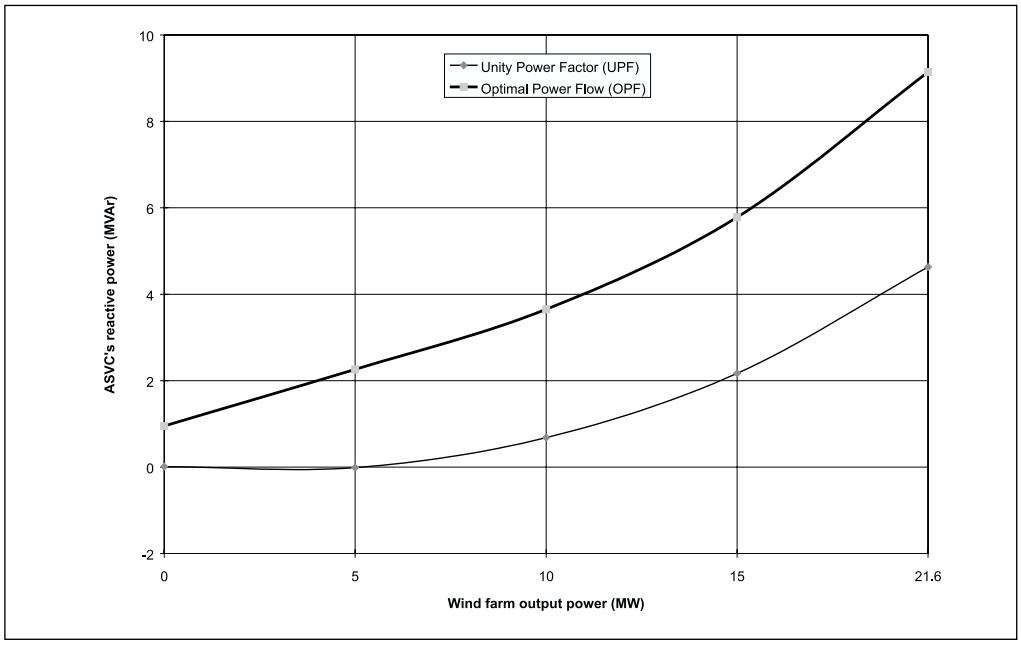

Fig 8.2(b): Comparison between Unity Power Factor (UPF) and Optimal Power Flow (OPF) control in terms of ASVC's reactive power requirement (maximum network load).

wind farm. A maximum allowable voltage fluctuation of +/- 5 % was assumed. The OPF was employed to compute the minimum reactive power that should be imported by the ASVC to maintain the voltage within these limits, and was compared with the UPF strategy.

When light loading of the distribution system coincides with the full active power output of the wind farm, the voltage rise effect may become significant, and voltages may increase above the maximum limit. The UPF control policy is inappropriate for maintaining the voltage under such critical conditions as shown in Tables 1 and 2. Instead of acting as a reactive source, the ASVC should import reactive power from the system and reduce the voltage rise effect. With the OPF control, the reactive power output of the wind farm is adjusted to maintain the voltage in the system within the permissible range. This is achieved by importing reactive power from the system (the ASVC acts as a reactive power sink), and thus reduces the effect of voltage rise. The minimum required reactive power import using this technique was determined for various levels of active power generation as shown in Figure 8.3(a). A successful voltage control was achieved only at the expense of an increase in network power losses as shown in Figure 8.3(b). This situation is expected to arise only occasionally and so the increase in network power losses would probably be tolerable. The alternative solution of shedding generation would incur higher overall costs.

		voltage (pu)	
Busbar	no ASVC	UPF	OPF
B2	1.030	1.030	1.030
B3	1.051	1.067	1.038
B4	1.051	1.067	1.038
B5	1.054	1.067	1.038
B6	1.077	1.108	1.050
B7	1.067	1.099	1.040

Table 8.1 : The effects of various reactive power compensation schemes on network voltage with rated wind farm output.

	no ASVC	UPF	OPF
Losses (MW)	1.90	1.72	2.19
QASVC (MVAr)	0	+4.5	-3.5

Table 8.2 : Total network losses and ASVC rating under various reactive power compensation schemes.

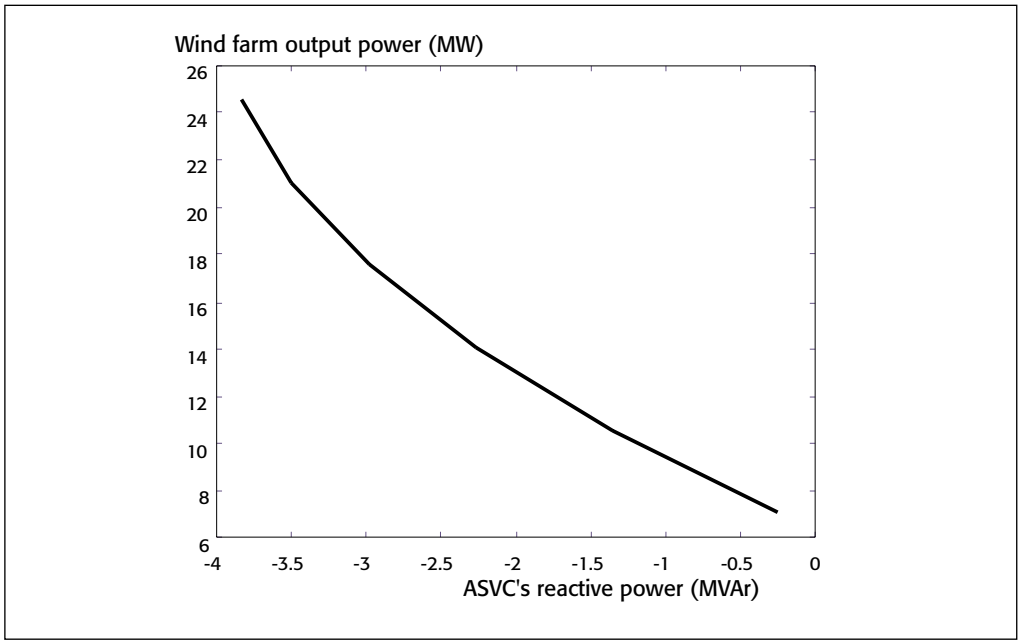

Fig 8.3(a): ASVC reactive power requirement for different levels of wind farm generation (minimum network load).

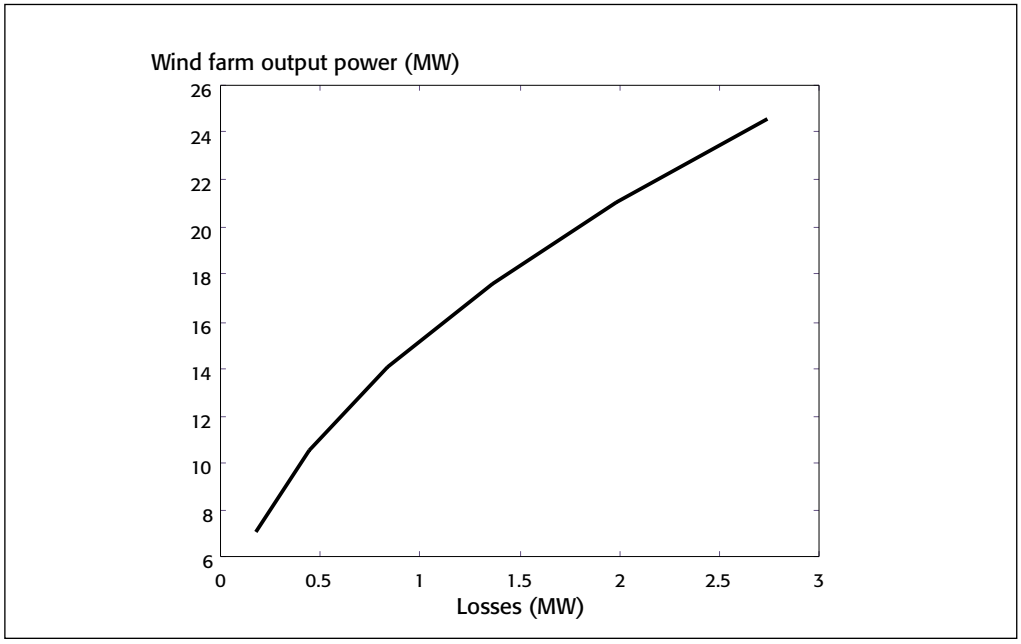

Fig 8.3(b): Network power losses for different levels of wind farm generation (minimum network load)

8.2.2 Dynamic Performance

Dynamic studies are required to investigate the transient behaviour of the network under various conditions and so appropriate dynamic analysis tools must be used. The electromagnetic transient program, PSCAD/EMTDC [9], has been used to investigate islanding phenomena and the mitigation of voltage fluctuations caused by blade passing frequency. An EMTDC model of the network, the wind farm and the ASVC was developed.

The ASVC is a three level design rated at +4.5/-3.5 MVAr and is connected to busbar B6 through a three phase D-Y transformer. It is operated in a Selective Harmonic Elimination Modulation (SHEM) mode to keep the total harmonic voltage distortion within acceptable limits. The asymmetrical rating of the ASVC is due to a 500 kVAr passive filter used to limit higher order harmonics. Two control techniques for the ASVC, based on the various established control strategies available in the literature [10-13], were implemented. A unity power factor technique used the reactive power drawn by the wind farm as the control variable for the reactive power output of the ASVC. The ASVC continuously supplies VArs to balance the reactive power demand of the wind farm up to its rating, beyond which a constant 4.5 MVAr is maintained. Alternatively, a voltage control technique maintained the voltage at the wind farm connection to a reference value by injecting or absorbing reactive power. The reference voltage of the wind farm was maintained using a proportional and integral control scheme.

Voltage Stability Performance

In a weak rural networks, where circuit impedance can be high, the voltage can be depressed by the reactive power drawn by the wind farm. In particular, when the real power produced by an induction generator exceeds its rated value, there is the possibility of voltage instability as large amounts of reactive power are absorbed [14]. This situation must be considered on wind farms as the power control of wind turbines is often imprecise. The use of an ASVC to actively control network voltage by locally supplying reactive power can reduce the likelihood of voltage instability.

To study the improvement in steady state stability of the network with the ASVC, investigations were carried out using the PSCAD/EMTDC model. The machine torque was increased from its 1 pu value and the voltage at the wind farm 33 kV busbar was measured. Figure 8.4 shows the wind farm 33 kV voltage plotted against the wind farm output power for the winter loads in the network. That figure clearly indicates the improvement of the steady state voltage stability limit when the ASVC generates 4.5 MVAr of reactive power.

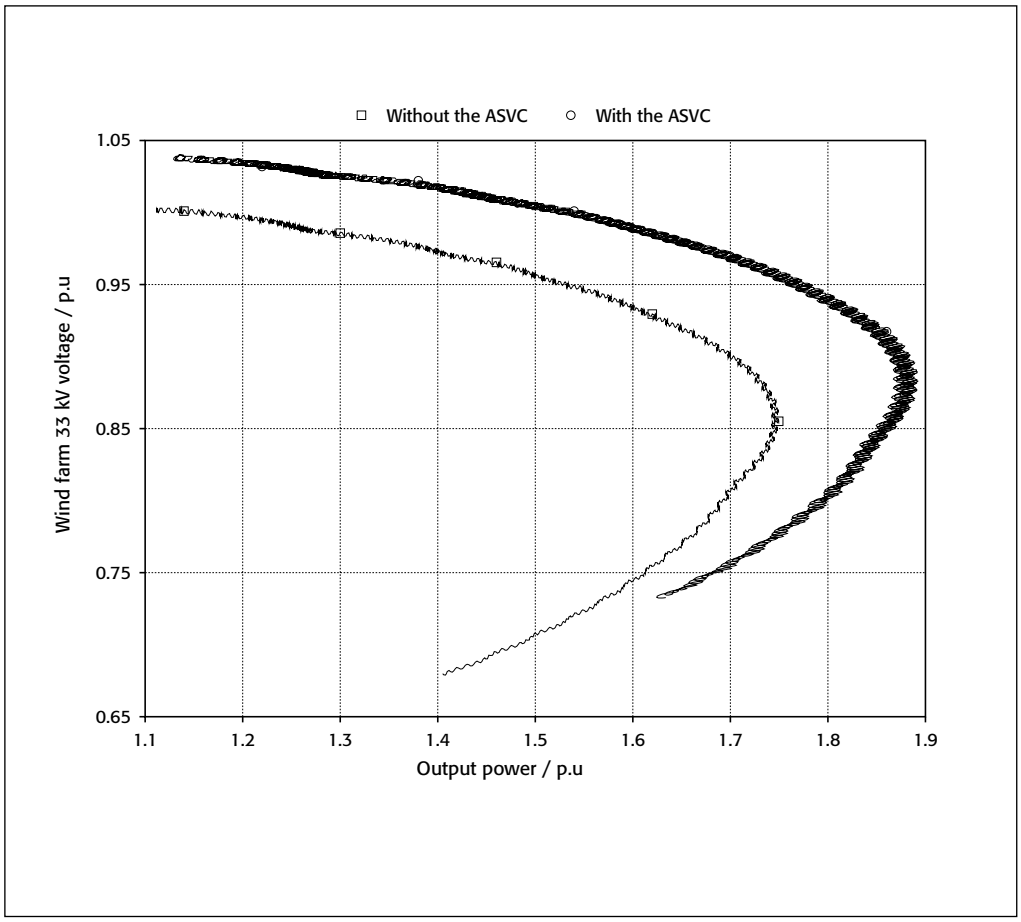

Fig 8.4: Wind farm 33 kV voltage versus wind farm output power with and without the ASVC.

Islanding

A wind farm may be isolated from the network as a result of a post-fault switching in the distribution network. This is generally referred to as "islanding" which may give rise to self-excitation of the wind turbine generators due to the presence of the PFC capacitors, thus increasing the voltage of the isolated network. Under an islanding condition, an ASVC can be used to absorb reactive power from the wind turbines, thus reducing the magnetic flux which supports the self-excitation [14,15].
In this study an islanding condition was studied by disconnecting the wind farm at the 33 kV busbar (B6). When modelling the induction machines under self-excitation conditions, the wind farm voltage increases and so it is neces-

sary to add the effect of saturation to the machine models. The machine saturation was modelled with two piece-wise linear curves. The unsaturated magnetising reactance was set to magnetising reactance plus the stator reactance and the saturated magnetising reactance was selected as 1/6th of the unsaturated reactance. Figure 8.5(a) shows the voltages at the wind farm 33 kV busbar and active and reactive power requirement of the wind farm when the wind farm is disconnected from the 33 kV system without the ASVC in service. Clearly the wind farm turbines are self-exciting and the voltage at the wind farm busbar starts increasing. The ASVC, operated under voltage control, was used to stabilise the wind farm voltage under this condition and Figure 8.5(b) shows the results obtained with the ASVC. The 33 kV voltage is maintained close to its set point value of 0.99 pu although there is a voltage transient at the instant of islanding caused by the delayed response of the phase locked loop control system of the ASVC.

Mitigation of voltage fluctuations

When a wind turbine blade passes its tower, it produces a pulsating torque in the induction generators, of up to 20 % of rated output thus creating a voltage fluctuation in the network around the wind farm. If the wind farm becomes synchronised, i.e. the blades on different wind turbines all pass the towers at the same time, then the power fluctuations at the blade passing frequency will add together. The network voltage fluctuations can then become very high.

When a wind farm is synchronised, the synchronous torque is transferred through the wind farm by voltage fluctuations on the circuit [16]. By stabilising the 33 kV voltage the synchronous torque can, no longer, be transferred. Stabilising the wind farm 33 kV is a very interesting application of an ASVC as both absorbing and generating modes of the ASVC can be used alternatively in this case.

To study the possibility of applying an ASVC to mitigate voltage fluctuations at blade passing frequency, a pulsating torque with magnitude variation ±20 % and frequency of 1.6 Hz was applied to the torque input of the wind farm generators. The ASVC was connected to the circuit using the voltage control technique described in Section 8.2.2. The results obtained with and without the ASVC are shown in Figure 8.6. A similar result was obtained with the 33 kV voltage signal passed through a washout filter or change function [11].

From Figure 8.6, it is clear that the ASVC can mitigate voltage fluctuations at the wind farm 33 kV busbar effectively. Due to the active power variations within the wind farm, the voltage at the wind farm 690 V busbar fluctuates even though the ASVC is in operation. However, eliminating the voltage fluctuations at the wind farm 33 kV is an important result as it should allow the synchronised operation of the turbines to be disturbed and the synchronism broken.

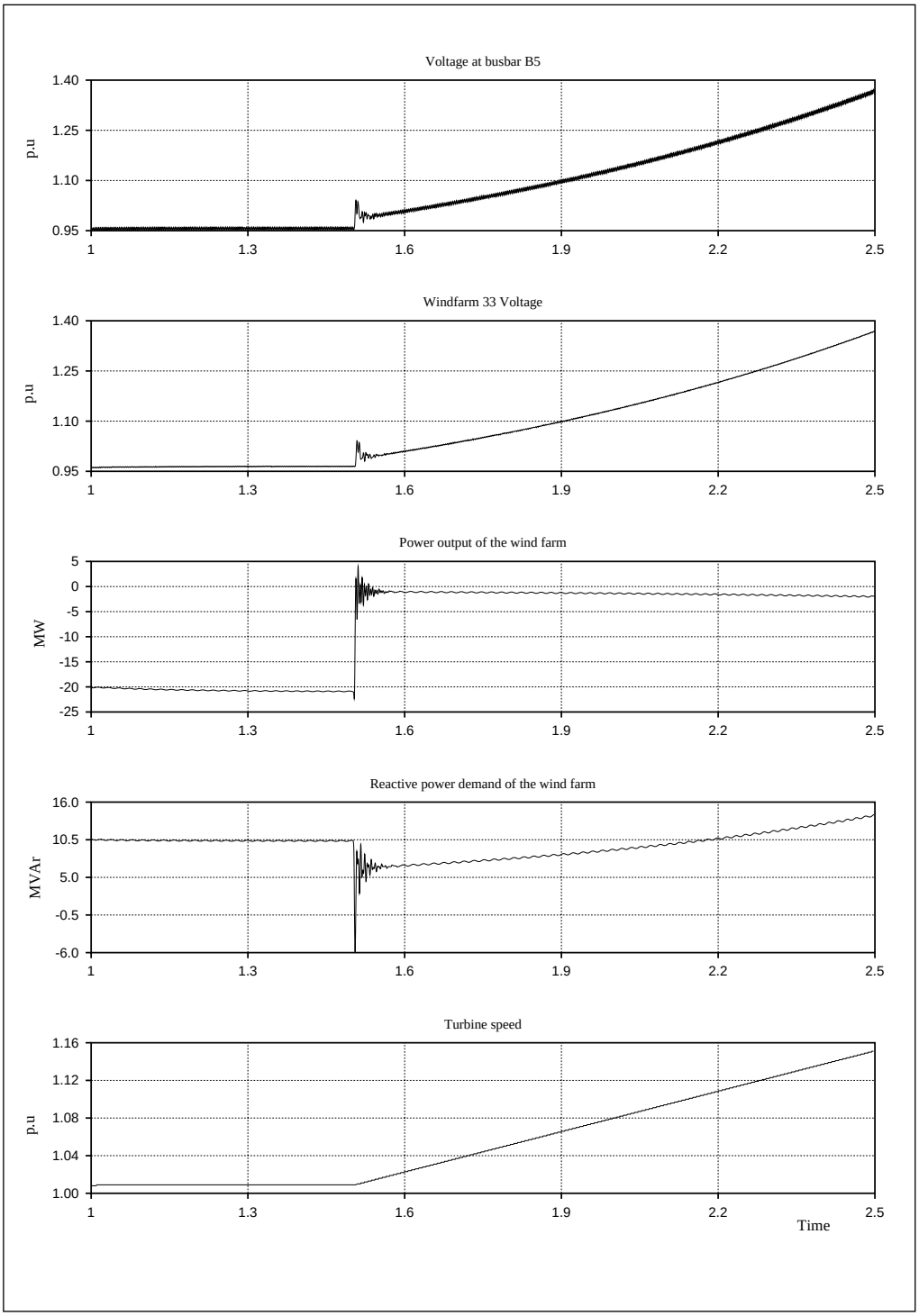

Fig 8.5(a): Islanding at the wind farm 33 kV busbar without the ASVC.

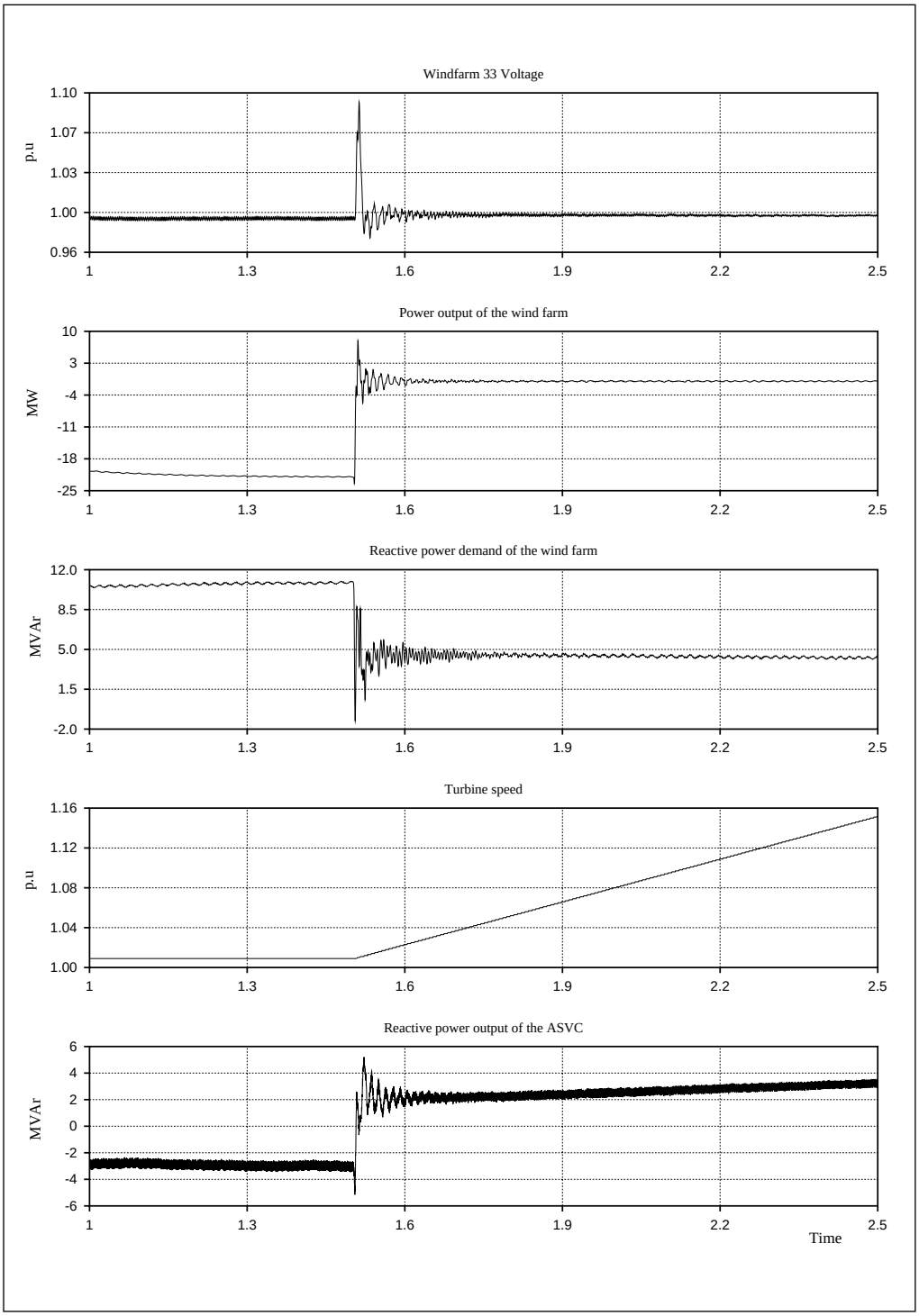

Fig 8.5(b): Islanding at the wind farm 33 kV busbar with the ASVC.

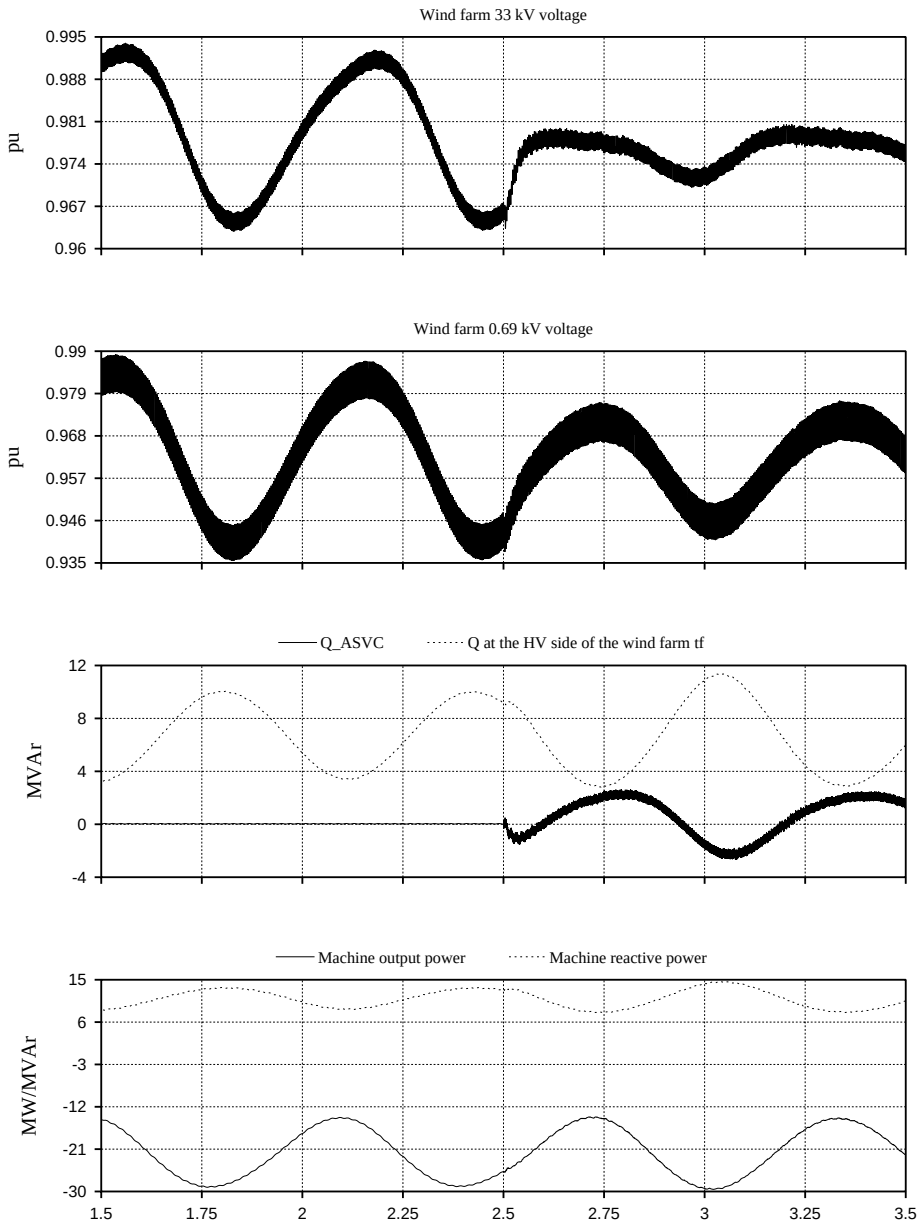

Fig 8.6: ASVC used to mitigate voltage fluctuations created by pulsating torque.

8.3 Study Case 2

Study Case 2 was a medium size wind farm (15 MW) sited in a remote area. The available distribution voltage levels were 20 kV and 66 kV and there was considerable interest in connecting the wind farm at 20 kV both to reduce costs and to minimise the environment impact of the long overhead circuits which would be required. However, this type of connection is characterised by a rather low ratio of fault level to wind farm rating (i.e 3.5), under normal operating conditions.
The main aspects of interest in the study case were: (1) steady state voltage, (2) distribution network losses and (3) voltage stability.

A simple representation of a section of the network to which the wind farm is connected, is shown in Figure 8.7(a). The wind farm is rated at 15 MW and was represented by thirty 500 kW stall regulated wind turbines. Each wind turbine is equipped with a local power factor capacitor of 187.5 kVAr. The connection of the wind farm to the electrical network will be at the 66/20 kV substation and so both 20 kV and 66 kV connections were considered. The connection circuits, 20 kV or 66 kV, would be approximately 15 km of overhead line with short underground sections at each end close to the utility and wind farm substations.

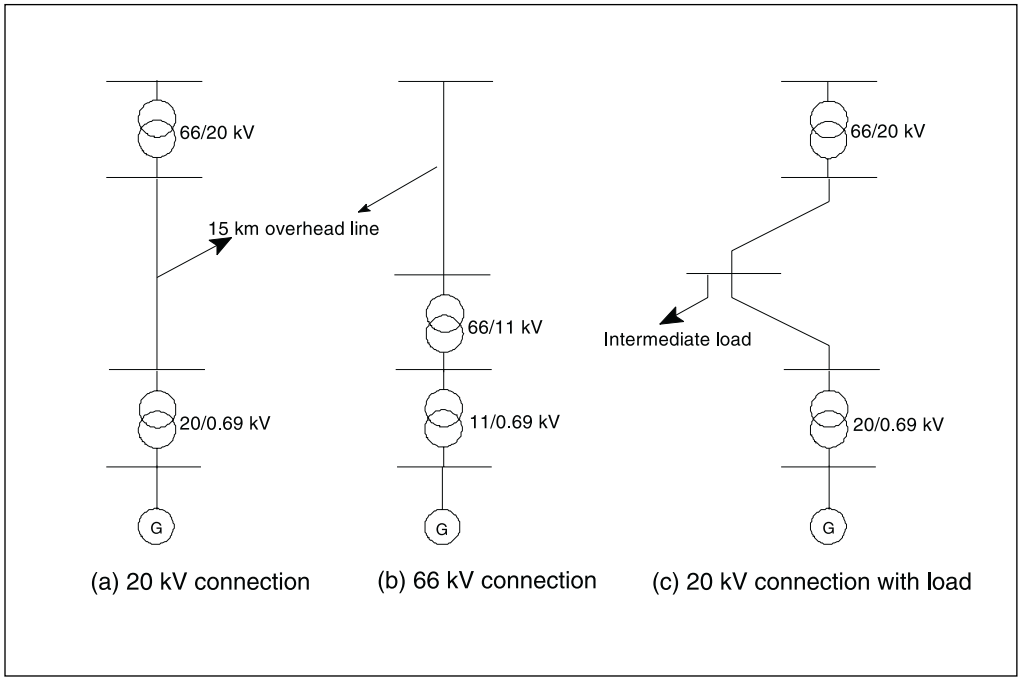

Fig 8.7: Simple representation of the wind farm with various options of connection - Study Case 2.

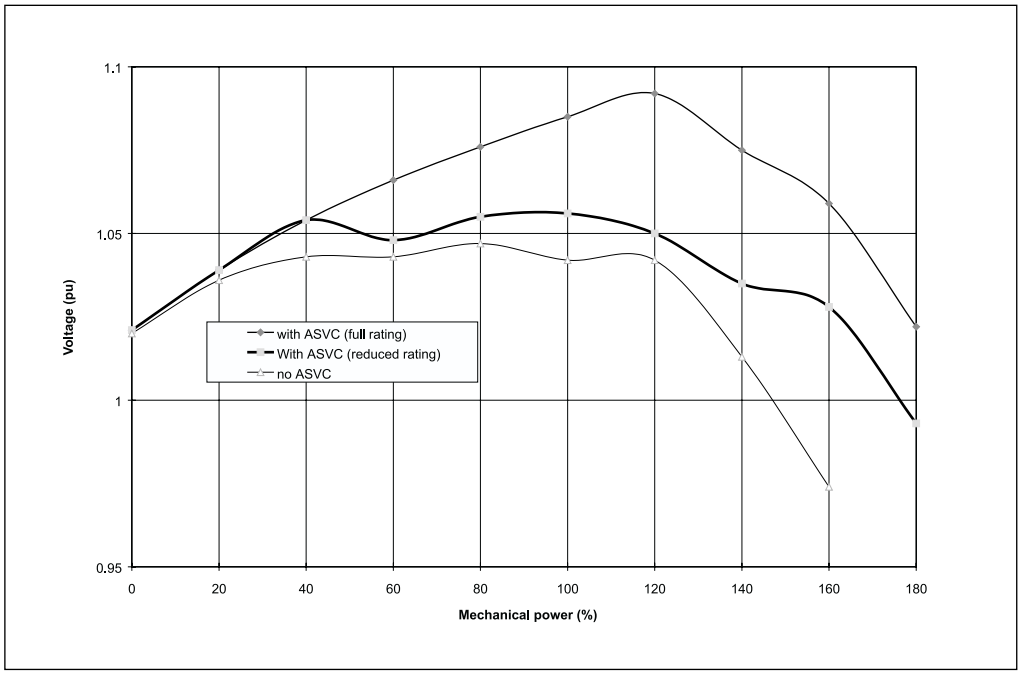

Fig 8.8: Voltage at 20 kV busbar with varying wind farm output.

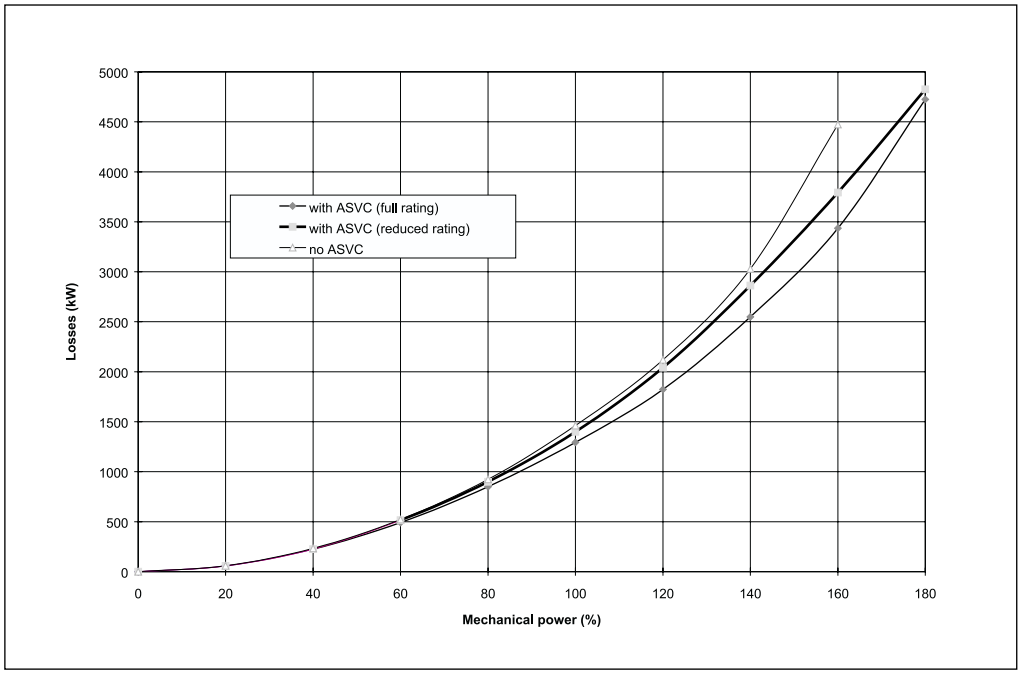

Fig 8.9: Variation of network losses with wind farm output.

The application of an ASVC for the compensation of the reactive power demand of this wind farm, during various operating conditions and with both options of connection, was investigated. The ASVC was used to balance the reactive power demand of the 20 kV or 66 kV circuit, up to its rating. These studies were carried out using the IPSA [17] software.

8.3.1 20 kV Connection

The voltage at the 66/20 kV Substation is kept constant at 20.4 kV (1.02 pu) using on-load tap changers of the 66/20 kV transformer. The power output of the wind farm was varied from zero to 160 %, after which the system becomes unstable. The corresponding voltages at the 20 kV busbar are shown in Figure 8.8. The kink in the voltage, at 60 % of mechanical power, is due to the operation of the transformer on-load tap changer. The 20 kV connection results in high losses of nearly 1.5 MW at rated output as shown in Figure 8.9.

The effect of adding a +/- 4 MVAr ASVC at the wind farm (20 kV busbar), using a unity power factor control scheme, was to increase the stability limit to 180 % and reduce losses by 168 kW at rated output as shown in Figure 8.9. This also led to excessive voltage on the 20 kV circuit, 9 % at full generation as shown in Figure 8.8, and therefore it would not be possible to apply the full rating of the ASVC (i.e +/- 4 MVAr). A reduced ASVC rating of +/- 2 MVAr was considered to supply part of the wind farm reactive power demand and to keep the wind farm 20 kV voltage within limits (0.94-1.06 pu). This strategy resulted in a stability limit of 180 % and a reduction in losses at rated wind farm output of 65 kW.

Apart from the high losses in the connecting circuit, the 20 kV connection without an ASVC appears to be acceptable. As the reduction in losses with the ASVC was modest it would appear to be difficult to justify the application of a compensator in this situation.

8.3.2 66 kV Connection

The wind farm is connected through a 66 kV circuit to the high voltage side of the 66/20 kV transformer, as shown in Figure 8.7(b). Two transformers, 66/11 kV and 11/0.69 kV, were used to step up the voltage of the wind turbines. The voltage at the 11 kV busbar is kept constant at 1.0 pu using the on-load tap changers.

Figure 8.10 shows the variation of the wind farm voltage with different levels of generation. The wind farm was shown to be stable up to 153 % of mechanical input power under normal conditions. The kinks in the voltage at the 66 kV busbar are due to on-load tap changer on the 66/11 kV transformers to keep the voltage at the 11 kV busbar constant at 1 pu. The 66 kV voltage connection circuit results in reasonable losses (750 kW at rated wind farm output) with only a small change in voltage at the wind farm (i.e, 0.08 %) as shown in Figures 8.10 and 8.11.

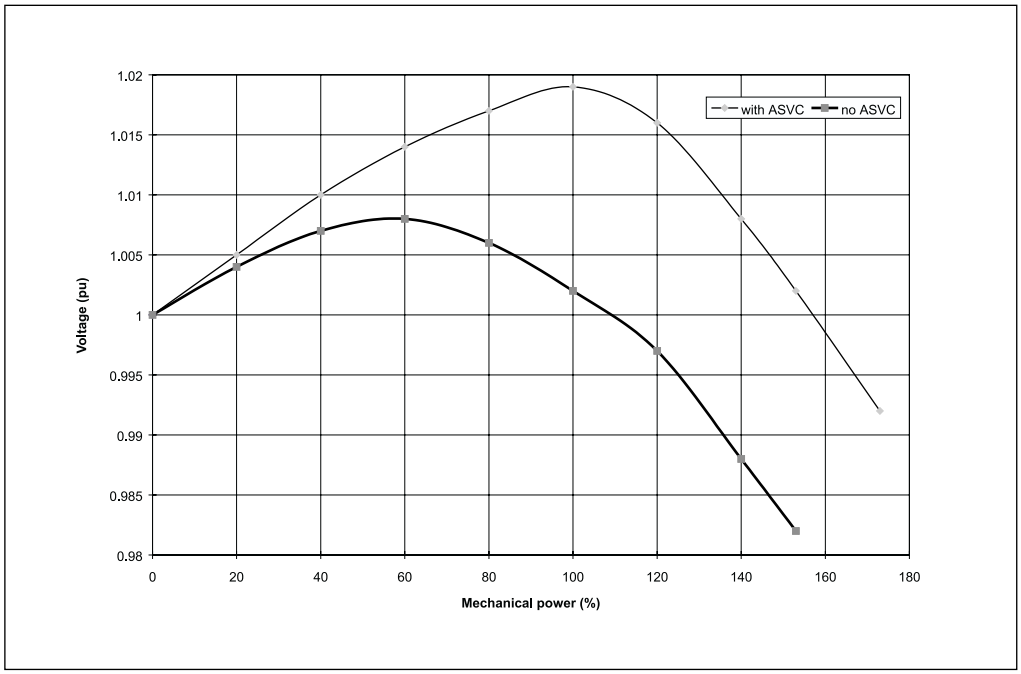

Fig 8.10: Voltage at 66 kV busbar with varying wind farm output.

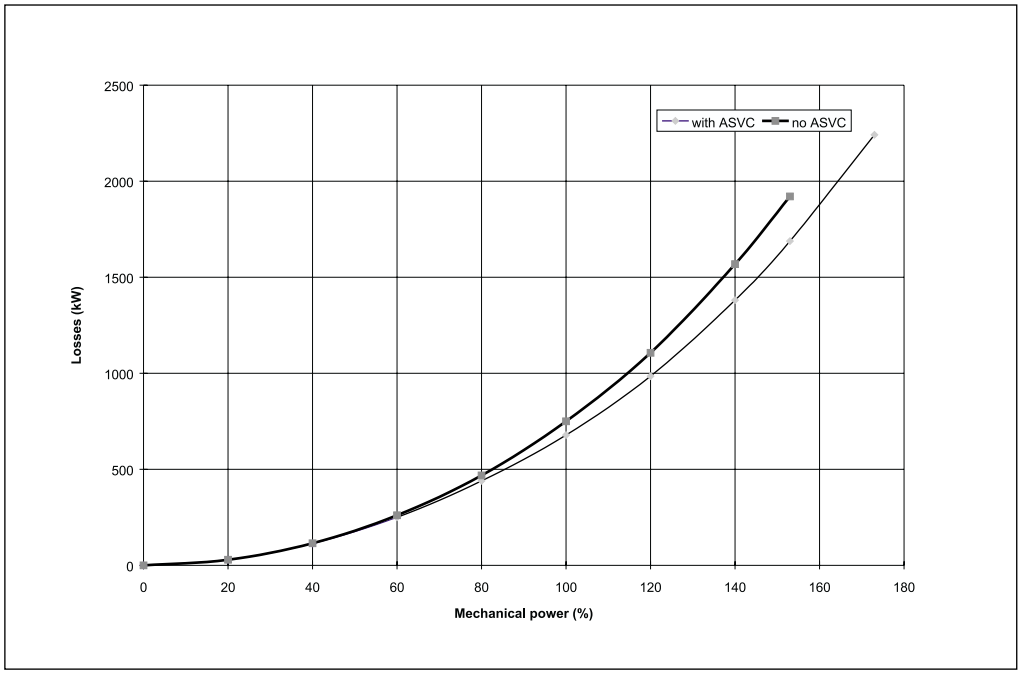

Fig 8.11: Variation of network losses with wind farm output.

The effect of applying a +/- 4 MVAr ASVC at the wind farm was to increase the stability limit to 173 % and to decrease the losses by 72 kW at rated wind farm output as shown in Figure 8.10 and 8.11 respectively. The 66 kV connection arrangement appears to be satisfactory without the ASVC and the reduction in the network losses was small, it is likely to be very difficult to justify the additional cost of the compensator.

8.3.3 20 kV Connection with Intermediate Load

The 20 kV circuit is very resistive and so the losses are high. The only effective way to reduce losses in this circuit is to connect a load to it. This is likely to be desirable as 20 kV is used as a distribution voltage in the network, to which the wind farm is connected, and consumers are supplied from fixed tap 20/0.4 kV transformers. In addition, the 20 kV overhead line is so long that it is likely that loads would be connected along it. A 5 MW, 0.98 power factor load block, representing peak loads, was connected at the mid-point of the circuit, as shown in Figure 8.7(c). Summer loads were assumed to be 10 % of winter loads.

The ASVC required to reduce losses and control the voltage of the 20 kV load busbar to within 0.98-1.02 pu, especially during summer loads, was rated at +/- 2 MVAr. The control strategy of the ASVC is to keep the voltage at the load busbar within the specified limits (i.e. +/- 2 %) by holding the voltage at the wind farm busbar constant at 1.02 pu. This latter corresponds to the 20 kV busbar voltage at rated output and maximum intermediate load when no ASVC is connected. This control strategy was shown to be satisfactory in controlling the load busbar voltage.

8.4 Study Case 3

Study Case 3 was that of a small wind farm connected to a rural 20 kV network. The object of this study was to investigate possible control strategies for the ASVC. Several of the voltage control techniques used on ASVCs applied to transmission systems were investigated and modelled.

A simplified equivalent circuit representation of the network is shown in Figure 8.12. The wind farm consisted of three 600 kW fixed speed wind turbine generators. The ASVC is connected at the high voltage side of the wind farm transformer and its role in controlling the reactive power requirements of the wind farm for various loads was investigated. The Matlab Power System Toolbox (PST) [18] was used for these studies.

8.4.1 The ASVC Characteristic

The ASVC characteristic, shown in Figure 8.13, was determined by the chosen voltage reference value and the slope of the control characteristic. The maximum and minimum ASVC currents define the operational boundary. The ASVC

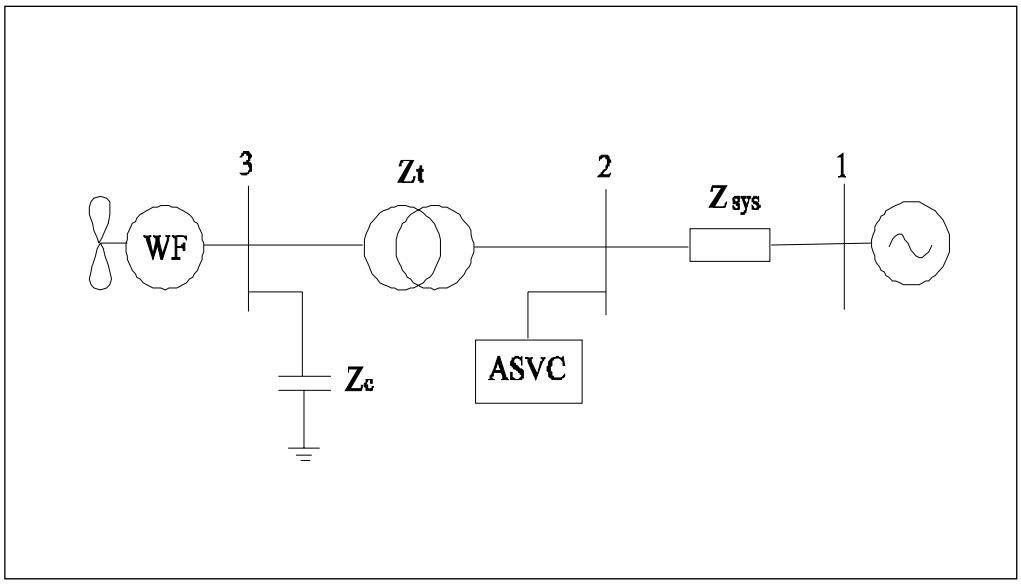

Fig 8.12: Simplified representation of the network with the wind farm – Study Case 3.

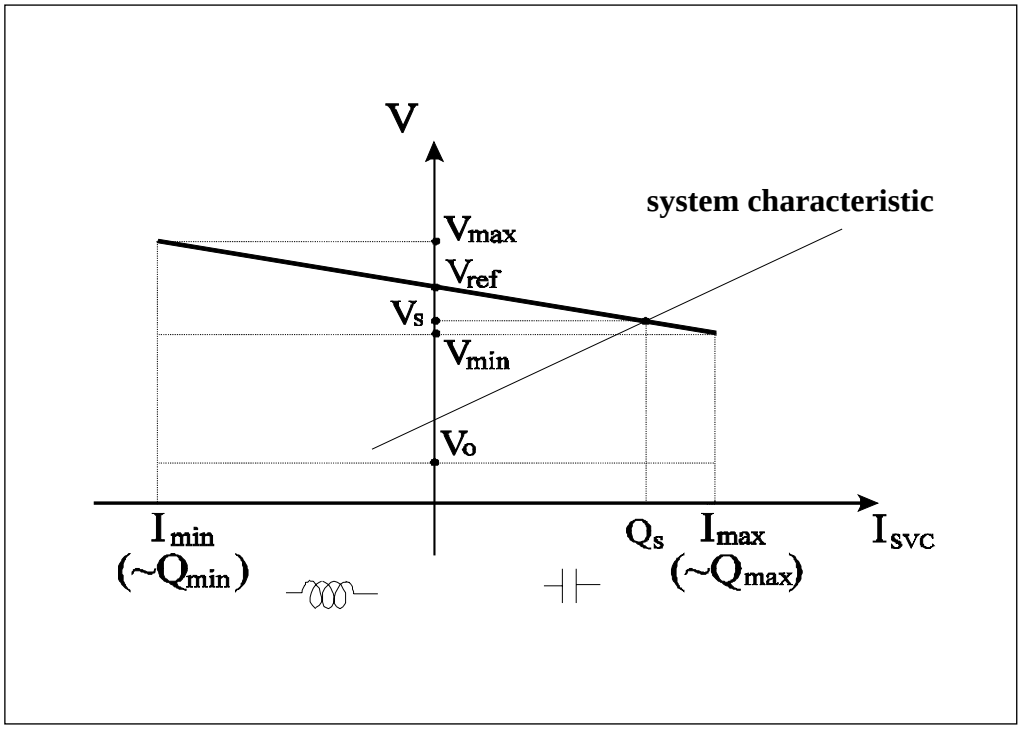

Fig 8.13: Output characteristic of the ASVC.

voltage for a particular operation condition is defined by the intersection of the system and ASVC characteristics. For voltages around the reference voltage, the ASVC characteristic is similar if expressed either as a function of the ASVC current or the reactive power capacity. The latter has been adopted in this work.

ASVC model for load flow studies

An ASVC model [19] has been implemented in the Matlab-PST load flow program. The ASVC busbar was represented as a special PQ node where the reactive power is a function of V_S, Q_{max} , Q_{min} (from the ASVC characteristic shown in Figure 8.13) as follows:

$$Q_s = V_s \left[\frac{Q_{max}}{V_{min}} (V_s - V_{max}) + \frac{Q_{min}}{V_{max}} (V_{min} - V_s) \right] \quad (1)$$

In the load flow program, the terms of the Jacobean matrix, which correspond to the ASVC busbar, were modified by adding the derivative of equation (1).

ASVC model for transient studies

A schematic diagram of the ASVC voltage control is illustrated in Figure 8.14. This is a simplified version of the control circuit described in reference [10]. For voltage control, the slope corrected actual system voltage signal is compared with the voltage reference value. The resulting voltage error signal ΔV ($\Delta V = V_{ref} - V_{act}$) is fed to the compensator block, whose output signal represents the required ASVC susceptance B_{ref} to correct and minimise the voltage error ΔV. The compensator block is represented by a lag function of the form (k/1+sT) to improve the ASVC response by responding to sudden changes in the network by smoothly changing to the appropriate voltage corresponding to the slope control characteistic. A Proportional-Integral controller may also be used, as suggested in reference [10]. This will allow a fast response to small voltage variations (Proportional component) and a zero voltage error signal control (Integral component). A further refinement is to use a “wash-out” filter to compensate voltage and power oscillations.

A superimposed slow reactive power control mode was added to the voltage control, once the ASVC currents or reactive power exceeded the minimum and maximum limits (I_{min} and I_{max} or Q_{min} and Q_{max}). The difference between the ASVC’s actual reactive power value and the reference value (Q_{min} and Q_{max}) is fed to a VAr regulator whose output, which is a voltage correction value, is added to the voltage reference ($_{Vref}$). This causes a shifting, along the ASVC’s voltage axis, of the voltage reference. Limits were imposed on the voltage correction value from the VAr regulator to avoid large deviations from the original selected reference voltage.

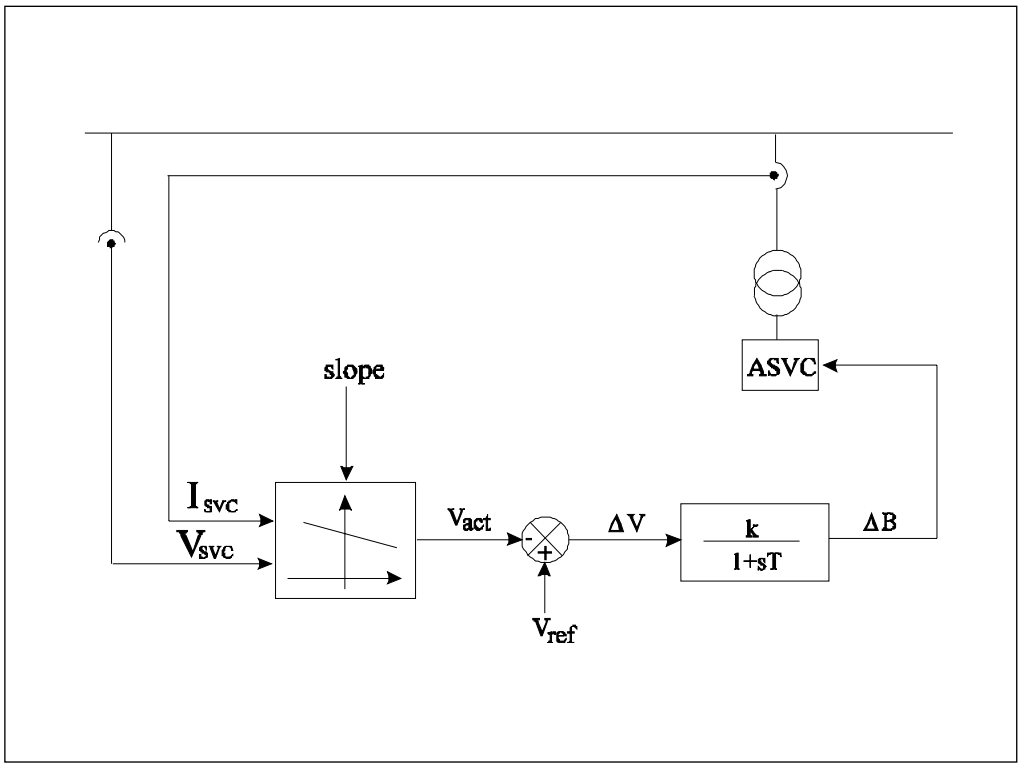

Fig 8.14: Schematic representation of an ASVC's voltage control strategy.

The original Matlab Power System Toolbox (PST) code for a conventional SVC device was based on the approach of correcting the voltage by varying the SVC susceptance. Therefore, for computational convenience, the ASVC voltage control was also based on variations of the 'ASVC susceptance'. However, B_{max} and B_{min} were not fixed values, but calculated at each time step as a function of the calculated voltage and maximum and minimum ASVC reactive power as follows:

$$B_{max} = \frac{Q_{max}}{V^2} \quad , \quad B_{min} = \frac{Q_{min}}{V^2} \tag{2}$$

8.4.2 Application of the ASVC

ASVC models were implemented in the load flow and transient Matlab PST programs. Several load flow simulations were performed to analyse the steady state response of the ASVC following changes in the reactive power demand of the wind farm. The results, checked against the system characteristic, indicate the adequacy of the ASVC model which was implemented.

The ASVC was also used to control the reactive power demand of the wind farm dynamically for various levels of generation. Two control strategies for the ASVC were implemented. The first used a voltage control scheme to keep the voltage at the ASVC busbar within the specified limits (-/+ 5 %) and along the slope characteristic. The second was to inject reactive power so that the reactive power flow between busbars 1 and 2 was zero (see Figure 9.12).

Although a number of studies have been carried out, only the results of one simulation are presented. Figure 8.15 shows changes in ASVC's voltage and reactive power following a change from a full wind farm generation to 50 % generation at time t = 1.3 sec (i.e., $Q_2 = 0$). The change in the level of generation causes a drop in the ASVC's voltage (from 1.0140 to 1.0120 pu) and reactive power (from 378 to 320 kVAr). The simulations were carried out with a value of gain k and time constant T chosen to be 50 and 0.5 respectively. The slow oscillations in the voltage and reactive power waveforms are due to the dynamics of the wind turbine induction generator as reflected in Figure 15(c) which shows the wind farm's generated power. The small stair-case variations in the waveforms are due to quantisation errors.

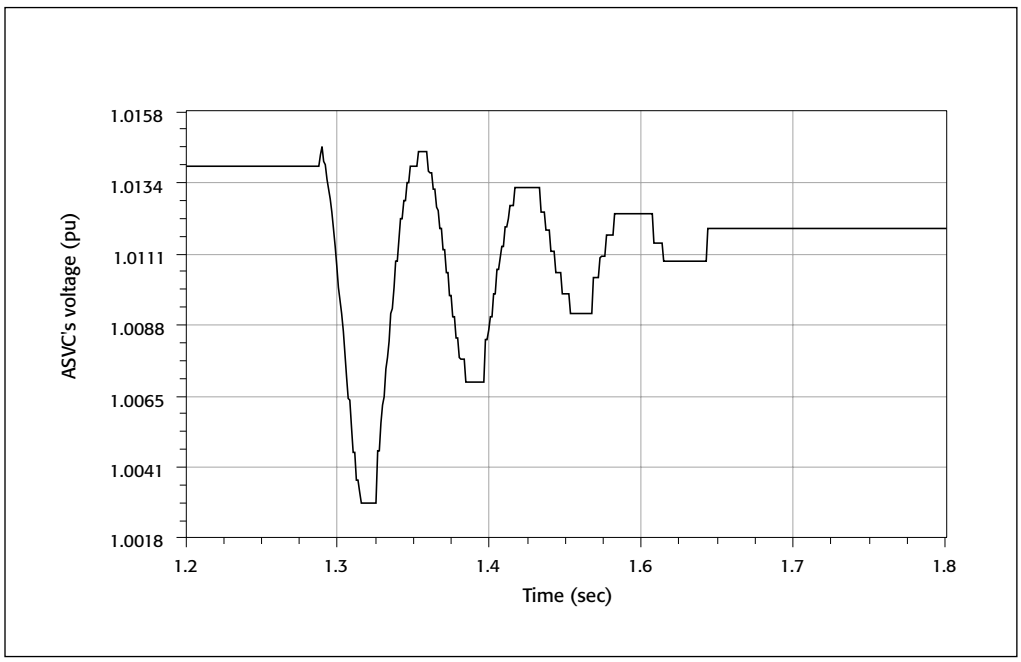

Fig 8.15(a): Variation of ASVC's voltage with changes in the wind farm generation.

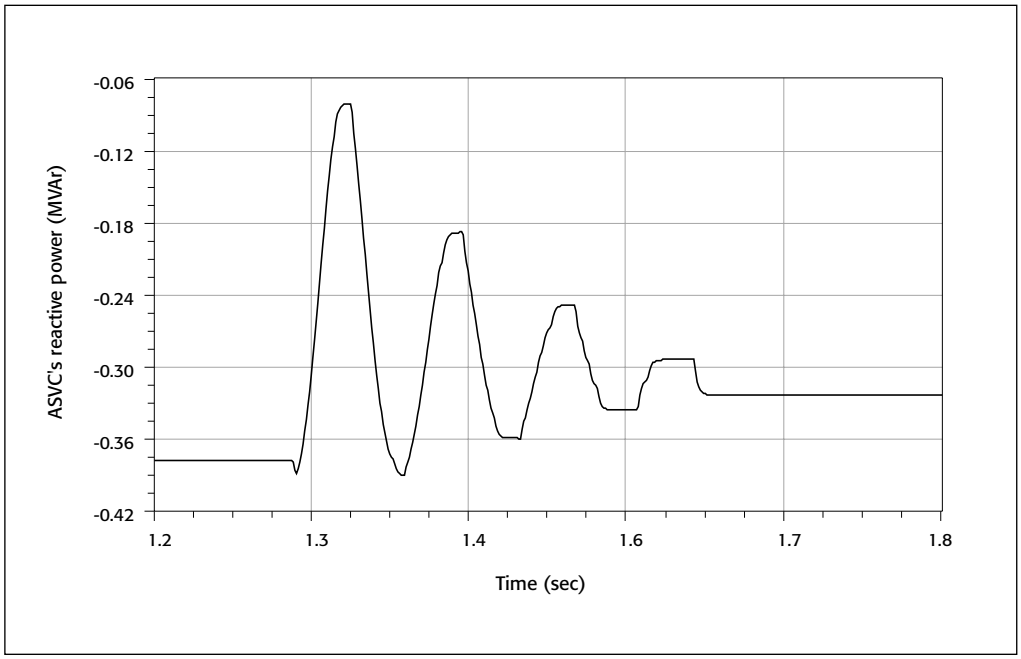

Fig 8.15(b): Variation of ASVC's reactive power with changes in the wind farm generation.

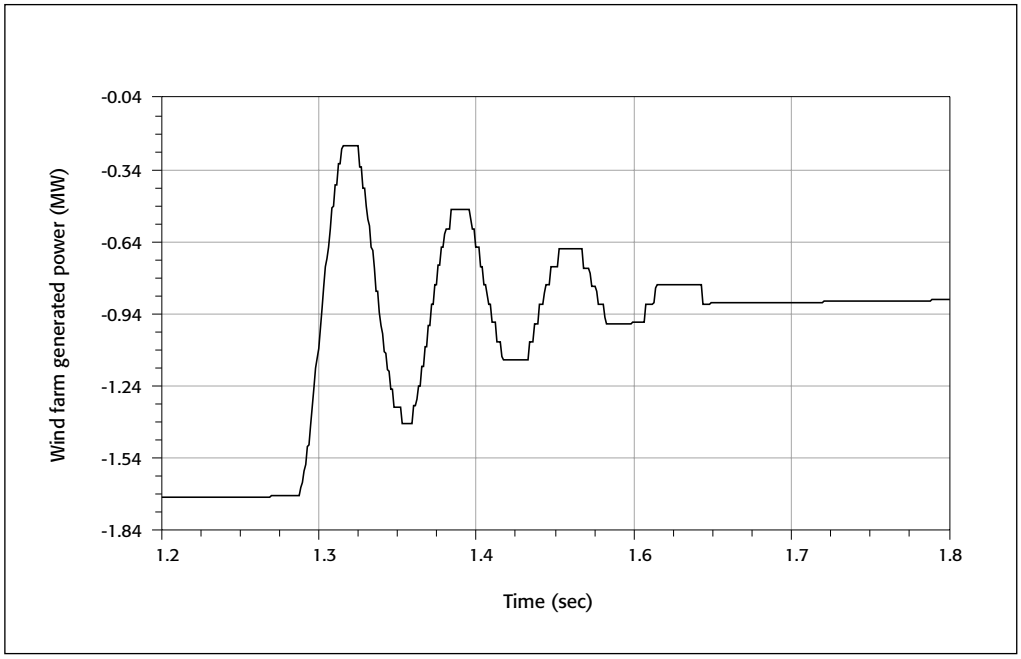

Fig 8.15(c): Variation of wind farm's generated power.

8.5 Conclusions

The application of Advanced Static VAr Compensators to different wind farms was investigated. Several strategies for steady state voltage and reactive power control of wind farms equipped with ASVCs were considered.

The unity power flow based strategy for controlling reactive power flows of a wind farm is likely to lead to close to minimal losses in real distribution networks. However, the unity power factor based control strategy may lead to an inefficient use of compensators in regulating the voltage in distribution systems in extreme circumstances, when the system is heavily or/and lightly loaded. The unity power factor based control may limit the active power output of embedded generators that can be accommodated, and therefore adversely influence the level of penetration of embedded generation particularly that connected to weak distribution systems.

The use of a unity power factor control technique and a voltage control scheme for the ASVC was also examined using an electromagnetic simulation. The ASVC was able to supply the reactive power requirements of the wind farm under various operating conditions, to control the network voltage actively and hence increase the permitted wind farm capacity and to improve the steady state stability limit of the network. Its application to prevent damaging over voltages which may occur under islanding conditions was demonstrated. The ASVC was also shown to mitigate voltage fluctuations at blade passing frequency successfully.

The operation of the ASVC with a unity power factor control scheme results in a reduction in total network losses but no increase in the penetration of embedded generation. The operation of the ASVC with a voltage control technique, operating on a conventional slope characteristic, would improve the steady state voltage stability of the network and increase the capacity of embedded generation that could be connected. This control technique can also prevent large overvoltages due to self-excitation at islanding if a controller with a fast enough speed of response is used. The control of transient voltage fluctuations, which may be caused by synchronised wind turbines, is also a natural consequence of a rapid voltage control scheme or may be implemented by a supplementary control signal of the voltage variations only.

The costs of connecting wind farms to distribution systems are mainly driven by the voltage level at which the connection is made and it is of considerable interest to developers and operators of wind farms to connect the generation at the lowest possible voltage level. On the other hand, in order to limit the effects of connecting wind farms on the rest of the system, high voltage connections are usually advocated by the utilities. The studies carried out on the wind farm of study case 2 show that a high voltage connection (66 kV) is likely to be the most suitable choice although a 20 kV connection is possible if the high losses can be accepted. On the basis of the steady state performance of the system the

only justification of an ASVC would appear to be if customer loads are connected to the 20 kV connecting circuit and then an ASVC would have a useful role in controlling the voltage of the high voltage side of the fixed tap 20/0.4 kV transformers.

The control strategy chosen for an ASVC depends on the system requirements. The use of the slope characteristic allows both voltage and reactive power control strategies to be performed simultaneously. The voltage control scheme is usually fast as compared to the slow acting reactive power control mode. Using a voltage control scheme, the voltage is controlled to within the specified limits by varying the injected or absorbed ASVC's reactive power. The reactive power control can be activated additional to the voltage control mode, to cater for deviations in reactive power between a desired and actual value by changing the reference voltage value. In this way, a unity power factor control scheme may be implemented.

References

1. P Gardner, "Technical and Commercial Aspects of the Connection of Wind Turbines to Electricity Supply Networks in Europe", Proceedings of the American Wind Energy Association Conference, March 1996.

2. K Bergmann et al., "Application of GTO-Based SVCs for Improved Use of the Rejsby Hede Wind Farm, 9th National Power Systems Conference, 19-21 December, Kanpur, India, 1996.

3. Z Saad-Saoud and N Jenkins, "The Application of Advanced Static VAr Compensators To Wind Farms", IEE Colloquium on Power Electronics for Renewable Energy, London, June 1997.

4. J E Hill, "A Practical Example of the Use of Distribution Static Compensator (D-STATCOM) to Reduce Voltage Fluctuations", IEE Colloquium on Power Electronics for Renewable Energy, London, June 1997.

5. J B Ekanayake, N Jenkins and C B Cooper, "Experimental investigation of an Advanced Static VAr Compensator", Generation, Transmission and Distribution, Proceedings of the IEE, Vol 142, No. 2, pp. 202-210, March 1995.

6. J B Ekanayake and N Jenkins, "Mathematical Models of a Three Level Advanced Static VAr Compensator", Generation, Transmission and Distribution, Proceedings of the IEE, Vol 44, No. 2, pp. 201-206, March 1997.

7. J B Ekanayake and N Jenkins, "A Three Level Advanced Static VAr Compensator", IEEE Transactions on Power Delivery, Vol. 11, No. 1, pp. 540-545, January 1996.

8. J B Ekanayake and N Jenkins, "Performance of a Three Level Advanced Static VAr Compensator", International Symposium on Electric Power Engineering, pp. 136-141, Stockholm Power Tech, June 1995.

9. Manitoba HVDC Research Centre, "EMTDC: Electromagnetic Transients Program Including DC Systems", 1994.

10. H Tyll and K Bergmann, "Use of Static VAR Compensators (SVCs) in High Voltage Systems", SRBE-KBVE, Les Compensateurs Statiques de Puissance Reactive, 22 March 1990, Brussels, Belgium.

11. J D Ainsworth, "Phase-Locked Oscillator Control System for Thyristor Controlled Reactors", Proceedings of the IEE, Vol. 135, Pt. C, No. 2, pp. 146-156, March 1988.

12. CIGRE WG38-01 Task Force No. 2, "Static VAR Compensators", 1986.

13. J D Ainsworth, "The Phase-Locked Oscillator - A New Control for Controlled Static Converter", IEEE Transactions on Power Apparatus and Systems, PAS-87, pp. 859-865, 1968.

14. Z Saad-Saoud and N Jenkins, "The Use of Advanced Static Var Compensators to Improve the Power Quality of Wind Farms", Proceedings of the 19th British Wind Energy Association Conference, BWEA 19, July 1997, Mechanical Engineering Publications.

15. T W Rasmussen, "An EMTDC Model of A Three Level Four MVAr Compensator", Proceedings of 32nd Universities Power Engineering Conference, UPEC 97, September 1997, UMIST, Manchester.

16. A Stampa and F Santjer, "Synchronism of Grid Connected Wind Energy Converters in a Wind Farm", DEWI Magazine, No. 7, August 1995 (in German).

17. A E Efthymiadis, A J B Heath and R D Youssef, "Interactive Power System Analysis (IPSA): User Manual", Version 9.3, Release 1.4, Power System Laboratory of UMIST, September 1997.

18. Cherry Tree Scientific Software, "Power System Toolbox (PST)", Canada, 1997.

19. R D Youssef, "Implicit Generator and SVC Modelling for Contingency Scheduling of Reactive Power Dispatch", IEE Proceedings on Generation, Transmission and Distribution, Vol 142, No. 5, September 1985.

Chapter 9

Conclusions

Nicholas Jenkins
Department of Electrical Engineering and Electronics
UMIST
PO Box 88
Manchester
M60 1QD
ENGLAND

Conclusions

The project successfully installed and commissioned an 8 MVAr GTO based Advanced Static VAr Compensator at the Rejsby Hede wind farm. This was the first application in the world of an ASVC used to improve the power quality of a large renewable energy generation plant.

The subsequent operating experience demonstrated that the ASVC was able dynamically to maintain the power factor of the wind farm at close to unity over a wide range of wind farm output power. The converter had a satisfactory harmonic performance although considerable studies were required at the design stage in order to achieve this.

A comprehensive monitoring system was designed, and constructed and installed at the wind farm and a large data set obtained for future analysis. Various system studies were carried out to investigate the use of ASVCs on other wind farm sites, particularly those with a low short circuit level relative to the wind farm capacity. It was shown that, in a number of situations, an ASVC is likely to be of significant benefit in improving various aspects of power quality.

In summary it may be concluded that the project was successful in developing and applying novel power electronic technology to a renewable energy system and that the research which has been completed will allow similar schemes to be implemented in the future.

Kent H. Søbrink
I/S Eltra

Ralf Stöber
Frank Schettler
Klaus Bergmann
SIEMENS

Nicholas Jenkins
Janaka Ekanayake (Visitor)
Zouhir Saad-Saoud,
Maria Luiza Lisboa,
Goran Strbac
UMIST

Jørgen Kaas Pedersen
Knud Ole Helgesen Pedersen
Technical University of Denmark

ISBN No.: 87–90707–05–2